

**An-Najah National University
Faculty of Graduate Studies**

**Determination of Some Fluoroquinolone Antibacterials
with DNA-Modified Electrodes and their Oxidation
by Potassium Hexacyanoferrate(III)**

**By
Ibrahim Diab Najeeb Abu-Shqair**

**Supervisor
Prof. Radi Daoud
Co-Supervisor
Prof. Mohammad Al-Subu**

*Submitted in Partial Fulfillment of the Requirements for the Degree of
Ph. D. of Science in Chemistry, Faculty of Graduate Studies, at An-
Najah National University, Nablus, Palestine*
2006



[Handwritten signature in blue ink]

**Determination of Some Fluoroquinolone Antibacterials
with DNA-Modified Electrodes and their Oxidation
by Potassium Hexacyanoferrate(III)**

By
Ibrahim Diab Najeeb Abu-Shqair

This Thesis was defended successfully on 05/06/2006 and approved by

Committee Members

Signature

1. Prof. Radi Daoud (Supervisor)

[Handwritten signature of R. Daoud]

2. Prof. Mohammad Al-Subu (Co - Supervisor)

[Handwritten signature of M. Al-Subu]

3. Dr. Nizam Diab (External Examiner)

[Handwritten signature of N. Diab]

4. Dr. Shokri Khalaf (Internal Examiner)

[Handwritten signature of S. Khalaf]

c

TO

MY PARENTS

MY WIFE AND MY CHILDREN

MY FAMILY AND FRIENDS

ACKNOWLEDGMENT

After thanking Allah, who granted me the power to finish this work, I would like to express my deep appreciation to my supervisors Prof. Radi Dauod and Prof. Mohammad Al-Subu for their fruitful supervision and encouragement during the research course.

I wish to thank all members of Chemistry Department, especially, Dr. Shokri Khalaf (Head of department), Prof. Hikmat Hilal, Dr. Waheed Al-Jundi, Dr Nidal Za'tar and Dr. Shehdi Jodeh for their help and encouragement.

I would like to thank Dr. Nizam Diab for his valuable suggestions and great help.

Special thanks to Dr. Zeid Qamheyyeh for providing the origin software and for solving the electrochemical equation, special thank also to Dr. Mohammad Mosmar, Dr. Isam Rashed, Dr. Mohammad Abu-Ja'far, Dr. Sameer Matter, Dr. Ayman Hussein for their fruitful help.

I would like to thank my friends Hussein Sharief, Daoud Abu-Safeyyeh, Amjad Izz El-Deen, Majdi Dwaikat and Amjad Shraim for thier great help.

Deep thanks to my friends and colleagues at Collage of Agriculture for their support. Thanks also to laboratory technicians and librarians for their cooperation during this work,

Special deep gratitude to my friends and family for their encouragement and support.

Ibrahim Abu-Shqair

Table of Contents

| Section | Title | Page |
|----------|--|-----------|
| | Committee Decision | II |
| | Dectation | III |
| | Acknowledgment | IV |
| | Table of Contents | V |
| | List of Tables | VII |
| | List of Figures | VIII |
| | Abstract | XIII |
| 1 | INTRODUCTION | 1 |
| 1.1 | Quinolones | 2 |
| 1.1.1 | Background and Uses | 2 |
| 1.1.2 | Mechanism of Action | 5 |
| 1.1.3 | Pharmacokinetics | 6 |
| 1.1.4 | Environmental Aspects | 6 |
| 1.1.5 | Photosensitivity of Quinolones | 7 |
| 1.1.6 | Determination of Quinolones | 8 |
| 1.1.6.1 | Electrochemistry | 8 |
| 1.1.6.2 | Capillary Electrophoresis | 9 |
| 1.1.6.3 | Chromatographic Methods | 11 |
| 1.1.6.4 | Microbiological Methods | 11 |
| 1.1.6.5 | Spectroscopy | 12 |
| 1.2 | DNA-Drug Interaction: Biosensors | 14 |
| 1.2.1 | DNA-Modified Electrodes | 23 |
| 1.2.1.1 | Electrochemical techniques | 23 |
| 1.2.1.2 | Physical adsorption onto carbon electrodes | 24 |
| 1.2.1.3 | Physical adsorption onto conducting polymers | 25 |
| 1.2.1.4 | Adsorption on gold electrodes | 25 |
| 1.2.1.5 | Adsorption on mercury electrodes | 25 |
| 1.2.2 | Drug-Modified Electrodes | 26 |
| 1.2.3 | Interaction in Solution | 26 |
| 1.3 | Chemical Oxidation of Quinolones | 26 |
| 2 | EXPERIMENTAL | 28 |
| 2.1 | Interaction of Quinolones with DNA | 29 |
| 2.1.1 | Reagents and Solutions | 29 |
| 2.1.2 | Instrumentation | 29 |
| 2.1.3 | Preparation of dsDNA-GCE | 30 |
| 2.1.4 | Methodology | 31 |
| 2.1.4.1 | Interaction of Quinolones with DNA in Solution | 31 |
| 2.1.4.2 | Interaction of Quinolones with DNA at Electrode Surface | 31 |
| 2.1.4.3 | Determination of Ciprofloxacin in Pharmaceutical Formulations | 32 |

| Section | Title | Page |
|----------------|---|-------------|
| 2.1.4.4 | Determination of Ciprofloxacin in Urine | 32 |
| 2.2 | Kinetics of Oxidation of Quinolones by $K_3Fe(CN)_6$ | 32 |
| 2.2.1 | Reagents and Solutions | 32 |
| 2.1.2 | Instrumentation | 33 |
| 2.1.3 | General Procedure for Kinetic Studies | 33 |
| 3 | RESULTS AND DISCUSSION | 34 |
| 3.1 | Interaction of Quinolones with DNA in Solution | 35 |
| 3.1.1 | UV-Visible Spectroscopy | 35 |
| 3.1.2 | Cyclic Voltammetric Studies | 37 |
| 3.2 | Interaction of Quinolones with DNA at the Electrode Surface | 45 |
| 3.2.1 | Effect of Scan Rate | 46 |
| 3.2.2 | Effect of pH | 46 |
| 3.2.3 | Effect of Accumulation Time | 48 |
| 3.2.4 | Effect of Accumulation Potential | 49 |
| 3.2.5 | Effect of Ionic Strength | 49 |
| 3.2.6 | Effect of Pulse Amplitude | 50 |
| 3.2.7 | Effect of Quinolone Concentration | 50 |
| 3.2.8 | Analytical Applications | 51 |
| 3.3 | Kinetics of Oxidation of Quinolones by Hexacyanoferrate (III) | 52 |
| 3.3.1 | Dependence on reactants concentration | 53 |
| 3.3.2 | Effect of added salts | 55 |
| 3.3.3 | Thermodynamic parameters | 55 |
| 4 | CONCLUSIONS AND FURTHER WORK | 58 |
| | SUGGESTIONS | |
| 4.1 | Conclusions | 59 |
| 4.2 | Suggestions for Future Work | 61 |
| | Tables | 62 |
| | Figures | 70 |
| | References | 120 |
| | Abbreviations | 151 |

List of Tables

| Table | Title | Page |
|-------------------|---|------|
| Table (1) | Absorption data for the interaction of ciprofloxacin with DNA | 63 |
| Table (2) | Absorption data for the interaction of norfloxacin with DNA | 63 |
| Table (3) | Absorption data for the interaction of enrofloxacin with DNA | 63 |
| Table (4) | Absorption data for the interaction of nalidixic acid with DNA | 63 |
| Table (5) | K values for the interaction of quinolones with DNA | 63 |
| Table (6) | Voltammetric behavior of CIP and CIP – DNA | 64 |
| Table (7) | Voltammetric behavior of NOR and NOR – DNA | 64 |
| Table (8) | Voltammetric behavior of ENR and ENR – DNA | 64 |
| Table (9) | Effect of addition of DNA on peak currents (CIP) | 64 |
| Table (10) | Effect of addition of DNA on peak currents (NOR) | 65 |
| Table (11) | Effect of addition of DNA on peak currents (ENR) | 65 |
| Table (12) | Electrochemical binding parameters for the interaction of quinolones with DNA | 65 |
| Table (13) | Relationship between DPASV peak currents and quinolone concentration | 66 |
| Table (14) | Effect of FQ concentration on reaction rate | 66 |
| Table (15) | Effect of $\text{Fe}(\text{CN})_6^{3-}$ concentration on reaction rate | 66 |
| Table (16) | Effect of OsO_4 concentration on reaction rate | 67 |
| Table (17) | Effect of hydroxide ion concentration on reaction rate | 67 |
| Table (18) | Effect of added $\text{K}_4\text{Fe}(\text{CN})_6$ on reaction rate | 67 |
| Table (19) | Effect of added salt on reaction rate | 68 |
| Table (20) | Effect of temperature on ciprofloxacin reaction rate | 68 |
| Table (21) | Effect of temperature on norfloxacin reaction rate | 68 |
| Table (22) | Effect of temperature on enrofloxacin reaction rate | 69 |
| Table (23) | Activation parameters for the catalysed oxidation of FQ's by hexacyanoferrate (III) | 69 |

List of Figures

| Figure | Title | Page |
|--------------------|---|------|
| Figure (1) | UV/Vis absorption spectra of acetate buffer solution (pH 5) containing 10 μM CIP in the presence of DNA (μM): (a) 0.00; (b) 10.0; (c) 20.0; (d) 30.0; (e) 40.0; (f) 50.0 | 71 |
| Figure (2) | UV/Vis absorption spectra of acetate buffer solution (pH 5) containing 10 μM NOR in the presence of DNA (μM): (a) 0.00; (b) 10.0; (c) 20.0; (d) 30.0; (e) 40.0 | 72 |
| Figure (3) | UV/Vis absorption spectra of acetate buffer solution (pH 5) containing 10 μM ENR in the presence of DNA (μM): (a) 0.00; (b) 10.0; (c) 20.0; (d) 30.0; (e) 40.0 | 73 |
| Figure (4) | UV/Vis absorption spectra of acetate buffer solution (pH 5) containing 10 μM NAL in the presence of DNA (μM): (a) 0.00; (b) 10.0; (c) 20.0; (d) 30.0; (e) 40.0 | 74 |
| Figure (5) | Plot of $A_0/(A-A_0)$ vs. $1/[\text{DNA}]$ | 75 |
| Figure (6) | Cyclic voltammograms of acetate buffer solution (pH 5) containing $3 \times 10^{-5}\text{M}$ CIP in the absence (a) and presence (b) of $1.2 \times 10^{-3}\text{M}$ DNA. Scan rate: 100mV/s. Initial potential: +0.3 V | 76 |
| Figure (7) | Cyclic voltammograms of acetate buffer solution (pH 5) containing $3 \times 10^{-5}\text{M}$ NOR in the absence (a) and presence of; (b) $1.5 \times 10^{-4}\text{M}$; (c) $6 \times 10^{-4}\text{M}$; (d) $9 \times 10^{-4}\text{M}$; (e) $1.2 \times 10^{-3}\text{M}$ DNA. Scan rate: 100mV/s. Initial potential: +0.3 V | 77 |
| Figure (8) | Cyclic voltammograms of acetate buffer solution (pH 5) containing $3 \times 10^{-5}\text{M}$ ENR in the absence (a) and presence (b) of $1.2 \times 10^{-3}\text{M}$ DNA. Scan rate: 100mV/s. Initial potential: +0.3 V | 78 |
| Figure (9) | Cyclic voltammograms of $\text{K}_4\text{Fe}(\text{CN})_6$ in the absence (a) and presence (b) of $1.2 \times 10^{-3}\text{M}$ DNA. Scan rate: 100mV/s. Initial potential: +0.3 V | 79 |
| Figure (10) | Plot of I_p vs $v^{1/2}$ of acetate buffer solution (pH 5) containing $4 \times 10^{-5}\text{M}$ CIP in the absence and presence of $1.6 \times 10^{-4}\text{M}$ DNA | 80 |
| Figure (11) | Plot of I_p vs $v^{1/2}$ of acetate buffer solution (pH 5) containing $3 \times 10^{-5}\text{M}$ NOR in the absence and presence of $1.2 \times 10^{-3}\text{M}$ DNA | 81 |

| Figure | Title | Page |
|--------------------|---|------|
| Figure (12) | Plot of I_p vs $v^{1/2}$ of acetate buffer solution (pH 5) containing $3 \times 10^{-5} M$ ENR in the absence and presence of $1.2 \times 10^{-3} M$ DNA | 82 |
| Figure (13) | Plot of E_p vs $\ln v$ of acetate buffer solution (pH 5) containing $3 \times 10^{-5} M$ CIP in the absence and presence of $1.2 \times 10^{-3} M$ DNA | 83 |
| Figure (14) | Plot of E_p vs $\ln v$ of acetate buffer solution (pH 5) containing $3 \times 10^{-5} M$ NOR in the absence and presence of $1.2 \times 10^{-3} M$ DNA | 84 |
| Figure (15) | Plot of E_p vs $\ln v$ of acetate buffer solution (pH 5) containing $3 \times 10^{-5} M$ ENR in the absence and presence of $1.2 \times 10^{-3} M$ DNA | 85 |
| Figure (16) | Binding curve of $3 \times 10^5 M$ CIP with DNA acetate buffer solution (pH 5). Scan rate: 100mV/s | 86 |
| Figure (17) | Binding curve of $3 \times 10^5 M$ NOR with DNA in acetate buffer solution (pH 5). Scan rate: 100mV/s | 87 |
| Figure (18) | Binding curve of $3 \times 10^5 M$ ENR with DNA in acetate buffer solution (0.2M, pH 5). Scan rate: 100mV/s | 88 |
| Figure (19) | Cyclic voltammograms of $1 \times 10^{-5} M$ CIP in acetate buffer solution (pH 5) at: (a) bare GC electrode and (b) DNA-modified GC electrode. (Scan rate: 100mV/s. Initial potential: +0.2 V. Accumulation time: 1.0 min) | 89 |
| Figure (20) | Cyclic voltammograms of $1 \times 10^{-5} M$ NOR in acetate buffer solution (pH5) at: (a) bare GC electrode and (b) DNA-modified GC electrode. (Scan rate: 100mV/s. Initial potential: +0.2 V. Accumulation time: 1.0 min) | 90 |
| Figure (21) | Cyclic voltammograms of $1 \times 10^{-5} M$ ENR in acetate buffer solution (pH5) at: (a) bare GC electrode and (b) DNA-modified GC electrode. (Scan rate: 100mV/s. Initial potential: +0.2 V. Accumulation time: 1.0 min) | 91 |
| Figure (22) | Differential-pulse anodic stripping voltammograms of $1 \times 10^{-5} M$ CIP in acetate buffer solution (pH 5) at (a) bare GC electrode and (b) DNA-modified GC electrode. (Scan rate: 10 mV/s. Initial potential: +0.4 V. Accumulation time: 1.0 min) | 92 |
| Figure (23) | Differential-pulse anodic stripping | 93 |

| Figure | Title | Page |
|--------------------|---|------|
| | voltammograms of 1×10^{-6} M CIP in acetate buffer solution (pH 5) at DNA-modified GC electrode at different scan rates (mV/s): (a) 5 (b) 10 (c) 20 (d) 50 (e) 100. (Initial potential: +0.4 V. Accumulation time: 1.0 min) | |
| Figure (24) | Effect of scan rate on the DPASV peak currents of 1×10^{-6} M drug in acetate buffer solution (pH 5) at DNA-modified GC electrode. (Initial potential: +0.4 V. Accumulation potential: 1.0 min) | 94 |
| Figure (25) | Differential-pulse anodic stripping voltammograms of 1×10^{-5} M CIP at DNA-modified GC electrode in acetate buffer solutions of different pH values: (a) pH 9, (b) pH 7, (c) pH 5, (d) pH 3.5. (Scan rate: 10 mV/s. Accumulation time: 1.0 min. | 95 |
| Figure (26) | Effect of pH on the DPASV peak currents of 1×10^{-5} M drug in acetate buffer solution at DNA-modified GC electrode. (Scan rate: 10 mV/s. Initial potential: +0.2 V. Accumulation potential: 1.0 min) | 96 |
| Figure (27) | Differential-pulse anodic stripping voltammograms of 1×10^{-5} M CIP at DNA-modified GC electrode in acetate buffer solution (pH 5) at different accumulation times (s): (a) 15, (b) 30, (c) 60, (d) 120. (Scan rate: 10 mV/s. Initial potential: +0.2 V) | 97 |
| Figure (28) | Effect of accumulation time on the DPASV peak currents of 1×10^{-5} M drug in acetate buffer solution (pH 5) at DNA-modified GC electrode. (Scan rate: 10 mV/s. Initial potential: +0.2 V) | 98 |
| Figure (29) | Differential-pulse anodic stripping voltammograms of 1×10^{-5} M CIP at DNA-modified GC electrode in acetate buffer solution (pH 5) at different accumulation potentials (V): (a) +0.8, (b) +0.6, (c) +0.4, (d) +0.2, (e) 0.0, (f) -0.2, (g) -0.4, (h) -0.6. (Scan rate: 10 mV/s. Initial potential: +0.2 V. Accumulation time: 30s) | 99 |
| Figure (30) | Effect of accumulation potential on the DPASV peak currents of 1×10^{-5} M drug in acetate buffer solution (pH 5) at DNA-modified GC electrode. (Scan rate: 10 mV/s. Initial potential: +0.2 V) | 100 |
| Figure (31) | Effect of ionic strength on the DPASV peak currents of 1×10^{-6} M drug in acetate buffer solution | 101 |

| Figure | Title | Page |
|--------------------|--|------|
| | (pH 5) at DNA-modified GC electrode. (Scan rate: 10 mV/s. Initial potential: +0.4 V. Accumulation time: 60s for CIP and NOR and 40s for ENR) | |
| Figure (32) | Differential-pulse anodic stripping voltammograms of 1×10^{-6} M CIP at DNA-modified GC electrode in acetate buffer solution (pH 5) at different pulse amplitudes (mV): (a) 25, (b) 50, (c) 100. (Scan rate: 10 mV/s. Initial potential: +0.4 V. Accumulation time: 30s) | 102 |
| Figure (33) | Differential-pulse anodic stripping voltammograms of different concentrations (μ M) of CIP at DNA-modified GC electrode in acetate buffer solution (pH 5): (a) 1.0, (b) 2.0, (c) 3.0, (d) 4.0, (e) 5.0. (Scan rate: 10 mV/s. Initial potential: +0.4 V. Accumulation time: 30s) | 103 |
| Figure (34) | Effect of CIP concentration on the DPASV peak currents in acetate buffer solution (pH 4) at bare and DNA-modified GC electrode. (Scan rate: 10 mV/s. Initial potential: +0.4 V. Accumulation time: 60s) | 104 |
| Figure (35) | Effect of NOR concentration on the DPASV peak currents in acetate buffer solution (pH 4) at DNA-modified GC electrode. (Scan rate: 10 mV/s. Initial potential: +0.4 V. Accumulation time: 60s) | 105 |
| Figure (36) | Effect of ENR concentration on the DPASV peak currents in acetate buffer solution (pH 4) at DNA-modified GC electrode. (Scan rate: 10 mV/s. Initial potential: +0.4 V. Accumulation time: 60s) | 106 |
| Figure (37) | Differential-pulse anodic stripping voltammograms of different samples of Ciprocare tablet solution. (Scan rate: 10 mV/s. Initial potential: +0.4 V. Accumulation time: 60s) | 107 |
| Figure (38) | Differential-pulse anodic stripping voltammograms of urine samples spiked with CIP. (Scan rate: 10 mV/s. Initial potential: +0.4 V, time: 60s) | 108 |
| Figure (39) | Effect of FQ concentration on reaction rate | 109 |
| Figure (40) | Effect of $K_3Fe(CN)_6$ concentration on reaction rate | 110 |
| Figure (41) | Effect of OsO_4 concentration on reaction rate | 111 |
| Figure (42) | Effect of hydroxide ion concentration on reaction rate | 112 |
| Figure (43) | Effect of added $K_4Fe(CN)_6$ on ciprofloxacin | 113 |

| Figure | Title | Page |
|--------------------|---|------|
| | reaction rate | |
| Figure (44) | Effect of added $K_4Fe(CN)_6$ on norfloxacin reaction rate | 114 |
| Figure (45) | Effect of added $K_4Fe(CN)_6$ on enrofloxacin reaction rate | 115 |
| Figure (46) | Effect of added salt on ciprofloxacin reaction rate | 116 |
| Figure (47) | Effect of added salt on norfloxacin reaction rate | 117 |
| Figure (48) | Effect added of salt on enrofloxacin reaction rate | 118 |
| Figure (49) | Effect of temperature on reaction rate | 119 |

**Determination of Some Fluoroquinolone Antibacterials
with DNA-Modified Electrodes and Their Oxidation
by Potassium Hexacyanoferrate(III)**

By

Ibrahim Diab Najeeb Abu-Shqair

Supervisor

Prof. Radi Daoud

Co-Supervisor

Prof. Mohammad Al-Subu

Abstract

UV-visible spectroscopic and electrochemical methods were used to study the interaction of some fluoroquinolones with calf-thymus DNA. UV-visible spectroscopy was used to evaluate the binding constants of drug-DNA complexes and to elucidate the nature of binding of these drugs with DNA. The interaction of the studied fluoroquinolones with DNA was investigated by cyclic voltammetry at a glassy carbon electrode with an irreversible electrochemical equation. The diffusion coefficients of both free and bound fluoroquinolones (D_f , D_b), the binding constant (K), and the binding site size (s) of fluoroquinolone-DNA complexes were obtained simultaneously by non-linear fit analysis of the experimental data. The results suggested that fluoroquinolones bind to DNA through an electrostatic mode of interaction with partial intercalation.

DNA-modified glassy carbon electrodes were used for the first time as a biosensor for the determination of the studied compounds. Differential-pulse anodic stripping voltammetry was used for investigating different factors that affect the oxidation of the studied fluoroquinolones at the DNA-biosensor. A method was proposed for the determination of ciprofloxacin concentration both in tablets and in a biological fluid (urine). The method was found to be sensitive, accurate, and inexpensive.

Kinetics of osmium tetroxide catalyzed-oxidation of the studied fluoroquinolones by potassium hexacyanoferrate (III) in alkaline medium were studied. The rate was found to be independent on the concentration of hexacyanoferrate (III), and first order with respect to both fluoroquinolone and OsO_4 . An empirical rate law was derived for the reaction, and the effect of various variables on the rate of reaction was studied. Thermodynamic parameters (E_a , ΔH^* , ΔS^* , ΔG^*) were also calculated.

CHAPTER 1

INTRODUCTION

1.1. Quinolones

1.1.1. Background and Uses:

The term quinolones is commonly used for the quinolone carboxylic acids or 4-quinolones; a group of synthetic antibacterial agents containing 4-oxo-1,4-dihydroquinoline skeleton (scheme1). The first analogue of this class , nalidixic acid, was synthesized in 1962 (1) and used for the treatment of urinary tract infections (2). It is more active against Gram-positive than Gram-negative organisms (3). The major metabolite of antibacterial activity is similar in spectrum and potency to that of the parent compound (4).

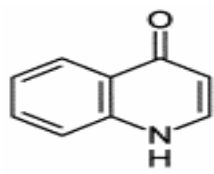
Different structural modifications in the quinoline nucleus have been made to increase antimicrobial activity and improve its performance. During 1980's, it was discovered that a fluorine atom at position 6 and

piperazine ring at position 7 greatly enhance the spectrum of activity of these antibiotics (5,6). Fluoroquinolones are extremely useful for the treatment of a variety of infections, including urinary tract infections, soft tissue infections, respiratory infections, bone-joint infections, typhoid fever, sexual transmitted diseases, prostatitis, community acquired pneumonia, acute bronchitis and sinusitis (5,7,8). Recently a relatively new approach to the rational design of antitumor agents has been introduced based on some new quinolone molecules (9). Ciprofloxacin, [1-cyclopropyl-6-fluoro-1,4-dihydro-4-oxo-7-(piperazinyl) -3-quinoline carboxylic acid], a typical second generation fluoroquinolone, has been in clinical use for more than a decade and sold for \$US 1.5 billion in 1996 (10). The drug has been the center of great interest and success, and more than 15000 articles have been published about it (11). Because of its efficiency in treatment of the infections caused by *Bacillus Anthracis* (Anthrax infections), and in connection with the outbreak of suspected anthrax biological warfare, significance of ciprofloxacin has increased enormously (12).

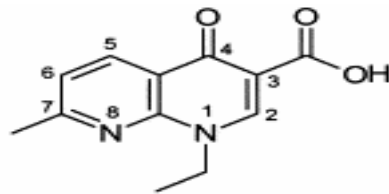
Norfloxacin, [1-ethyl-6-fluoro-1,4-dihydro-4-oxo-7-(piperazinyl)-3-quinoline carboxylic acid], is one of the 4-quinolone synthetic antibiotics. It is active against Gram-positive and Gram-negative bacteria and is widely used in the treatment of urinary infections with good penetration of the infected sites. About 30% of the oral dose is excreted unchanged in the urine within 24 hours, thus producing high urinary concentrations (13).

Quinolones, however, are not limited to clinical applications. They are also widely used to treat and prevent veterinary diseases in animals intended for human consumption and commercially farmed fish such as salmon and catfish. Enrofloxacin, [1-cyclopropyl-6-fluoro-1,4-dihydro-4-

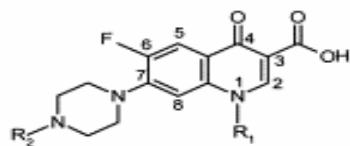
oxo-7-(4-ethyl-1-piperazinyl)-3-quinoline carboxylic acid], another member of the fluoroquinolones family, is administered to cattle, pigs, chicken, turkeys, sheep, rabbits, and dogs to control bacterial infections caused by sensitive organisms (14).



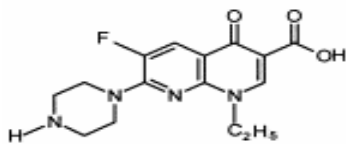
4-oxo-1,4-dihydroquinoline



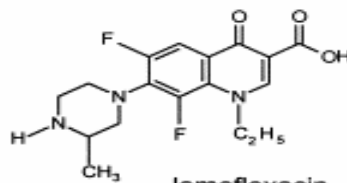
nalidixic acid



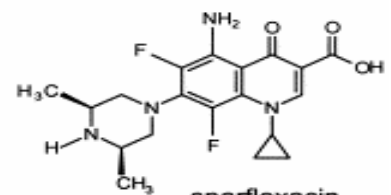
ciprofloxacin: $R_1 = \text{cyclopropyl}$, $R_2 = \text{H}$
 norfloxacin: $R_1 = \text{ethyl}$, $R_2 = \text{H}$
 enrofloxacin: $R_1 = \text{cyclopropyl}$, $R_2 = \text{ethyl}$
 pefloxacin: $R_1 = \text{ethyl}$, $R_2 = \text{methyl}$



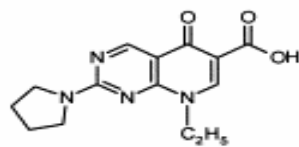
enoxacin



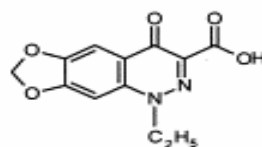
lomefloxacin



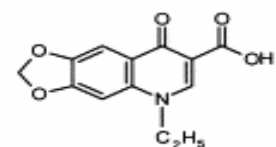
sparfloxacin



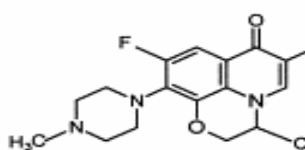
piromidic acid



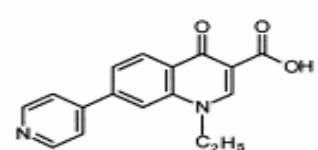
cinoxacin



oxolinic acid



ofloxacin



rosoxacin

Scheme 1. Some quinolones and related structures.

1.1.2. Mechanism of Action:

Quinolones are active against the DNA-gyrase enzyme, a type II topoisomerase. It is believed that DNA-gyrase introduces negative supercoils in DNA (15) by wrapping the DNA around the enzyme. The enzyme then catalyzes the breakage of a segment of the wrapped DNA, the passage of a segment of the same DNA through the break and finally the religation of the break (16). In this way, DNA “knots” are resolved and the DNA is exposed for replication process.

DNA-gyrase is essential for all bacteria and is therefore an excellent target for antibiotics. Quinolones turn the action of gyrase against the bacteria by blocking the strand passage and thereby hindering proper replication of DNA. This eventually leads to cell death.

Currently several structural models have been suggested to account for the action of quinolones. In common, all suggested models require a direct interaction between the drug and either single or double-stranded DNA (17-19). One of these models suggests that Mg^{2+} plays an important role in the drug binding to a DNA-gyrase complex (19-22). However the exact mechanism of action is still unclear and several points such as: (i) preference for single- or double-strand DNA binding; (ii) the role of Mg^{2+} ions; (iii) groove binding versus classical interaction need to be addressed (11). Thus, contribution to deeper insight into the mechanism of interaction of this class of antibiotics with DNA is important for a better understanding of their therapeutic efficiency (23).

1.1.3. Pharmacokinetics:

After oral administration, fluoroquinolones are well absorbed (bioavailability of 80-95%) and distributed widely in body fluids and tissues. Serum half-lives range from 3 hours (norfloxacin and ciprofloxacin) up to 10 hours (pefloxacin) or longer (sparfloxacin). Oral absorption is impaired by divalent cations including those in antacids. Serum concentrations of intravenously administered drug are similar to those of orally administered drug. Concentrations in prostate, kidney, neutrophils, and macrophages exceed serum concentrations. Most fluoroquinolones are eliminated by renal mechanisms, either tubular secretion or glomerular filtration (24).

1.1.4. Environmental Aspects:

A significant part of body administered quinolones is excreted intact and introduced into the nature through wastewater (25). Because of the extensive usage of these drugs, the presence of quinolones in aquatic environment has been reported. Concentrations of 249 to 405 ng/L of ciprofloxacin and 45 to 120 ng/L of norfloxacin have been detected in domestic waste water in Switzerland (26,27). Higher concentrations of some fluoroquinolones (0.6-2 mg/L) were recently detected in wastewaters in the US. Moderate concentrations of 0.02 mg/L and 0.12 mg/L were also reported for ciprofloxacin and norfloxacin respectively for samples from 139 surface streams across the US (28). A range of concentrations of 0.7 to 124.5 mg/L of ciprofloxacin found in a Swiss hospital waste water (29).

The contamination with quinolone antibiotics may cause a threat to the ecosystem and human health by increasing the drug resistance of bacteria (30). Antibiotic-resistant bacteria have been isolated from different

environments including rivers, streams, drinking water, and waste water treatment plant effluents (31,32). Fluoroquinolones, especially ciprofloxacin have been linked to the genotoxicity of waste water effluents in German and Swiss hospital wastewaters for causing primary DNA damage in bacteria (25).

Fluoroquinolones have been shown to be relatively resistant to microbial degradation (33-35). However, other studies have reported extensive degradation of ciprofloxacin and enrofloxacin by certain fungi species (36).

Photodegradation of fluoroquinolones by direct uv photolysis or radical- mediated photolysis has been reported (37-41). Depending on the reaction conditions, more than ten photodegradation products including dealkylation, defluorination and hydroxylation have been identified.

Sorption to soil, sediments or dissolved organic matter is another important environmental sink for fluoroquinolones (42-44), which might result in a fewer amount of freely available antibacterial agents and thus reduce their photodegradation and biodegradation (45).

1.1.5. Photosensitivity of Quinolones:

Drug-induced photosensitivity can be divided into phototoxicity and photoallergy. Phototoxicity is the adverse response to the combined actions of a chemical agent such as a drug and a physical agent such as the UV radiation . The quinolone antibiotics are typical photosensitizers (46). Phototoxicity owing to these drugs was caused by the reactive oxygen species (ROS) (47). Oxygen- dependent release of ROS induces phototoxic damage on cell surface, DNA and lysosome (48-50). Clinically,

phototoxicity shows features of exaggerated sunburns. Long-term intake of a photosensitizer may induce contract of ocular lens or photo-aging of skin (51). Quinolone antibiotics were able to induce photocarcinogenesis. Fluoroquinolones, such as lomefloxacin or flumequine exhibited increased photocarcinogenic potentials (52,53). Most quinolones show phototoxicity in various *in vitro* methods, which examine fluorescence or phototoxic killing of organisms or phototoxic destruction of cells, and *in vivo* methods, which measure swellings or erythema (46).

Quinoline antibiotics also induce photoallergy, another feature of UV-induced skin lesion. This photoallergy shows features of allergic contact dermatitis in the exposed areas. Without uv irradiation, they are usually inert, however, under uv light, quinolones are activated to bind with skin proteins which becomes complete antigen and induces allergic dermatitis (54,55).

1.1.6. Determination of Quinolones :

Determination of quinolones in different samples has been achieved by different techniques, among these are:

1.1.6.1. Electrochemistry:

Voltammetric and polarographic methods have gained a considerable interest for the determination of pharmaceuticals. Beside their suitability for the analysis of trace materials in complicated systems, these methods are sufficiently sensitive and selective. Over the last 15 years, direct determination of quinolones has been investigated by electrochemical methods, with polarographic methods being favored in the early 1990s (56). The presence of a carbonyl group attached to the quinolones nucleus,

in conjunction with carboxylic acid group initiated several polarographic studies for this class of compounds (57).

Differential-pulse polarography (DPP) technique (58) and adsorptive stripping voltammetry (ASV) (59) were used for the determination of norfloxacin in tablets. Anodic stripping technique (ASV) was also used for the determination of ofloxacin in tablets (60). Linear sweep voltammetry (61) and DPP (62) were also investigated for the determination of ofloxacin in its pure form, medicinal preparations and biological fluids. Square-wave adsorptive voltammetry using glassy carbon electrodes was reported for the analysis of norfloxacin in urine (63). Ciprofloxacin was determined in urine by ASV at mercury and carbon paste electrodes (64).

Enrofloxacin in formulations and biological fluids was determined by direct current, alternating current and DPP (65). AdSV was also used for the determination of enrofloxacin in commercial formulations and urine samples (66). Nalidixic acid was polarographically determined in urine (67). ASV was applied for the determination of nalidixic acid in pharmaceuticals, human urine and serum (68). Other quinolones such as, levofloxacin (69), fleroxacin (70), moxifloxacin (71), trovafloxacin (72), and lomefloxacin (73) were determined by voltammetry.

1.1.6.2. Capillary Electrophoresis:

In recent years, capillary electrophoresis (CE) has gained popularity as a separation technique for routine analysis and its applications are wide spread in many fields of analytical chemistry (74). CE is a good alternative to liquid chromatography in drug analysis (75). It combines high resolution and easy automation with modest sample requirements and low solvent consumption (76,77). CE has a very good sensitivity based on mass

detection. This is important when the size of the sample is very limited, as when analyzing a single cell. However, CE is not sufficiently sensitive when based on concentration especially compared to HPLC.

To take full advantage of the separation power of CE for trace analysis of biological samples, detection sensitivity has to be increased. Several highly sensitive detection systems, such as laser-induced fluorescence detectors and electrochemical detectors have been reported (78-80).

Another method is to increase the sample loadability of the system. Electrophoretic analyte-focusing techniques are an elegant way of increasing loadability in CE. These techniques are based on applying local differences in electrical field strength during the injection on focusing step to enable the analyte ions to stack (81-84). Because of complexity of biological samples, it is generally hard to inject them directly into the analytical instrument. Several pre-treatment methods have been carried out to analyze quinolones in biological samples, such as deproteinization (85-87), liquid-liquid extraction (88-90) and solid-phase extraction (SPE) (91-94). SPE was used in the determination of ciprofloxacin, enrofloxacin, and flumequine in pig plasma sample by CE (95). CE was also applied to the separation of ciprofloxacin and sarafloxacin in chicken muscle samples (74). Electrophoresis behavior of six quinolones with piperazinyl substituent has also been studied (96). The simultaneous separation of nine quinolones from biological and environmental samples, using capillary electrophoresis has been reported recently (113).

1.1.6.3. Chromatographic Methods:

Few studies have reported the use of gas chromatography (GC) and thin layer chromatography (TLC) for the analysis of quinolones. GC was used for the determination of nalidixic acid in plasma (97) and drug tablets (98). A GC method was also described for the determination of cinoxacin in capsules (99) and in pharmaceuticals (100). TLC was used for the determination of nalidixic acid in pharmaceuticals and in plasma (101). TLC was proposed for the simultaneous determination of norfloxacin, ciprofloxacin and pefloxacin in urine (102). TLC was also applied to the screening of quinolone residues in milk (103).

High performance liquid chromatography (HPLC) is the most frequently applied technique for the determination of quinolones, because of its specificity, sensitivity, rapidity and robustness (104). There have been numerous reports describing the analysis of single and various combinations of fluoroquinolones in biological fluids, foods and environmental samples using either UV or fluorescence as the method of detection (105-111). An HPLC method describing the simultaneous separation of six fluoroquinolones with fluorescence detection was reported (112).

1.1.6.4. Microbiological methods :

Microbiological inhibition tests are used for the determination of antibiotics. The minimum inhibitory concentrations (MICs) of 63 quinolones was determined against 14 references and clinical strains of the *Mycobacterium avium*-*Microbacterium intracellulare* complex (57). Recently, 27 antibacterial agents including four quinolones (ciprofloxacin,

enrofloxacin, norfloxacin, flumequinone) in milk were detected by specific microbiological method (Eclipse 100) (114).

1.1.6.5. Spectroscopy:

Different spectroscopic methods have been used for the determination of quinolones, among these are:

1.1.6.5.1. UV-Spectroscopy :

Quinolones absorb light in the uv region of the spectrum, and various methods for the determination of quinolones are based on measuring their absorbance in this region. Norfloxacin was determined in capsules by measuring the absorbance of its solution in 0.4 M NaOH at 273 nm (115). Ciprofloxacin was determined in tablets by measuring the absorbance of the sample in dilute HCl at 283 nm. Ciprofloxacin in urine was determined by following its absorbance in 0.01M NaOH at 335 nm (57). UV-spectroscopy was also applied for the determination of naladixic acid (116). Fleroxacin in human serum and in dosage forms was determined by uv-spectrophotometry (117).

1.1.6.5.2. Visible Spectrophotometry:

Quinolones react with metal ions to form colored complexes that can be utilized for their determination. Ciprofloxacin and norfloxacin were determined through their reaction with iron (III) in sulfuric acid media, and measuring the absorbance of the corresponding complexes at 447 and 430 nm respectively (118). Ferric nitrate was also used for the determination of ciprofloxacin (119). A spectrophotometric study on the interaction between norfloxacin and three metal ions (Al^{3+} , Mg^{2+} , Ca^{2+}) was also reported (120).

Spectrophotometric methods were also described for the determination of quinolones through charge transfer complex formation with Π -acceptors. P-benzoquinone and p-nitrophenol are examples of such acceptors (57). Ciprofloxacin, enrofloxacin and pefloxacin were determined through complex formation with three different acceptors, namely; chloranilic acid, tetracyanoethylene and 2,3-dichloro-5,6-dicyano-p-benzoquinone (121).

Quinolones were also determined spectrophotometrically through ion-pair complex formation. Ciprofloxacin was determined by using bromocresol purple or bromophenol blue. Methyl orange and bromothymol blue were also used for ciprofloxacin determination at 425 nm and 410 nm respectively (122).

1.1.6.5.3. Spectrofluorimetry:

Quinolones can be determined by measuring the fluorescence of the native compounds or their derivatives. Moxifloxacin was determined in tablets human urine and serum by measuring its fluorescence at 465 nm after excitation at 287 nm (123). Levofloxacin in pharmaceutical and biological fluids was determined by measuring its fluorescence at 494 nm after excitation at 282 nm (124). Nalidixic acid was determined in urine by measuring its fluorescence at 350/435 nm (125).

Complexation of quinolones with metals to produce fluorescent chelates has been used for the development of fluorimetric methods for the determination of these compounds. Norfloxacin, sparfloxacin and flumequine in their pharmaceutical dosage or in biological fluids were determined through complexation with Al (III)(126-128).

Tb (III) was used for the determination of levofloxacin in tablets and serum (129). Ciprofloxacin and Enrofloxacin in animal tissues were determined by terbium-sensitized luminescence (130). The ternary-complex formation of nalidixic acid with Tb (III) was used for its determination in formulation and biological fluids (131). Spectrofluorimetric methods were developed for the determination of eight quinolone antibacterials, including ciprofloxacin, norfloxacin and nalidixic acid. The methods depend on the chelation of each of studied drugs with zirconium, molybdenum, vanadium and tungsten (132). Recently, spectrofluorimetric methods based on the charge-transfer reaction of certain fluoroquinolones as Π -electron donors were described. Ciprofloxacin, perfloxacin and fleroxacin were determined through transfer reaction with 7,7,8,8-tetracyanoquinodimethane as Π -electron acceptor (133). The fluorescence intensity of the complexes was enhanced in 21-35 fold higher than that of the fluoroquinolones.

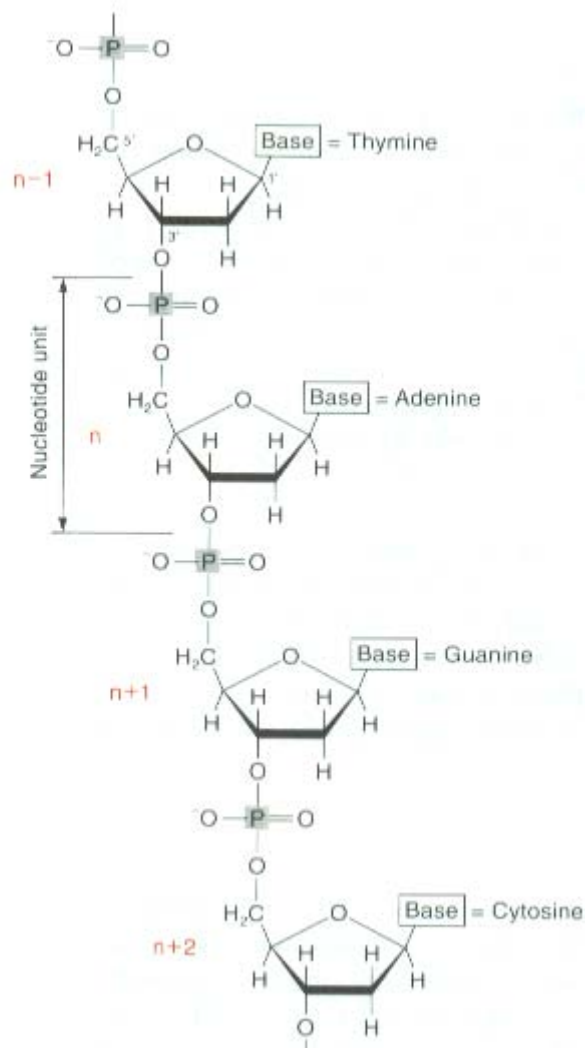
1.2. DNA-Drug Interaction; Biosensors

Nucleic acid plays a critical role as it bears heritage information and guides the biological synthesis of proteins and enzymes, through replication and transcription of genetic information in living cells (134).

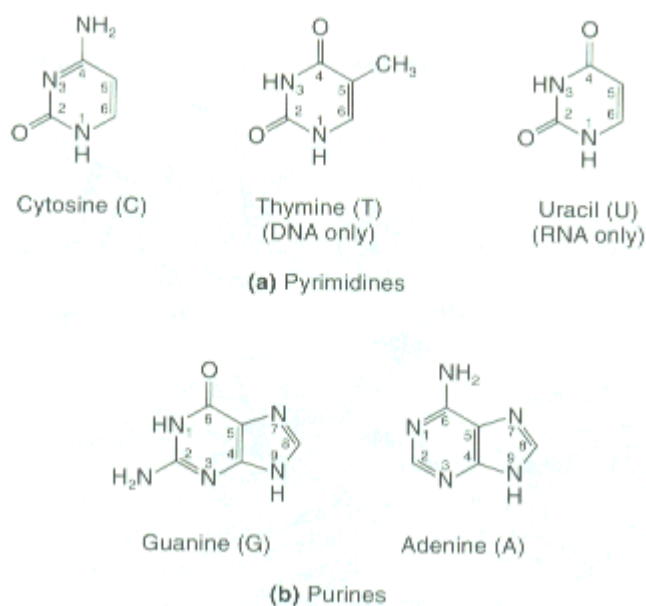
DNA is a polymer of deoxyribonucleotides. As shown in scheme 2, phosphodiester linkages join adjacent residues to form a sugar-phosphate polymer backbone. Linked to each sugar is one of the nucleotide bases, the purines; adenine and guanine, and the pyrimidines; cytosine and thymine. The unit comprising only a sugar and a base is referred to as a nucleoside, whereas nucleotides contain additional 5'- or 3'-phosphate groups.

Schemes 3 and 4 show the structures of the nucleoside bases of DNA and their base-pairing schemes.

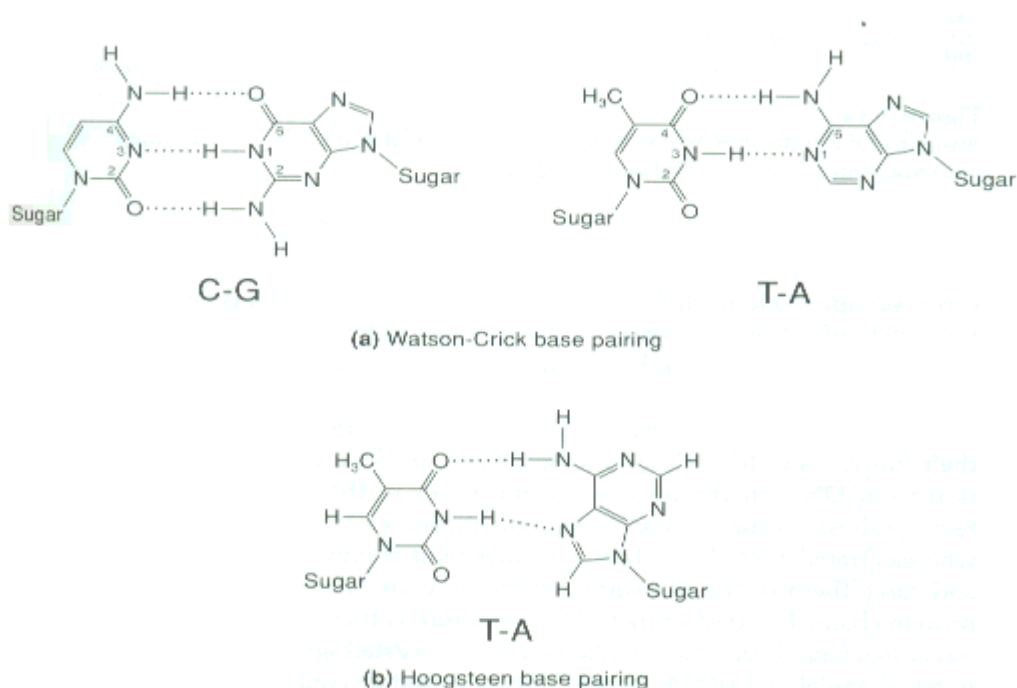
Watson-Crick base-pairing is responsible for linking the two DNA strands into a double helix. An alternative scheme sometimes encountered is Hoogsteen base-pairing which is also shown in scheme 4.



Scheme 2. Structures of the phosphodiester backbone of DNA.



Scheme 3. Chemical structures of nucleoside bases.



Scheme 4. Base – pairing schemes that occur in nucleic acids.

The latter is more Both single- and double–stranded forms of DNA exist, but common and will be discussed. Double–stranded DNA may have one out of three different forms. The structural features of these forms are

illustrated in scheme 5. The structure of the most common, or B-form, of DNA is a right-handed double helix characterized by major and minor grooves, and parallel Watson-Crick base pairs stacked on one another at 3.4 Å spacing. A pitch of 35 Å corresponds to 10.4 base pairs per turn. A second type of DNA is the A-form, having a deep major groove and parallel base pairs that are no more perpendicular to the helix axis. The Z-DNA is a fascinating left-handed variant seen for sequences having alternating stretches of purine-pyrimidine nucleoside, with no deep grooves. Characteristics of the three types are compared in scheme 5.

| | A-DNA | B-DNA | Z-DNA |
|--|-------------------|---------------------|---|
| Shape | Broadest | Intermediate | Most elongated |
| Rise per base pair | 2.3 Å | 3.4 Å | 3.8 Å |
| Helix diameter | 25.5 Å | 23.7 Å | 18.4 Å |
| Screw sense | Right-handed | Right-handed | Left-handed |
| Glycosidic bond | <i>anti</i> | <i>anti</i> | <i>anti</i> for C,T <i>syn</i> for G |
| Base pairs per turn of helix | 11 | 10.4 | 12 |
| Pitch per turn of helix | 25.3 Å | 35.4 Å | 45.6 Å |
| Tilt of base pairs from normal to helix axis | 19° | 1° | 9° |
| Major groove | Narrow and deep | Wide and deep | Flat |
| Minor groove | Broad and shallow | Narrow and deep | Narrow and deep |

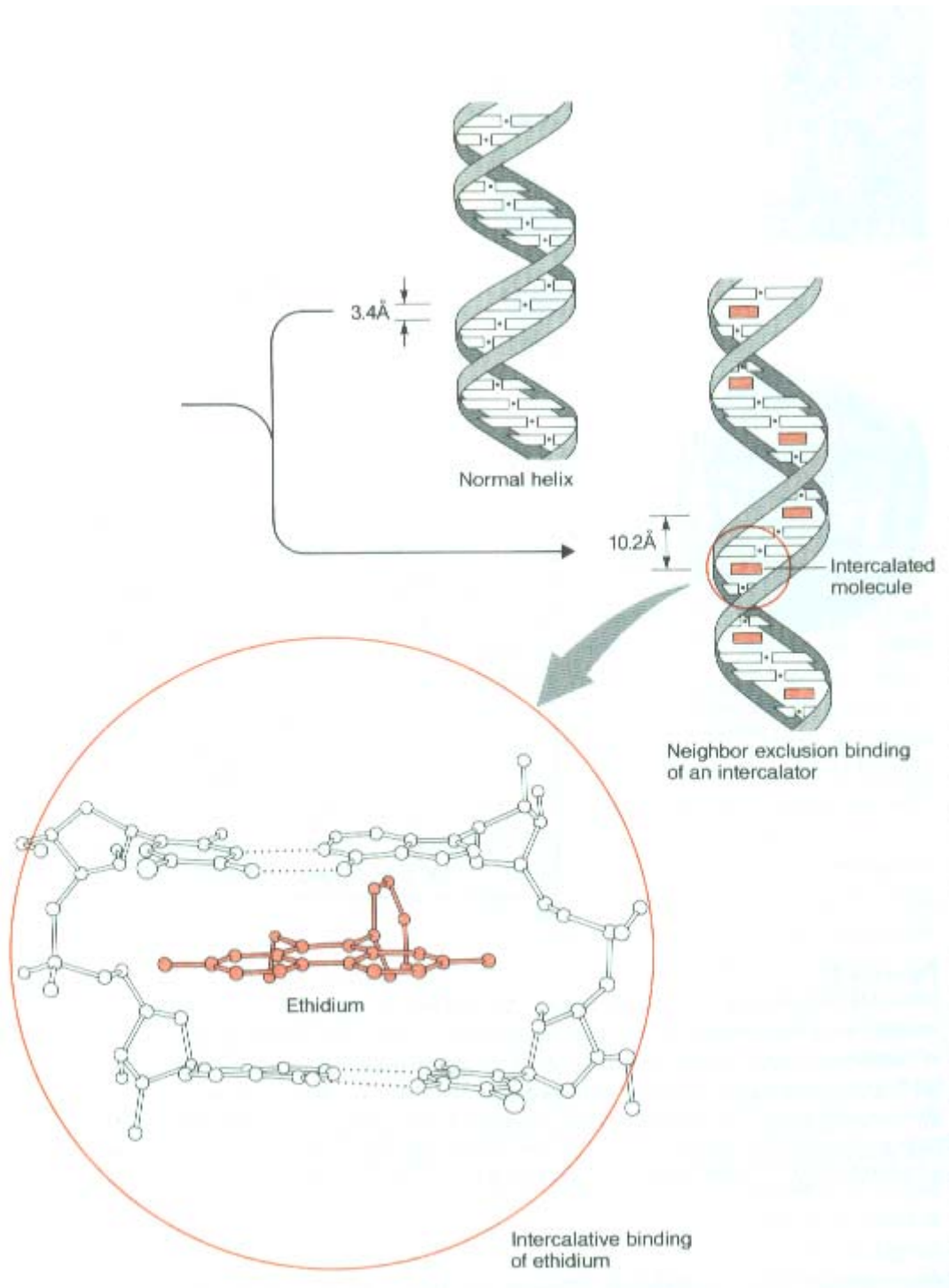
Scheme 5. Structural features and parameters of A-, B-, and Z-DNA.

The interaction of drugs with DNA is one of the most important aspects in drug discovery and development. These interactions are responsible for the desired action of such drugs, but may also lead, at least in part, to the unwanted toxic effects. The binding nature and dynamics of small molecules bind to DNA is an important fundamental issue on life science and is useful in clarifying the structure and function of DNA, understanding the action mechanism of some anti-tumor and anti-viral

drugs and the origin of some diseases. Also, compounds which bind to DNA with high affinity can influence expression of genetic information and therefore, affect cell proliferation and differentiation (135).

Basically, there are different manners for binding to double helical DNA(136): (i) intercalation of the molecule between adjacent base pairs. Fused – ring organic heterocycles such as ethidium bromide bind to duplex DNA by intercalation, occupying every other interbase pair site at saturation (Scheme 6) (137). Direct proof of this “neighbor exclusion” binding model was provided by the X-ray diffraction patterns of polycrystalline DNA fibers containing intercalated platinum terpyridine (hydroxyl ethanethiolate) complex, [Pt(terpy)(HET)]. The platinated sample exhibited a clear 10.2 Å reflections along the meridian in the X-ray diffraction pattern corresponding to the nearest Pt - Pt repeat distance along the helix axis in the intercalated structure.

Other types of binding to DNA include: (ii) non-covalent groove binding interactions involving contact with the inner surface of major or minor groove of DNA double helix (e.g. triostin), (iii) covalent binding (e.g. mitomycin), (iv) cations binding along the outer surface of DNA double helix, via electrostatic interactions with phosphate anions (e.g. dodecyl trimethylammonium bromide).



Scheme 6. Binding to DNA via intercalation.

Following these bindings, changes to both DNA and binder molecules occur, which cause alteration of thermodynamic stability and changes in functional properties of DNA (138).

Many techniques have been reported for studying the interaction between drugs and DNA such as DNA-foot printing (139), nuclear magnetic resonance (NMR) (140,141), mass spectroscopy (MS) (142), spectrophotometry (143), FT-IR and Raman spectroscopy (144-147), molecular modeling (148-150), equilibrium dialysis(151,152), capillary electrophoresis (153-156), surface plasmon resonance (157-159), and electric linear dichroism (160-165).

Electrochemical investigation of drugs-DNA interaction has gained a growing interest in recent years. It can yield a useful complement to other methods and provide a good evidence for the interaction mechanism. Electrochemical approach can also be used for the quantification of these drugs.

Biosensors are small devices, which utilize biological reactions for detecting target analytes (167). A typical biosensor usually consists of three components; a recognition element, a signal transducing structure and an amplification/processing element. A great progress in the development of electrochemical sensors for DNA hybridization and DNA damage, achieved in recent years, suggests that these sensors may soon become important tools in medicine and other areas of practical life of the 21st century. The main advantages of electrochemical devices are their low-cost, fast response, simple design, small dimensions and low power requirements (166). Various transduction mechanisms such as, electrochemical, thermal and optical are employed (168). Depending on

the nature of the recognition element, biosensors are divided into two main types; bioaffinity and biocatalytic devices. The first type depends on the selective binding of the target analyte to a surface confined ligand partner (e.g. antibody and oligonucleotide). In the second type an immobilized biomolecule is used for recognizing the target substance such as sensor strips with immobilized glucose oxidase that are used for personal monitoring of diabetes(169).

Electrochemical DNA biosensors comprise a nucleic acid recognition layer, which is immobilized over an electrochemical transducer. The role of the nucleic acid layer is to detect changes that occur in the DNA structure during interaction with DNA-binding molecules or to selectively detect a specific sequence of DNA. The signal transducer must determine the change that has occurred at the recognition layer due to the binding molecules or due to the hybridization; converting this into an electronic signal which then be relayed to the end user (170). Observing the electrochemical signal related to DNA-DNA interactions or DNA-drug interactions can provide evidence for the interaction mechanism, the nature of the complex formed, binding constant, binding site size and the role of free radicals generated during interaction in the drug action.

The mechanism of interaction between drugs and DNA can be explained electrochemically by studying the behavior of drug in the absence and presence of DNA. Different types of working electrodes may be used such as, carbon paste electrode (CPE) (171-178), glassy carbon electrode (GCE) (179-187), gold electrode (188), hanging mercury drop electrode (HMDE) (189-191), pencil graphite electrode (PGE) (192,193), screen-printed electrodes (SPE) (194), carbon fiber column electrode

(CFCE) and carbon fiber disk electrode (CFDE) (195). The three-electrode system used consists of a working electrode, a reference electrode (Ag/AgCl or saturated calomel electrode) and an auxiliary (Pt-wire) electrode. Different electrochemical techniques can be used for investigating drug-DNA interactions. The most common techniques are cyclic voltammetry (196), square wave voltammetry (197,198), and differential pulse voltammetry (199). The interaction mechanism can be investigated by three different ways; DNA-modified electrode, drug-modified electrode and interaction in solution, these are described below:

1.2.1. DNA – modified electrodes:

To prepare electrochemical DNA sensors, the immobilization of the DNA probe should be considered. Different procedures are used to immobilize DNA on transducer surfaces. The techniques that are used to immobilize double-stranded DNA will be investigated only. Adsorption is the most common method to immobilize dsDNA on surfaces. It does not require reagents or special nucleic acid modifications. The main disadvantage of this method is that the nucleic acid may desorb from the surface due to the hybridization condition. The adsorption of dsDNA can be accomplished by one of the following procedures:

1.2.1.1. Electrochemical techniques:

This kind of immobilization can be used to detect small molecules (drugs, carcinogens, pollutants) that interact with DNA, using the dsDNA as recognition element of affinity biosensors. These molecules interact with dsDNA through either intercalative or electrostatic binding. The DNA biosensing of these molecules consists of three steps; dsDNA immobilization by electrochemical adsorption, analyte interaction and

transduction(200). The probe dsDNA was first immobilized on a carbon surface by polarizing the bare electrode for 1 minute at high potential (+1.8V) (vs. Ag/AgCl) followed by adsorptive accumulation for 2 minutes at +0.5V (vs. Ag/AgCl) in electrolyte containing dsDNA. The dsDNA-coated electrode was then placed in a stirred sample solution of the analyte for a given time(200).

There are two schemes for biosensors to produce electrochemical signals that are concentration dependent. The first includes the detection of non-electroactive analytes through the competitive binding displacement of a redox marker from the DNA- coated surface. The second depends on the changes in the intrinsic anodic (guanine or adenine) signal of the DNA-coated transducer, due to the dsDNA analyte binding event (200).

1.2.1.2. Physical adsorption onto carbon electrodes:

In this method, DNA biosensor is prepared by covering a glassy carbon electrode with a dsDNA solution and leaving the electrode to dry. This sensor is either used directly after being soaked in water for a certain time to remove unadsorbed DNA (194). Otherwise, the DNA-modified electrode is conditioned in a buffer solution at +1.4V for 5 minutes. Afterwardes it is immersed in a solution of single-stranded DNA, where several differential pulse voltammograms are recorded between 0 and +1.4V until stable peak currents are obtained for guanine and adenine oxidation. At this stage, the DNA biosensor reaches the maximum activity for electroanalytical applications (186). This electrode is then used to pre-concentrate drugs on the surface and to study the interaction mechanism of these drugs with DNA by means of cyclic, differential pulse or square wave voltammetry (201,202).

1.2.1.3. Physical adsorption onto conducting polymers:

In this method DNA is immobilized on a glassy carbon electrode previously modified with a polymer (e.g. polypyrrole, PPy) film (203). The polymer modified electrode is prepared by cyclic voltammetric electro-oxidation of aqueous solution of pyrrole. This electrode is immersed in an acid solution of DNA for 1 minute. Then the surface is washed to remove non-adsorbed DNA.

1.2.1.4. Adsorption on gold electrodes:

Gold electrodes are modified by dropping a small volume of DNA solution on their surfaces. This is followed by air drying overnight and rinsing to remove unadsorbed DNA (204).

1.2.1.5. Adsorption on mercury electrodes:

The DNA can be determined and characterized by the hanging mercury drop electrode (HMDE) using adsorptive stripping voltammetry. This can be done by DNA immobilization through a short incubation of an HMDE in a DNA solution. Then DNA transduction in a voltammetric cell containing the background electrolyte. However, it was shown that no significant hybridization takes place at the mercury electrode (205). This is probably because of the strong hydrophobic interaction between the probe bases and the electrode surface. Thus, probe bases are not accessible to form specific base pair with the target DNA approaching from solution. On the other hand, mercury surfaces seem to be suitable for the detection of DNA damage. Nucleic acids are electroactive species that produce well-defined voltammetric peaks reflecting small damage to the double helical DNA. However, the application of the HMDE as part of a hybridization biosensor is rather impractical (206).

1.2.2. Drug-modified electrodes:

In this type of modification, the drug is first immobilized on the electrode surface. The electrochemical signals of the drug are monitored and then the changes in these signals after interaction with DNA are observed. Adriamycin modified glassy carbon electrode was used to study the interaction between adriamycin and DNA. The modified electrode was prepared by immersing a glassy carbon electrode in a 5 μ M adriamycin solution for 10 minutes at a deposition potential of +0.4 V. Afterwards, the electrode was rinsed with deionized water and transferred to DNA solution where voltammetric measurements were performed (185).

1.2.3. Interaction in solution:

For studying the interaction in solution, drug and DNA are placed in the same solution. The changes in the electrochemical signal of drug-DNA complex are compared with the signals obtained for DNA or drug alone in solution (206).

1.3. Chemical Oxidation of Quinolones:

The use of oxidizing agents in attacking particular groups in simple and large molecules has received a great attention. Among these is potassium hexacyanoferrate (III) (207-212), a one electron oxidant with a redox potential of 0.36V. Although hexacyanoferrate (III) has some advantages that make it suitable for the oxidation of several organic substrates (213); in particular, its stability over the entire pH scale and being a moderate oxidant, its reactions with some nitrogen containing compounds are not facile and require the presence of a catalyst (214,215). Osmium tetroxide has been used widely for catalyzing such reactions (216-220).

CHAPTER 2

EXPERIMENTAL

2.1. Interaction of Quinolones with DNA

2.1.1. Reagents and Solutions:

Calf thymus DNA (sodium salt type 1), was purchased from Sigma and was used, as received, without further purification. Solutions of DNA gave ratios of UV absorbance at 260 and 280 nm (A_{260}/A_{280}) of 1.8 – 1.9, indicating that DNA was sufficiently free from protein(221). The concentration of DNA solution expressed in M of nucleotide phosphate (NP), was determined by UV absorbance at 260 nm using molar extinction coefficient (ϵ) of $6600 \text{ cm}^{-1}\text{M}^{-1}$ (221).

Single stranded DNA (ssDNA) solution was prepared by a previously reported method(186). Exactly 3 mg of DNA were dissolved with 0.5 mL of 65% pure perchloric acid, then 0.5 mL of 9M NaOH was added to neutralize the solution. The volume was completed to 10 mL with 0.2M pH 5 acetate buffer solution and the solution was kept at 4°C .

Ciprofloxacin hydrochloride, norfloxacin, Enrofloxacin and nalidixic acid were obtained from Sigma. Stock solutions of 10^{-3} M were prepared by dissolving the appropriate amount of the drug with 1 mL of 0.1M glacial acetic acid and then diluting to the mark of 10 mL volumetric flask with distilled water. The solutions were kept at 4.0°C and used within one week. Acetate buffer (0.2M) solution was used as supporting electrolyte.

2.1.2. Instrumentation:

All voltammetric measurements were carried out using an EG & G polarographic analyzer/stripping voltammeter model 264B coupled with 303A stand, 305 automatic stirrer and RE 0150 X-Y recorder.

All experiments were performed using an electrochemical cell of 10 mL with a three electrode system consisting of a bare glassy carbon electrode (GCE) or a dsDNA-modified glassy carbon electrode (dsDNA-GCE) as a working electrode, a platinum wire as an auxiliary electrode and an Ag/AgCl as a reference electrode. The pH measurements were carried out using HANNA pH meter model HI 8424.

UV-visible spectra were obtained using Shimadzu UV-VIS-NIR Scanning Spectrophotometer, model UV3101PC.

Origin software (vergin 6.1) was used for nonlinear fit analysis of the experimental data (I_p vs. R) based on the chemical equation.

2.1.3. Preparation of dsDNA-GCE:

A glassy carbon electrode (0.071 cm^2) was polished with alumina powder and was then rinsed thoroughly with distilled water. The dsDNA-modified electrode was prepared by a previously established method (186), consisting of covering the GCE surface with 3 mg dsDNA dissolved in 80 μL of pH 5 acetate buffer solution. The electrode was left to dry and then it was placed in an electrochemical cell containing acetate buffer (pH 5) and conditioned at +1.4 V during 5 minutes. Afterwards, it was immersed in ssDNA solution and several differential pulse voltammograms were recorded between 0 and +1.4 V (vs Ag/AgCl) to check that no electrochemical reaction is taking place on the surface of the modified electrode in the supporting electrolyte. The conditioning process was repeated until stable peak currents were obtained for guanine and adenine oxidation. At this stage, the DNA biosensor reached the maximum activity for electrochemical applications (181), and was then dried at room temperature. This procedure is known to lead to the formation of a

relatively thick DNA layer with good conductivity on the electrode surface (222).

2.1.4. Methodology:

2.1.4.1. Interaction of Quinolones with DNA in Solution

A) UV-visible spectroscopy:

The desired concentration of the drug (10^{-5} M) was prepared by placing 100 μ L of the stock (10^{-3} M) drug solution into 10.0 mL volumetric flask. Different volumes (100, 200, 300, 400 and 500 μ L) of 10^{-3} μ M stock dsDNA solution were added to achieve various concentrations (10-50 μ M) of DNA. The volume was then completed to 10.0 mL with acetate buffer solution and absorption spectra were recorded in 1 cm optical path length quartz cell at 25 $^{\circ}$ C.

B) Cyclic Voltammetry:

A volume of 10.0 mL of the buffer solution was pipetted into a clean dry voltammetric cell. Exactly 300 μ L of the stock (10^{-3} M) drug solution and different volumes of stock DNA solution were added to the cell to achieve the required concentrations. The solution was stirred at a slow rate for 1 minute, then cyclic voltammograms were recorded between + 0.20 V and + 1.20 V at a scan rate of 100 mV/s.

2.1.4.2. Interaction of Quinolones with DNA at Electrode Surface:

A dsDNA-GCE was soaked in 10 mL buffer solution containing a certain concentration of the drug. The solution was stirred for a certain time (usually 1 minute) at the selected accumulation potential (usually 0V). Cyclic voltammograms or differential-pulse anodic stripping

voltammograms were then recorded. The modified electrode was regenerated by scanning it in a blank buffer solution until blank voltammograms are obtained. The electrode was stable for one week of constant use.

2.1.4.3. Determination of Ciprofloxacin in Pharmaceutical Formulations

Ciprofloxacin in Ciprocare tablets was analyzed as follows; Five tablets were weighed and grinded to a fine powder. A weight equivalent to one tablet was transferred quantitatively to 500.0 mL volumetric flask and dissolved with 10.0 mL of 0.1 M glacial acetic acid. The volume was then completed to the mark with distilled water and then filtered to remove insoluble additives. Three milliliters of the filtrate were then diluted to 10.0 mL with distilled water. A portion of this solution (100 μ L) was added to a cell containing 10.0 mL buffer solution and differential-pulse voltammograms were recorded. The amount of ciprofloxacin was calculated from a previously prepared calibration curve.

2.1.4.4. Determination of Ciprofloxacin in Urine

Urine sample (3.0 mL) was spiked with 1.0 mL of 10^{-3} M ciprofloxacin solution. A volume of 100 μ L of this solution was added to a cell containing 10.0mL buffer solution and determined as before (section 2.1.4.3).

2.2. Kinetics of Oxidation of Quinolones by $K_3Fe(CN)_6$:

2.2.1. Reagents and Solutions:

Potassium hexacyanoferrate (III) (Riedel-dehaen), osmium tetroxide, ciprofloxacin. HCl, norfloxacin, enrofloxacin and nalidixic acid (sigma)

were used as received. Stock solution of the drug (0.5M) was prepared by dissolving the desired amount of the drug and further dilution was performed using distilled water. The stock solution was kept in the refrigerator at 4.0°C for not more than one week.

2.2.2. Instrumentation:

Absorption measurements and pH measurements were performed using the same instruments in section 2.1.2.

2.2.3. General Procedure for Kinetic Studies:

Kinetics for the oxidation of the quinolones under study were followed spectrophotometrically by measuring the absorbance of potassium hexacyanoferrate (III) with the progress of time at 420 nm.

The desired hydroxide ion concentration was achieved using standard sodium hydroxide solution. Sodium chloride solution was added to adjust the ionic strength of the reaction mixture to the required value. The required volumes of the drug, potassium hexacyanoferrate (III) and the required reagents were added to the reaction flask and mixed well. A portion of the reaction mixture was transferred to the cell and the absorbance was recorded at appropriate intervals right after mixing.

CHAPTER 3

RESULTS AND DISCUSSION

3.1. Interaction of Quinolones with DNA in Solution:

The interaction of the studied quinolones with DNA in solution was studied by UV-visible spectroscopy and cyclic voltammetry at a bare glassy carbon electrode. UV-visible spectroscopy is useful to explore the nature of binding between quinolones and DNA, and to estimate the magnitude of the binding constant (K). On the other hand, cyclic voltammetry provides a more detailed picture about the type of interaction between the studied quinolones and DNA. Several parameters describing the interaction of the studied drugs with DNA such as, diffusion coefficients (D_f , D_b), binding constant (K), and the binding site size (s) were calculated by analyzing the experimental data.

3.1.1. UV-Visible Spectroscopy:

The interaction of ciprofloxacin (CIP), norfloxacin (NOR), enrofloxacin (ENR), and nalidixic acid (NAL) with dsDNA in solution was studied by UV-visible spectroscopy. Figures (1-4) show the absorption spectra of the four quinolones in the absence and in the presence of various concentrations of dsDNA at pH 5 acetate buffer solution. A continuous decrease in the absorbance maxima of the four drugs was observed with the gradual increase in the concentration of DNA in solution. This hypochromic effect is probably due to the interaction between the electronic states of the intercalating drug chromophores and those of the DNA bases (223). The strength of this electronic interaction is expected to decrease as the distance of separation between the chromophore and DNA bases increases(224). The apparent hypochromism observed suggests a close proximity of the quinolone chromophores to the DNA bases. In addition, a small red shift was observed for the maxima of the drugs with

the addition of DNA. This is explained by assuming that the drugs might slide into the base pairs of DNA upon binding, and thus preventing the formation of hydrogen bonding with the solvent water molecules. The hypochromic effect and the red shift in UV-visible spectra upon binding to DNA are considered as indications of an intercalating mode of interaction(225).

Based on variations in absorption spectra of the studied quinolones upon binding to DNA, the binding constant, K, was calculated from the equation (226):

$$A_0/(A-A_0) = \epsilon_G/(\epsilon_{H-G} - \epsilon_G) + \epsilon_G/(\epsilon_{H-G} - \epsilon_G) \times 1/K[\text{DNA}] \quad (1)$$

Where:

A_0 : Absorbance of drug in the absence of DNA.

A : Absorbance of drug in the presence of DNA.

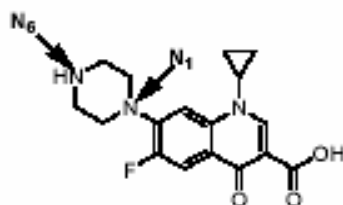
ϵ_G : Absorption coefficient of drug.

ϵ_{H-G} : Absorption coefficient of drug-DNA complex.

Using absorbance data present in Figures (1-4) and Tables (1-4), the plot of $A_0/(A-A_0)$ versus $1/[\text{DNA}]$ was linear as shown in Figure (5). From the slopes and intercepts of the straight lines obtained, the values of the binding constants were calculated and tabulated in Table (5). The values of K obtained indicate that these drugs have certain affinities toward DNA.

The results in Table (5) reveals that norfloxacin and ciprofloxacin have higher binding constant values than those of enrofloxacin and

nalidixic acid. The former quinolones (CIP and NOR), differs only in the substituent (cyclopropyl versus ethyl) at the nitrogen atom of the aromatic heterocyclic ring.



The fact that ciprofloxacin and norfloxacin have comparable binding constant values suggests that the piperazine ring plays an important role in binding to DNA. This explains the small K value of nalidixic acid. The smaller K value of enrofloxacin compared to that of ciprofloxacin and norfloxacin, may be explained by the increased steric hindrance of the ethyl group at the outer nitrogen (N_6) of the piperazine ring in enrofloxacin compared to hydrogen atom in ciprofloxacin and norfloxacin. In addition, the absence of the hydrogen atom of the outer nitrogen (N_6) of the piperazine ring prevents the formation of a hydrogen bonding between enrofloxacin and DNA. Both factors are expected to weaken the binding of enrofloxacin to DNA, and hence, a smaller K value is obtained. However, larger values of K (ca 10^4 - 10^5 M^{-1}) were obtained for molecules that bind strongly to DNA such as anti tumor drugs (227,228).

3.1.2. Cyclic Voltammetric Studies:

Cyclic voltammograms of the various quinolones, both in the absence and presence of dsDNA at a bare glassy carbon electrode in acetate buffer (0.2 M, pH 5.0) are presented in Figures (6-8). Ciprofloxacin, norfloxacin and enrofloxacin showed a single anodic peak, which corresponds to the oxidation of these compounds, most probably at the

piperazine moiety (69,177,229). In the reverse scan no cathodic peaks were observed, this indicates an irreversible process. No oxidation peaks were observed for nalidixic acid which lacks the piperazine ring under the present conditions (figure not shown). This confirms that oxidation occurs, as suggested above, at the piperazine ring.

Addition of calf thymus dsDNA to a solution of the quinolone, caused a marked decrease in the peak current height and a shift of the peak potential to more positive values as shown in Figures (6-8). This might be attributed to the binding of the quinolones to the bulky and slowly diffusing DNA, which results in a considerable decrease in the apparent diffusion coefficient. The shift of peak potential to more positive values indicates that these drugs have properties of intercalative binders (230). In order to demonstrate that the decrease in current was due to the slow diffusion rate of quinolone - DNA complex, and not to the increased viscosity of the solution or the blockage of the electrode surface by DNA adsorption, a special cyclic voltammetry experiment was performed in $K_4Fe(CN)_6$ solution in the absence and also in presence of DNA. In these solutions, the ions of $Fe(CN)_6^{4-}$ do not interact with DNA because of the coulombic repulsions between their negative charges. Figure (9) shows that the addition of DNA to $Fe(CN)_6^{4-}$ solution affected the current only slightly and no shift of peak potentials was observed. This confirms that there is no obvious effect on diffusion from the changed viscosity of the solution. This indicates also that there is no significant obstruction of the electrode surface from DNA adsorption. Thus the great decrease in current in CV experiments (Figures 6-8), can be attributed to the diffusion of the drug bound to DNA with large molecular weight.

The change in current and shift in potential upon DNA addition can be used to quantify the binding of the studied quinolones to DNA. The association of an electroactive molecule (EM) with a binding site (S) composed of s base pairs on a DNA duplex, to form a complex (EM-S) can be expressed as:



The equilibrium constant of this reaction is given by:

$$K = C_b / (C_f C_s) \quad (3)$$

Where, K is the equilibrium constant of the EM-S complex, and C_b , C_f and C_s are the equilibrium concentrations of EM-S, free EM and free S, respectively. The total concentration of the electroactive molecule, C_t , is given by the equation:

$$C_t = C_b + C_f \quad (4)$$

The total concentration of binding sites, $C_{NP} / 2s$, along a DNA duplex can be expressed as follows:

$$C_{NP} / 2s = C_b + C_s \quad (5)$$

Where, C_{NP} is the concentration of nucleotide phosphate, which is determined by UV spectrometry at 260 nm, and s is the binding site size (base pairs, bp) of the electroactive molecule interacting with DNA. It means the number of DNA base pairs occupied (or covered) by a binding molecule.

The ratio of the nucleotide phosphate concentration and the total concentration of electroactive molecule can be defined as R :

$$R = C_{NP} / C_t \quad (6)$$

R is varied when cyclic voltammetric experiments are carried out. For an irreversible reaction at 25°C, the total anodic current (I_p) with any R can be calculated by (231):

$$I_p = B [(\alpha n)_f^{1/2} D_f^{1/2} C_f + (\alpha n)_b^{1/2} D_b^{1/2} C_b] \quad (7)$$

Where, $B = 2.99 \times 10^5 n A \nu^{1/2}$.

α : electron transfer coefficient

n : no. of electrons.

A : electrode surface area.

Making appropriate substitutions of C_f and C_b an equation for I_p is obtained (180):

$$I_p = B \{ (\alpha n)_f^{1/2} D_f^{1/2} C_t + [(\alpha n)_b^{1/2} D_b^{1/2} - (\alpha n)_f^{1/2} D_f^{1/2}] [b - (b^2 - 2K^2 C_t^2 R/s)^{1/2}] / (2K) \} \quad (8)$$

Where; $b = 1 + KC_t + KRC_t/(2s)$.

The above equation is valid for the assumption of non-cooperative, non-specific binding to DNA with the existence of one type of discrete binding site. The diffusion coefficients of EM and EM-DNA (D_f , D_b), the binding constant (K) and the binding site size (s) of EM-DNA can be obtained by non-linear fit analysis of the experimental data (I_p and R) according to the above equation.

The peak currents (I_p) of the studied quinolones and quinolone - DNA complexes were examined as a function of scan rate (ν). The results

are shown in Tables (6-8). The plots of I_p vs $v^{1/2}$ for both the free and bound quinolones are shown in Figures (10-12). The plots were linear for both free and bound quinolones indicating an irreversible electrode process without surface adsorption. This means that the oxidation process was controlled by of the electroactive species to the electrode surface(231). Furthermore, the smaller linear slope of quinolone-DNA complex demonstrates that the quinolone can bind with DNA in solution, forming quinolone-DNA adduct with large molecular weight, resulting in a considerable decrease in the apparent diffusion coefficient (232).

The relationship between E_p and $\ln v$ over the studied range (0.005 - 0.1 V) was plotted for quinolones and quinolone-DNA complexes according to the classical equation of peak potential for an irreversible electrode process (233):

$$E_p = E^{o'} + RT/(anF) \{0.780 + 0.5 \ln [anDFv/(RT)] - \ln k^o\} \quad (9)$$

Where;

$E^{o'}$: the formal electrode potential.

α : electron transfer coefficient.

k^o : the standard heterogeneous rate constant.

R: universal gas constant = 8.3145 J/mol.K

F: Farady = 96,485 coulomb.

D: diffusion coefficient.

According to the above equation the relation between E_p and $\ln v$ should be linear. The plots of E_p versus $\ln v$ are presented in Figures (13-

15) . The values of αn can be obtained from the slope of the straight lines. In the absence of DNA, the slopes of E_p vs $\ln v$ for ciprofloxacin, norfloxacin, and enrofloxacin were 0.0237, 0.0218 and 0.019 respectively. The values of αn were calculated to be 0.541, 0.588, and 0.675 respectively.

In the presence of DNA the slopes of E_p vs $\ln v$ for ciprofloxacin, norfloxacin, and enrofloxacin were 0.0132, 0.0139 and 0.0092 respectively. The values of αn were calculated to be 0.972, 0.923, and 1.395 respectively.

The results of the CV experiments in the drug solution at various concentrations of DNA are summarized in Tables (9-11). A non linear fit analysis of the data to equation (8) yielded the binding curves shown in Figures (16-18). The diffusion coefficients of both free and bound ligands (D_f , D_b), the binding constant (K) and the binding site size (s) were simultaneously obtained by non-linear fit analysis of the electrochemical data. These parameters are shown in Table (12).

The results illustrate that the quinolones under study bind to dsDNA. Ciprofloxacin and norfloxacin bind to DNA more strongly than enrofloxacin as can be concluded from the binding constant values. However, the binding constant values for the quinolone–DNA complex (10^5) are smaller than those obtained for molecules that are known to bind strongly to DNA such as anti-tumor drugs ($K \geq 10^7$) (180,230,232). This indicates a weaker binding between quinolones and DNA.

The type of interaction between the studied quinolones and DNA cannot be judged easily. The calculated binding site size (s) is a fraction for the studied drugs (0.07 – 0.11). This indicates that these drugs cannot

be considered as typical intercalators. The positive shift in oxidation potentials for the drugs upon binding to DNA, suggests that intercalative properties of these drugs cannot be ruled out completely. On the other hand, the small values of the binding constants and binding site size require a non–intercalative (electrostatic) mode of interaction with DNA.

Mechanism of Interaction Between Quinolones and DNA:

The mechanism of interaction between quinolones and DNA is not yet fully understood. A great deal of contrast has introduced into the literature about the manner in which these drugs can bind to DNA. In this study, an effort is made to combine the outcome of electrochemical techniques with other reported methods in order to give a better understanding of the mode of interaction between quinolones and DNA.

¹H NMR studies were used to prove the existence of predominantly minor groove ciprofloxacin–duplex interactions, and to excluded classic intercalation between ciprofloxacin and DNA (11). Other NMR studies suggested that norfloxacin exhibits both an intercalation–like interaction and non–specific groove binding to DNA (140).

Electric linear dichroism showed that norfloxacin is capable of interacting with DNA via both minor and major groove contacts (164). However, another study using the same technique excluded the groove binding mode or surface binding of norfloxacin (165).

UV–melting curves and fluorescence emission spectra suggested that ciprofloxacin has at least two different binding modes; a non–specific binding to DNA molecules, which is electrostatically driven, and a specific non–electrostatically controlled binding. The effect of ciprofloxacin on the

change in intrinsic viscosity suggested that ciprofloxacin has the properties of an intercalative binder (234).

The results obtained in this study can contribute with the following conclusions:

(i) binding between the studied quinolones and dsDNA does exist, as can be concluded from the binding constant (K) values obtained by uv-visible spectrometry and cyclic voltammetry.

(ii) the small value of the binding constants (compared to other typical intercalators) and the very small binding site size (*s*), favors non-intercalative or at least partial-intercalative binding to DNA.

(iii) the hypochromic effect, along with the red shift in absorbance maxima of the studied drugs, upon binding to DNA, supports an intercalative mode of interaction.

(iv) the positive shift in oxidation potential for the studied drugs upon binding to DNA, requires intercalative binding between the studied drugs and dsDNA.

(v) the results are obtained for *in vitro* experiments, which may not necessarily be representative for *in vivo* experiments.

(v) other factors that may favor one type of binding over the other are needed to be studied in more details in order to give a better understanding of the mode of interaction between the studied quinolones and DNA.

(vii) Regarding the results of this study, it can be concluded that electrostatic interaction with partial intercalation is the most probable mechanism of interaction between the studied quinolones and DNA.

3. 2. Interaction of Quinolones with DNA at the Electrode Surface:

Cyclic voltammetry and differential-pulse anodic stripping voltammetry, were used for investigating the electrochemical oxidation behavior of fluoroquinolones at the DNA-modified glassy carbon electrode, as a potential biosensor for the determination of these drugs.

A). Cyclic Voltammetry:

Cyclic voltammograms obtained after the accumulation of the quinolone at a bare glassy carbon electrode and dsDNA-modified glassy carbon electrode, from $1.0 \times 10^{-5} \text{M}$ quinolone in acetate buffer solution for 1.0 min at open circuit conditions are shown in Figures (19-21).

For both types of electrodes (i.e. bare and DNA-modified glassy carbon electrodes), one wave was observed in the forward scan and no waves were obtained in the reverse direction, which characterizes irreversible electrode processes.

A comparison between the current response for the drug on bare and DNA-modified glassy carbon electrodes (Figures 19-21) shows that the DNA-modified electrodes exhibit a larger anodic signal for the oxidation of ciprofloxacin, norfloxacin and enrofloxacin. This behavior reflects the binding of the studied drugs with surface-confined DNA layer. The presence of the nucleic acid coating at the glassy carbon electrode surface greatly enhances the sensitivity for the studied drugs. In addition, the DNA-modified glassy carbon electrode showed a shift in the oxidation wave of the studied drugs to less positive potentials.

B). Differential-Pulse Anodic Stripping Voltammetry:

Differential-pulse anodic stripping voltammograms of ciprofloxacin at a bare GC electrode and DNA-modified GC electrode are shown in

Figure (22). In addition to the ability of the modified electrode to pre-concentrate the studied drugs, a better peak shape was obtained at the DNA-modified electrode as compared to the unmodified GC electrode.

The effect of several factors on the electrochemical behavior of the studied quinolones at DNA-modified glassy carbon electrodes was studied using differential-pulse anodic stripping voltammetry as discussed below:

3.2.1. Effect of Scan Rate:

The effect of scan rate (v) on the peak current of 1.0×10^{-5} M of the drug was examined using differential-pulse anodic stripping voltammetry. Figure (23) shows the voltammogram obtained for ciprofloxacin at different scan rates. The relation between peak heights and scan rate is presented in Figure (24). A linear plot of peak current versus scan rate is obtained within the studied range (10 - 100 mV/s) for the studied drugs at dsDNA-modified GC electrode. The peak potential (E_p) shifts toward more positive values with increasing scan rate for the oxidation of ciprofloxacin, norfloxacin and enrofloxacin. This is expected for an irreversible electrode process.

3.2.2. Effect of pH:

The influence of pH on the oxidation of ciprofloxacin, norfloxacin and enrofloxacin was investigated. Figure (25) shows differential - pulse anodic stripping voltammograms for ciprofloxacin at various pH values. A plot of peak currents versus pH (Figure 26) shows that the peak current is maximum in the pH interval 3.5 - 5.0.

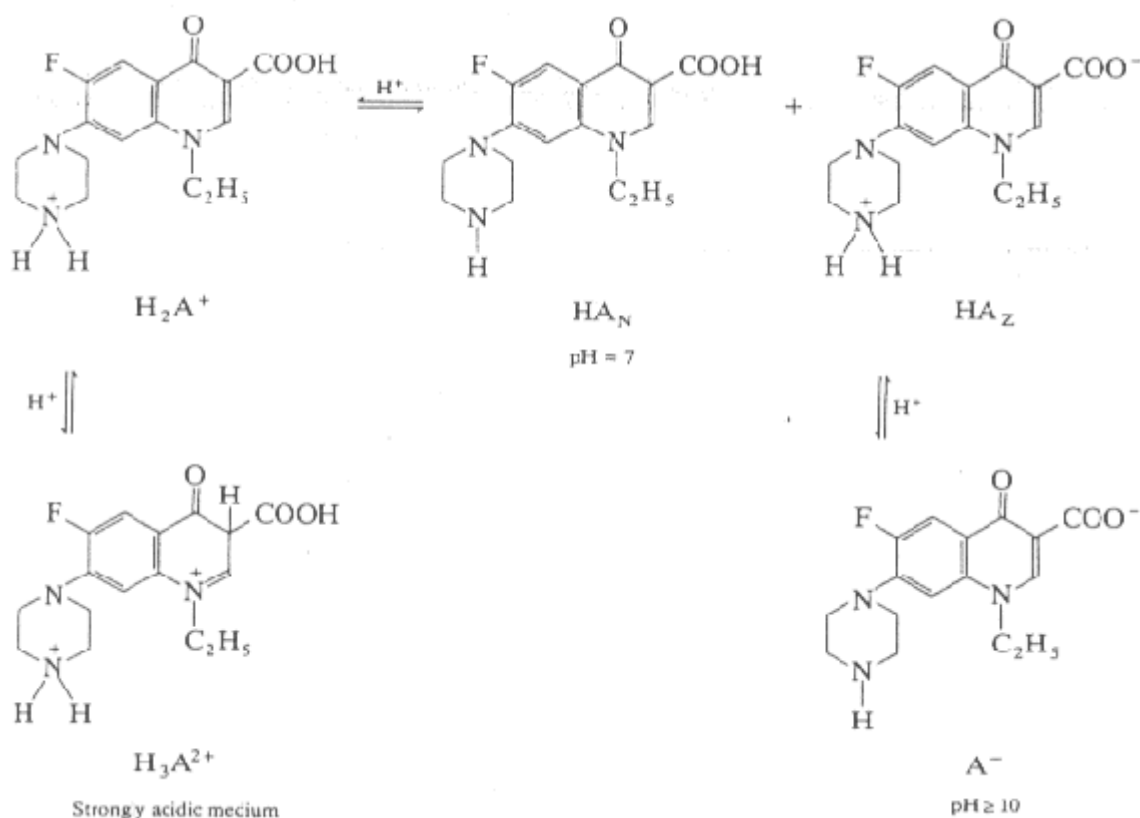
The fluoroquinolones under study possess two ionizable functional groups; a carboxylic group and a basic piperazinyl group. Ciprofloxacin,

norfloxacin and enrofloxacin can exist in four possible forms; cations, neutral unionized species, zwitterions and anions depending on the given pH. The acid–base equilibria for norfloxacin in aqueous media are indicated in scheme (7).

Considering the electrostatic attachment, one can expect that the cationic form that exists at acidic pH binds more strongly than the other forms present at neutral and basic pH values.

The peak currents are attributed to the irreversible oxidation of the piperazine moiety of the studied fluoroquinolones (69,177). The number of electrons transferred per molecule was calculated to be two for similar molecules containing the piperazine moiety (229).

For the quinolones under study, it was found that the peak potentials shift to less positive values with increasing pH, and the peak heights decrease markedly at $\text{pH} \geq 7.0$.



Scheme 7. Acid – Base equilibria for norfloxacin in aqueous media.

3.2.3. Effect of Accumulation Time:

The effect of accumulation time on the current response was examined at the dsDNA-modified electrode. The binding of the studied drugs to dsDNA depends on the accumulation time. Differential-pulse anodic stripping voltammograms for ciprofloxacin at different accumulation times are shown in Figure (27). The dependence of peak heights on the accumulation time for 1.0×10^{-5} M of the drug in acetate buffer (0.2 M, pH 5) at a dsDNA-modified glassy carbon electrode is presented in Figure (28). These results show a current increase within 30 s for ciprofloxacin and a leveling off at longer accumulation times. For norfloxacin and enrofloxacin the peak height increased up to 60 s then leveled off after.

3.2.4. Effect of Accumulation Potential:

The effect of accumulation potential on the oxidation of 1.0×10^{-5} M of the drug was examined at the dsDNA-modified electrode using differential-pulse anodic stripping voltammetry. Figure (29) shows the voltammograms obtained for ciprofloxacin at different accumulation potentials. The relation between peak heights and accumulation potential is presented in Figure (30). The peak currents for ciprofloxacin, norfloxacin and enrofloxacin are affected only slightly within the studied potential range (-0.6 - +0.6 V). Thus, open circuit accumulation was chosen for conducting analysis of the present work.

3.2.5. Effect of Ionic Strength:

The interaction of the studied quinolones with dsDNA immobilized at the glassy carbon electrode was investigated under different ionic strength conditions. Figure (31) shows the differential - pulse peak currents for the studied drugs at various concentration of NaCl. The peak current response for ciprofloxacin, norfloxacin and enrofloxacin decreased with increasing the ionic strength. This suggests that these compounds bind to the double helix of DNA by a combined effect of intercalative and electrostatic interaction with the anionic phosphate moieties. It may be assumed that the positively charged drug molecules are electrostatically attached to the negatively charged phosphate backbone of dsDNA at low ionic strength conditions. This interaction overcomes the intercalative interaction. At higher ionic strength, the drugs start to intercalate between the double helix because the ionic shielding of the negative charges on the DNA is established. In solutions of high ionic strength, where electrical

neutrality is ensured, the anodic signal decreases, which indicates that less drug molecules associate with dsDNA.

3.2.6. Effect of Pulse Amplitude:

The effect of pulse amplitude on the oxidation of 1.0×10^{-6} M ciprofloxacin at the modified glassy carbon electrode was investigated and illustrated in Figure (32). It was found that the peak current increases as the pulse amplitude increases. On the other hand, the peak potential is shifted to less positive values as pulse amplitude increased in the anodic direction.

3.2.7. Effect of Quinolone Concentration:

The effect of drug concentration on the oxidation of the studied quinolones at the modified glassy carbon electrode was investigated. Differential-pulse anodic stripping voltammograms for different concentrations of ciprofloxacin are illustrated in Figure (33). The dependence of the differential-pulse peak current on the studied quinolones' concentration at a dsDNA-modified glassy carbon electrode as well as at the bare glassy carbon electrode is shown in Figures (34-36). The relationship between the peak current and ciprofloxacin concentration was found to be linear over the range 1.0–10.0 μ M, with a slope of 0.716 μ A/ μ M and intercept of 1.26 μ A. The detection limit (based on standard deviation) was calculated to be 1.17×10^{-7} . The precision of the method was determined from five repeated measurements of the peak height of 1.0×10^{-6} M drug. The percentage relative standard deviation (%RSD) was calculated to be 2.05%.

The relationship between the peak current and norfloxacin concentration (Figure (35)) was found to be linear over the same range; 1.0–10.0 μM , with a slope of 0.897 $\mu\text{A}/\mu\text{M}$ and intercept of 1.40 μA . The detection limit was calculated to be 9.30×10^{-8} . The percentage relative standard deviation (%RSD) was calculated to be 1.44%.

The relationship between the peak current and enrofloxacin concentration (Figure 36) was found to be linear over the range 1.0– 9.0 μM , with a slope of 0.713 $\mu\text{A}/\mu\text{M}$ and intercept of 1.40 μA . The detection limit was calculated to be 1.14×10^{-7} . The percentage relative standard deviation (%RSD) was calculated to be 2.16%.

The relation between peak currents and the concentration of the studied drugs was also investigated at the bare glassy carbon electrode. The results are shown in Table (13).

3.2.8. Analytical Applications:

The DNA-modified glassy carbon electrode as a biosensor was applied for the determination of ciprofloxacin as a representative of the studied fluoroquinolones both in tablets and in urine.

A). Analysis of Pharmaceutical Samples:

The validity of the method for the determination of ciprofloxacin by differential-pulse voltammetry at a dsDNA-modified glassy carbon electrode was examined by assaying ciprofloxacin in the commercially available Ciprocare tablets (250 mg/tablet) according to the procedure described in section (2.1.4.3). The quantitative determination of ciprofloxacin was based on the linear correlation between the peak currents and ciprofloxacin concentration.

The optimum conditions for analysis were, pH 4 (acetate buffer), 60 s accumulation time, 10 mV/s scan rate, open circuit, and 50 mV pulse height. These parameters were chosen according to the best peak definition and reproducibility of measurements.

Analysis of five different drug samples using the previously constructed calibration curve (Figure 34), gave a mean recovery of 96.70 % of Ciprocare tablet, with RSD of 1.95 %. Figure (37) shows the reproducibility of the method (three of five measurements are shown).

B). Analysis of Urine:

Ciprofloxacin in urine was determined with reference to a re-established calibration curve (section 2.1.4.4). Analysis of five different dilute samples of urine showed a mean recovery of 94.5 % of the spiked urine samples. The RSD was determined to be 6.55 %. The reproducibility of the method is shown in Figure (38).

The proposed method of analysis is sensitive and accurate, so it can be used for the determination of the studied drugs in pharmaceuticals as well as biological fluids (urine), since it combines good detection limits with relatively short time and inexpensive instrumentation.

3.3. Kinetics of Oxidation of Quinolones by Hexacyanoferrate:

The rate of oxidation of quinolones (NAL, CIP, NOR and ENR) by $K_3Fe(CN)_6$ was investigated by following the absorbance of $K_3Fe(CN)_6$ at 420 nm versus time. Alkaline hexacyanoferrate (III) showed almost no reaction with the studied quinolones in the absence of the catalyst. The absorbance versus time plots were linear for the oxidation of the fluoroquinolones (CIP, NOR, and ENR) by $K_3Fe(CN)_6$ in alkaline medium

catalyzed by osmium tetroxide, indicating that the order of reaction with respect to $K_3Fe(CN)_6$ is zero. Nalidixic acid showed no reaction with $K_3Fe(CN)_6$ even in the presence of the catalyst. This suggests that piperazine ring is the active site for oxidation of fluoroquinolones (FQ) by hexacyanoferrate (III). The same behavior was observed in the electrochemical oxidation of these compounds.

The rate of reaction of FQ's with $K_3Fe(CN)_6$ was represented by the negative slope of the straight absorbance versus time lines obtained. The reproducibility of the pseudo-first-order rate constant (k) from replicate runs was within $\pm 3\%$. The dependence of the reaction rate on various parameters was investigated. These parameters included concentration of reactants, catalyst, hydroxide ion, potassium hexacyanoferrate (II) and other salts, as well as temperature.

3.3.1. Dependence on reactants concentration

Kinetics were followed out at various initial concentrations of the desired reactant while keeping other parameters constant. The order of reaction with respect to each reactant is represented by the slope of the straight lines obtained from the plot of logarithms of the rates versus logarithms of the corresponding initial concentrations.

The dependence of the reaction rate on FQ concentration is represented in Table(14) and Figure(39). It was found that the rate increases with increasing the initial concentration of FQ. The order of reaction with respect to FQ was found to be nearly unity (0.916 for CIP, 0.986 for NOR and 0.913 for ENR).

Comparison of the reactivities of the FQ's points out to the inner nitrogen (N_1) of the piperazine ring to be the rate-limiting reactive site. For example, CIP and NOR differ only in the substituent (i.e., cyclopropyl versus ethyl) at the nitrogen atom of the aromatic heterocyclic ring. The fact that CIP and NOR have comparable reactivities suggests that the reaction center is unlikely associated with nitrogen atom of the heterocyclic ring. ENR differs from CIP only in its ethyl substituent at the outer nitrogen (N_6) of the piperazine ring. However, the rates of these two compounds are comparable (even a slower rate is observed for ENR). The rate of oxidation of aliphatic amines was found to follow the order; primary < secondary < tertiary owing to the increased basicity of nitrogen atom of the amine. Tertiary amines reacted at an average 4-fold faster rate than secondary amines(235). If the rate-limiting step was associated with the outer nitrogen atom (N_6), then ENR (a tertiary amine) would react faster than CIP (a secondary amine)- a scenario that was clearly not observed in the experiments.

The reactions followed zero-order dependence on potassium hexacyanoferrate (III) concentration as shown in Table (15) and Figure (40).

The effect of osmium tetroxide on the reaction rate is shown in Table (16) and Figure(41). It was found that the rate of reaction is directly proportional to the concentration of OsO_4 . The order of reaction with respect to OsO_4 was found to be about one for the studied FQ's. Species such as OsO_4 , $[OsO_4(H_2O)_2]$, $[OsO_4(H_2O)(OH)]^-$ and $[OsO_4(OH)_2]^{2-}$ coexist in fast equilibria with each other, as different forms of Os (VIII), in basic medium(218). Since the present reaction medium is strongly basic, then the total $[Os(VIII)]$ can be assumed as $[OsO_4(OH)_2]^{2-}$ (218).

The dependence of the rate on initial hydroxide ion concentration is given in Table (17) and Figure (42). It was found that the rate increased slightly with increasing the hydroxide ion concentration in the reaction medium.

3.3.2. Effect of added salts

The reaction of FQ's with $K_3Fe(CN)_6$ in the presence of OsO_4 was carried out at different concentrations of potassium hexacyanoferrate (II). It was found that the rate decreases with increasing the concentration of $K_4Fe(CN)_6$ as shown in Table (18) and Figures (43-45). This indicates that $Fe(CN)_6^{4-}$ is involved in a reversible step that could affect the rate determining step.

Addition of different potassium salts to keep a constant ionic strength has no effect (within experimental error) on the reaction rates for the studied FQ's, as shown in Table (19) and Figures (46-48).

Addition of chlorides showed that sodium and potassium have no specific effect on the rate, whereas ammonium has. Being acidic, ammonium ion consumes some OH^- and thus affects the production of the assumed active form of the catalyst $[OsO_4(OH)_2]^{2-}$. The resulting ammonia could also inhibit the reaction through the formation of a complex with Os(VIII), *per say*, $[OsO_4(NH_3)_2]$.

3.3.3. Thermodynamic parameters

The activation parameters of the catalyzed reaction between the studied fluoroquinolones and $Fe(CN)_6^{3-}$ were calculated by carrying out the reaction at different temperatures (Table 23). Using the experimental rate equation:

$$\text{Rate} = k[\text{FQ}][\text{OsO}_4] \quad (11)$$

The rate constants were calculated at these different temperatures (Tables 20-22).

The energy of activation was calculated according to Arrhenius equation:

$$K = A e^{-E_a/RT} \quad (12)$$

Where;

k: specific rate constant

A: frequency factor

E_a: energy of activation

R: gas constant

T: absolute temperature

The plot of lnk versus 1/T (Figure 49) was linear with a slope of - E_a/RT, hence E_a was calculated. The entropy [ΔS*], the enthalpy [ΔH*] and the free energy [ΔG*] of activations were calculated from the following relations respectively (236):

$$\text{Log}(k/T) = \text{Log}(k_B/h) + \Delta S^*/4.57 - E_a/4.57T \quad (13)$$

Where k, T and E_a have the same significance as before.

h: Plank's constant = 6.625X10⁻²⁷ erg. sec

k_B: Boltzman constant = 1.381X10⁻¹⁶ erg. deg

$$\Delta H = E_a - RT \quad (14)$$

And

$$\Delta G = \Delta H - T\Delta S \quad (15)$$

The positive values of ΔS^* indicates that the transition states are less ordered than the reactants. The constancy of ΔG^* values indicates a common mechanism of oxidation for the FQ's studied.

CHAPTER 4

CONCLUSIONS AND FURTHER WORK SUGGESTIONS

4.1. CONCLUSIONS

The following conclusion can be drawn from the results of this work:

4.1.1. Interaction of FQ's with DNA in Solution

- 1) A hypochromic effect and a red shift was observed in the UV absorbance maxima of the studied FQ's upon addition of DNA. This suggests an intercalative mode of interaction.
- 2) The positive shift in the oxidation potential of the studied FQ's upon binding to DNA also supports an intercalative mode of interaction.
- 3) The small values of the binding constants (K) for the drug-DNA complexes, obtained by CV and UV-visible spectroscopy, in addition to the small site size (s), favored non-intercalative or partial intercalative binding to DNA.
- 4) The results of this work suggest electrostatic interaction with partial intercalation as the most probable mode of interaction between the studied FQ's and DNA.

4.1.2. Interaction of FQ's with DNA at the Electrode Surface

- 1) CV measurements showed that the DNA-modified glassy carbon electrode exhibits a larger anodic signal for the oxidation of the FQ's.
- 2) DP-ASV studies revealed that the DNA-modified electrode has the ability to pre-concentrate the drug, leading to an enhanced sensitivity for the drug and a better peak definition.
- 3) The factors affecting the electrochemical oxidation of the studied FQ's at the modified-electrode were investigated, and optimum conditions were

specified as; 10 mV/s scan rate, pH 4, 1.0 min accumulation time at open circuit conditions.

4) Analysis of ciprofloxacin both in tablets and in urine was performed according to the proposed method. The concentration of CIP was calculated from a pre-established calibration curve. The method showed high sensitivity, accuracy with good detection limits.

4.1.3. Kinetics of Oxidation of FQ's with catalyzed- $K_3Fe(CN)_6$

1) The rate of oxidation of the studied FQ's followed the order:



2) The studied drugs followed zero-order kinetics with respect to $K_3Fe(CN)_6$, and the rate law was found experimentally to be;

$$\text{Rate} = k[FQ][OsO_4]$$

3) The rate of oxidation for the studied compounds enhanced with increasing the concentration of hydroxide ion, and decreased with increasing the concentration of $K_4Fe(CN)_6$. However, the rate was not affected by the concentration of the added salts.

4) The thermodynamic parameters were calculated for the oxidation process by exploring the dependence of the reaction rate constant (k) on temperature.

4.2. SUGGESTIONS FOR FUTURE WORK

For a better understanding of drug-DNA interactions and their applications, the following experiments are suggested as future work:

- 1) Using other types of electrodes for studying the interaction of the studied FQ's with DNA.
- 2) Investigating the electrochemical behavior of other FQ's and deducing trends based on variation between their structures.
- 3) Applying the technique followed in this work to study drugs of different categories such as anti-tumor drugs that are known to intercalate with DNA.
- 4) Using additional techniques to confirm the mechanism of interaction suggested by the present study.
- 5) Studying more factors and conditions, such as ionic strength and pH, that may participate in clarifying the mechanism of interaction between FQ's and DNA.
- 6) Trying new methods of modification with DNA (e.g. electrodeposition) and investigating their suitability.
- 7) Investigating biomaterials other than DNA (e.g. enzymes), as potential biosensors for the determination of FQ's.

TABLES

Table (1): Absorption data for the interaction of ciprofloxacin with DNA
[CIP] = 10 μ M, [DNA] = 10-50 μ M, pH = 5

| [DNA] μ M | A ₀ | A | A ₀ /(A-A ₀) | 1/[DNA] $\times 10^{-5}M^{-1}$ |
|---------------|----------------|------|-------------------------------------|--------------------------------|
| 10 | 0.81 | 0.73 | -10.12 | 1.0 |
| 20 | | 0.66 | -5.40 | 0.5 |
| 30 | | 0.57 | -3.38 | 0.33 |
| 40 | | 0.48 | -2.45 | 0.25 |
| 50 | | 0.40 | -1.97 | 0.20 |

Table (2): Absorption data for the interaction of norfloxacin with DNA
[NOR] = 10 μ M, [DNA] = 10 – 40 μ M, pH = 5

| [DNA] μ M | A ₀ | A | A ₀ /(A-A ₀) | 1/[DNA] $\times 10^{-5}M^{-1}$ |
|---------------|----------------|------|-------------------------------------|--------------------------------|
| 10 | 0.74 | 0.67 | -9.25 | 1.0 |
| 20 | | 0.59 | -4.93 | 0.5 |
| 30 | | 0.49 | -2.96 | 0.33 |
| 40 | | 0.43 | -2.38 | 0.25 |

Table (3): Absorption data for the interaction of enrofloxacin with DNA
[ENR] = 10 μ M, [DNA] = 10 - 40 μ M, pH = 5

| [DNA] μ M | A ₀ | A | A ₀ /(A-A ₀) | 1/[DNA] $\times 10^{-5}M^{-1}$ |
|---------------|----------------|------|-------------------------------------|--------------------------------|
| 10 | 0.72 | 0.63 | -8.00 | 1.0 |
| 20 | | 0.53 | -3.78 | 0.5 |
| 30 | | 0.46 | -2.76 | 0.33 |
| 40 | | 0.37 | -2.05 | 0.25 |

Table (4): Absorption data for the interaction of nalidixic acid with DNA
[NAL] = 10 μ M, [DNA] = 10 – 50 μ M, pH = 5

| [DNA] μ M | A ₀ | A | A ₀ /(A-A ₀) | 1/[DNA] $\times 10^{-5}M^{-1}$ |
|---------------|----------------|-------|-------------------------------------|--------------------------------|
| 10 | 0.89 | 0.755 | -6.60 | 1.0 |
| 20 | | 0.620 | -3.30 | 0.5 |
| 30 | | 0.470 | -2.11 | 0.33 |
| 40 | | 0.370 | -1.72 | 0.25 |

Table (5): K values for the interaction of quinolones with DNA

| Drug | CIP | NOR | ENR | NAL |
|--------------------------------------|------|------|------|------|
| K($\times 10^{-2}$)M ⁻¹ | 6.33 | 7.78 | 3.62 | 2.29 |

Table (6): Voltammetric behavior of CIP and CIP – DNA
[CIP] = 3×10^{-5} M in acetate buffer solution (pH 5) after 1 min accumulation
at open circuit conditions. b: Addition of 1.2×10^{-3} M DNA (R = 40).

| ν (V/s) | E_p (V) | E_p^b (V) | I_p (μ A) | I_p^b (μ A) |
|-------------|-----------|-------------|------------------|--------------------|
| 0.005 | 0.810 | 0.855 | 0.058 | 0.032 |
| 0.010 | 0.820 | 0.860 | 0.108 | 0.046 |
| 0.020 | 0.845 | 0.870 | 0.158 | 0.088 |
| 0.05 | 0.860 | 0.880 | 0.274 | 0.172 |
| 0.100 | 0.880 | 0.895 | 0.454 | 0.275 |

Table (7): Voltammetric behavior of NOR and NOR – DNA
[NOR] = 3×10^{-5} M in acetate buffer solution (pH 5) after 1 min
accumulation at open circuit conditions.
b: Addition of 1.2×10^{-3} M DNA (R = 40).

| ν (V/s) | E_p (V) | E_p^b (V) | I_p (μ A) | I_p^b (μ A) |
|-------------|-----------|-------------|------------------|--------------------|
| 0.005 | 0.820 | 0.860 | 0.070 | 0.038 |
| 0.010 | 0.830 | 0.865 | 0.115 | 0.064 |
| 0.020 | 0.845 | 0.875 | 0.166 | 0.096 |
| 0.05 | 0.865 | 0.890 | 0.288 | 0.185 |
| 0.100 | 0.885 | 0.90 | 0.461 | 0.282 |

Table (8): Voltammetric behavior of ENR and ENR – DNA
[ENR] = 3×10^{-5} M in acetate buffer solution (pH 5) after 1 min
accumulation at open circuit conditions.
b: Addition of 1.2×10^{-3} M DNA (R = 40).

| ν (V/s) | E_p (V) | E_p^b (V) | I_p (μ A) | I_p^b (μ A) |
|-------------|-----------|-------------|------------------|--------------------|
| 0.005 | 0.790 | 0.840 | 0.036 | 0.022 |
| 0.010 | 0.810 | 0.850 | 0.084 | 0.044 |
| 0.020 | 0.820 | 0.855 | 0.134 | 0.070 |
| 0.05 | 0.835 | 0.860 | 0.247 | 0.168 |
| 0.100 | 0.850 | 0.870 | 0.428 | 0.243 |

Table (9): Effect of addition of DNA on peak currents
[CIP] = 3×10^{-5} M in acetate buffer solution (pH 5) after 1 min accumulation
at open circuit conditions. Scan rate : 100 mV/s.

| No. | [DNA] (10^{-4} M) | R | I_p (μ A) |
|-----|----------------------|----|------------------|
| 1 | 0.00 | 0 | 0.454 |
| 2 | 1.50 | 5 | 0.404 |
| 3 | 3.00 | 10 | 0.368 |
| 4 | 6.0 | 20 | 0.324 |
| 5 | 9.0 | 30 | 0.294 |
| 6 | 12.0 | 40 | 0.275 |

Table (10): Effect of addition of DNA on peak currents

[NOR] = 3×10^{-5} M in acetate buffer solution (pH 5) after 1 min accumulation at open circuit conditions. Scan rate : 100 mV/s.

| No. | [DNA] (10^{-4} M) | R | I_p (μ A) |
|-----|----------------------|----|------------------|
| 1 | 0.00 | 0 | 0.461 |
| 2 | 1.50 | 5 | 0.410 |
| 3 | 3.00 | 10 | 0.382 |
| 4 | 6.0 | 20 | 0.336 |
| 5 | 9.0 | 30 | 0.300 |
| 6 | 12.0 | 40 | 0.284 |

Table (11): Effect of addition of DNA on peak currents

[ENR] = 3×10^{-5} M in acetate buffer solution (pH 5) after 1 min accumulation at open circuit conditions. Scan rate : 100 mV/s.

| No. | [DNA] (10^{-4} M) | R | I_p (μ A) |
|-----|----------------------|----|------------------|
| 1 | 0.00 | 0 | 0.428 |
| 2 | 1.50 | 5 | 0.4382 |
| 3 | 3.00 | 10 | 0.341 |
| 4 | 6.0 | 20 | 0.292 |
| 5 | 9.0 | 30 | 0.262 |
| 6 | 12.0 | 40 | 0.243 |

Table (12): Electrochemical binding parameters for the interaction of quinolones with DNA.

3×10^{-5} mol/L quinolone titrated with DNA in acetate buffer solution (pH 5). Scan rate 100 mV/s.

| Quinolone | $10^6 D_f$ (cm^2/s) | $10^7 D_b$ (cm^2/s) | $10^{-5} K$ (cm^3/mol) | s (bp) |
|-----------|---------------------------------------|---------------------------------------|--|--------|
| CIP | 2.34 | 1.85 | 2.89 | 0.10 |
| NOR | 2.22 | 1.76 | 2.91 | 0.11 |
| ENR | 1.69 | 0.67 | 1.92 | 0.07 |

Table (13): Relationship between DPASV peak currents and quinolone concentration.

Acetate buffer solution (pH5). Scan rate: 10 mV/s. Initial potential: + 0.4 V. Accumulation time: 60 s.

| Compound | Electrode | Slope ($\mu\text{A}/\mu\text{M}$) | Intercept (μA) | Linearity Range (μM) | R^2 |
|----------|-----------|--|--------------------------------|---|-------|
| CIP | Bare | 0.120 | 0.212 | 1.0 - 8.0 | 0.99 |
| | Modified | 0.716 | 1.268 | 1.0 - 10.0 | 0.99 |
| NOR | Bare | 0.131 | 0.229 | 1.0 - 8.0 | 0.99 |
| | Modified | 0.897 | 1.403 | 1.0 - 10.0 | 0.99 |
| ENR | Bare | 0.107 | 0.188 | 1.0 - 7.0 | 0.99 |
| | Modified | 0.713 | 1.406 | 1.0 - 9.0 | 0.98 |

Table (14): Effect of FQ concentration on reaction rate:

$[\text{K}_3\text{Fe}(\text{CN})_6] = 1 \times 10^{-3} \text{M}$, $[\text{OsO}_4] = 1 \times 10^{-5} \text{M}$, $[\text{OH}^-] = 0.1 \text{M}$, temperature = 25°C , $\mu = 0.15$

| $10^2 [\text{FQ}] \text{ M}$ | -Log rate | | |
|------------------------------|-----------|------|------|
| | CIP | NOR | ENR |
| 0.5 | 2.02 | 2.04 | 2.26 |
| 1.0 | 1.68 | 1.73 | 1.87 |
| 2.0 | 1.43 | 1.41 | 1.67 |
| 3.0 | 1.30 | 1.28 | 1.53 |

Table(15): Effect of $\text{Fe}(\text{CN})_6^{3-}$ concentration on reaction rate:

$[\text{FQ}] = 0.01 \text{M}$, $[\text{OsO}_4] = 1 \times 10^{-5} \text{M}$, $[\text{OH}^-] = 0.1 \text{M}$, temperature = 25°C , $\mu = 0.15$

| $10^4 [\text{K}_3\text{Fe}(\text{CN})_6] \text{M}$ | -Log rate | | |
|--|-----------|------|------|
| | CIP | NOR | ENR |
| 4.0 | 1.72 | 1.76 | 1.89 |
| 6.0 | 1.69 | 1.72 | 1.86 |
| 8.0 | 1.67 | 1.74 | 1.86 |
| 10.0 | 1.68 | 1.73 | 1.88 |
| 12.0 | 1.66 | 1.70 | 1.87 |

Table (16): Effect of OsO₄ concentration on reaction rate:

[FQ] = 0.01M, [K₃Fe(CN)₆] = 1x10⁻³ M, [OH⁻] = 0.1M, temperature = 25°C, μ =0.15

| 10 ⁵ [OsO ₄] M | -Log rate | | |
|---------------------------------------|-----------|------|------|
| | CIP | NOR | ENR |
| 0.5 | 1.92 | 2.06 | 2.14 |
| 1.0 | 1.68 | 1.73 | 1.86 |
| 2.0 | 1.44 | 1.62 | 1.70 |
| 3.0 | 1.35 | 1.43 | 1.59 |
| 4.0 | 1.25 | 1.30 | 1.45 |

Table (17): Effect of hydroxide ion concentration on reaction rate:

[FQ] = 0.01M, [K₃Fe(CN)₆] = 1x10⁻³ M, [OsO₄] = 1x10⁻⁵ M, temperature = 25°C, μ =0.15

| [NaOH] M | -Log rate | | |
|----------|-----------|------|------|
| | CIP | NOR | ENR |
| 0.020 | 2.08 | 2.14 | 2.21 |
| 0.050 | 1.86 | 1.96 | 2.04 |
| 0.075 | 1.78 | 1.85 | 1.96 |
| 0.100 | 1.68 | 1.73 | 1.86 |

Table (18): Effect of added K₄Fe(CN)₆ on reaction rate:

[FQ] = 0.01M, [K₃Fe(CN)₆] = 1x10⁻³ M, [OsO₄] = 1x10⁻⁵ M, [OH⁻] = 0.1M temperature = 25°C, μ = 0.15

| 10 ⁴ [K ₄ Fe(CN) ₆]M | -Log Rate | | |
|--|-----------|------|------|
| | CIP | NOR | ENR |
| 0.0 | 1.68 | 1.73 | 1.86 |
| 5.0 | 1.75 | 1.81 | 1.89 |
| 10.0 | 1.80 | 1.88 | 1.91 |
| 15.0 | 1.85 | | 1.95 |
| 20.0 | 1.88 | 1.95 | 1.98 |

Table (19): Effect of added salt on reaction rate:

[FQ] = 0.01M, [K₃Fe(CN)₆] = 1x10⁻³M, [OsO₄] = 1x10⁻⁵M, [OH⁻] = 0.1M
 temperature = 25^oC, μ = 0.15

| Salt | -Log Rate | | |
|--------------------|-----------|------|------|
| | CIP | NOR | ENR |
| NaCl | 1.68 | 1.73 | 1.86 |
| NH ₄ Cl | 1.85 | 1.86 | 1.95 |
| KCl | 1.69 | 1.75 | 1.88 |
| KBr | 1.70 | 1.71 | 1.82 |
| KI | 1.68 | 1.75 | 1.83 |

Table (20): Effect of temperature on ciprofloxacin reaction rate:

[CIP] = 0.01M, [K₃Fe(CN)₆] = 1x10⁻³M, [OsO₄] = 1x10⁻⁵M, [OH⁻] = 0.1M,
 μ = 0.15

| T(^o C) | 10 ³ /T (K ⁻¹) | 10 ² [Rate] | 10 ⁻⁵ k | lnk |
|--------------------|---------------------------------------|------------------------|--------------------|-------|
| 15 | 3.47 | 1.46 | 1.46 | 11.89 |
| 20 | 3.41 | 1.82 | 1.82 | 12.11 |
| 25 | 3.36 | 2.1 | 2.1 | 12.25 |
| 30 | 3.30 | 2.65 | 2.65 | 12.48 |
| 37 | 3.22 | 3.38 | 3.38 | 12.73 |

Table (21): Effect of temperature on norfloxacin reaction rate:

[NOR] = 0.01M, [K₃Fe(CN)₆] = 1x10⁻³M, [OsO₄] = 1x10⁻⁵M, [OH⁻] =
 0.1M, μ=0.15

| T(^o C) | 10 ³ /T (K ⁻¹) | 10 ² [Rate] | 10 ⁻⁵ k | lnk |
|--------------------|---------------------------------------|------------------------|--------------------|-------|
| 15 | 3.47 | 1.31 | 1.31 | 11.76 |
| 20 | 3.41 | 1.64 | 1.64 | 11.90 |
| 25 | 3.36 | 1.85 | 1.85 | 12.11 |
| 30 | 3.30 | 2.39 | 2.39 | 12.35 |
| 37 | 3.22 | 3.11 | 3.11 | 12.64 |

Table (22): Effect of temperature on enrofloxacin reaction rate:

[ENR] = 0.01M, [K₃Fe(CN)₆] = 1x10⁻³M, [OsO₄] = 1x10⁻⁵M, [OH⁻] = 0.1M, μ= 0.15

| T(°C) | 10 ³ /T (K ⁻¹) | 10 ² [Rate] | 10 ⁻⁵ k | lnk |
|-------|---------------------------------------|------------------------|--------------------|-------|
| 20 | 3.41 | 1.01 | 1.01 | 11.52 |
| 25 | 3.36 | 1.38 | 1.38 | 11.83 |
| 30 | 3.30 | 1.79 | 1.79 | 11.98 |
| 40 | 3.19 | 2.57 | 2.57 | 12.45 |

Table (23): Activation parameters for the catalyzed oxidation of FQ's by potassium hexacyano ferrate(III) in alkaline medium:

| FQ | Ea(kJ) | ΔS*(J) | ΔH*(kJ) | ΔG*(kJ) |
|-----|--------|--------|---------|---------|
| CIP | 27.90 | 59.48 | 25.42 | 7.69 |
| NOR | 30.12 | 66.74 | 27.64 | 7.75 |
| ENR | 34.45 | 80.62 | 35.97 | 11.94 |

FIGURES

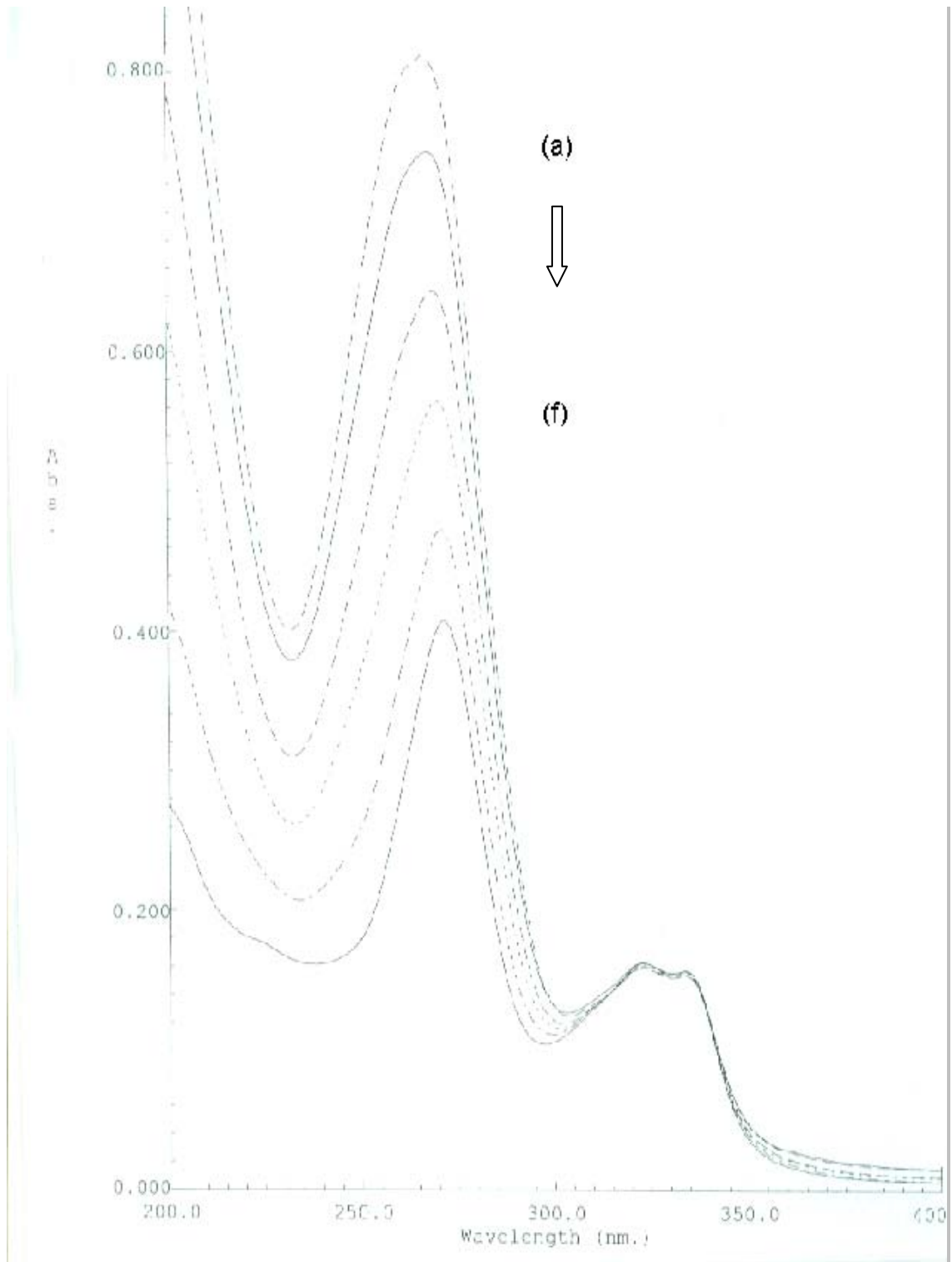


Figure (1): UV/Vis absorption spectra of acetate buffer solution (pH 5) containing 10 μM CIP in the presence of DNA (μM): (a) 0.00; (b) 10.0; (c) 20.0; (d) 30.0; (e) 40.0; (f) 50.0

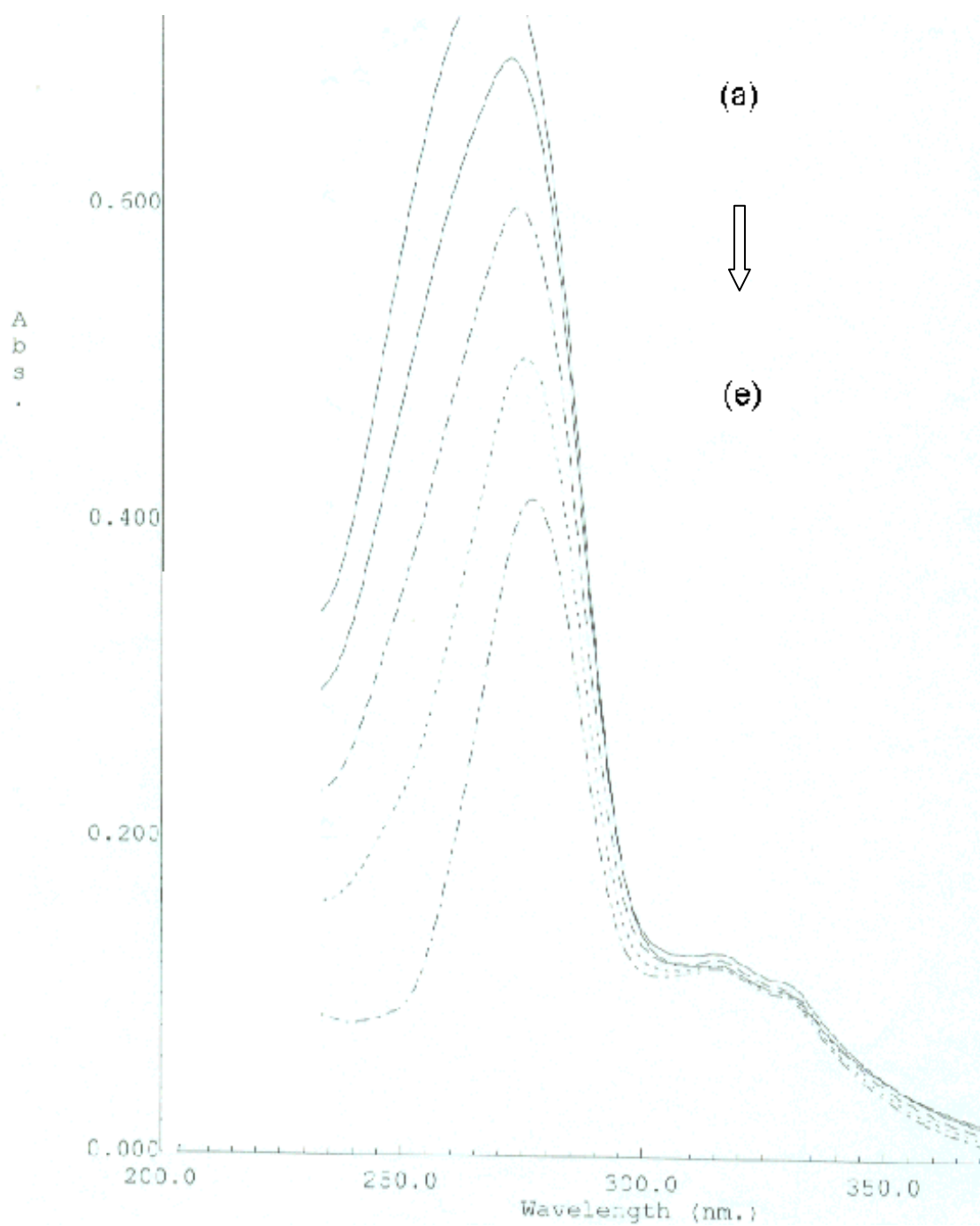


Figure (2): UV/Vis absorption spectra of acetate buffer solution (pH 5) containing 10 μM NOR in the presence of DNA (μM): (a) 0.00; (b) 10.0; (c) 20.0; (d) 30.0; (e) 40.0

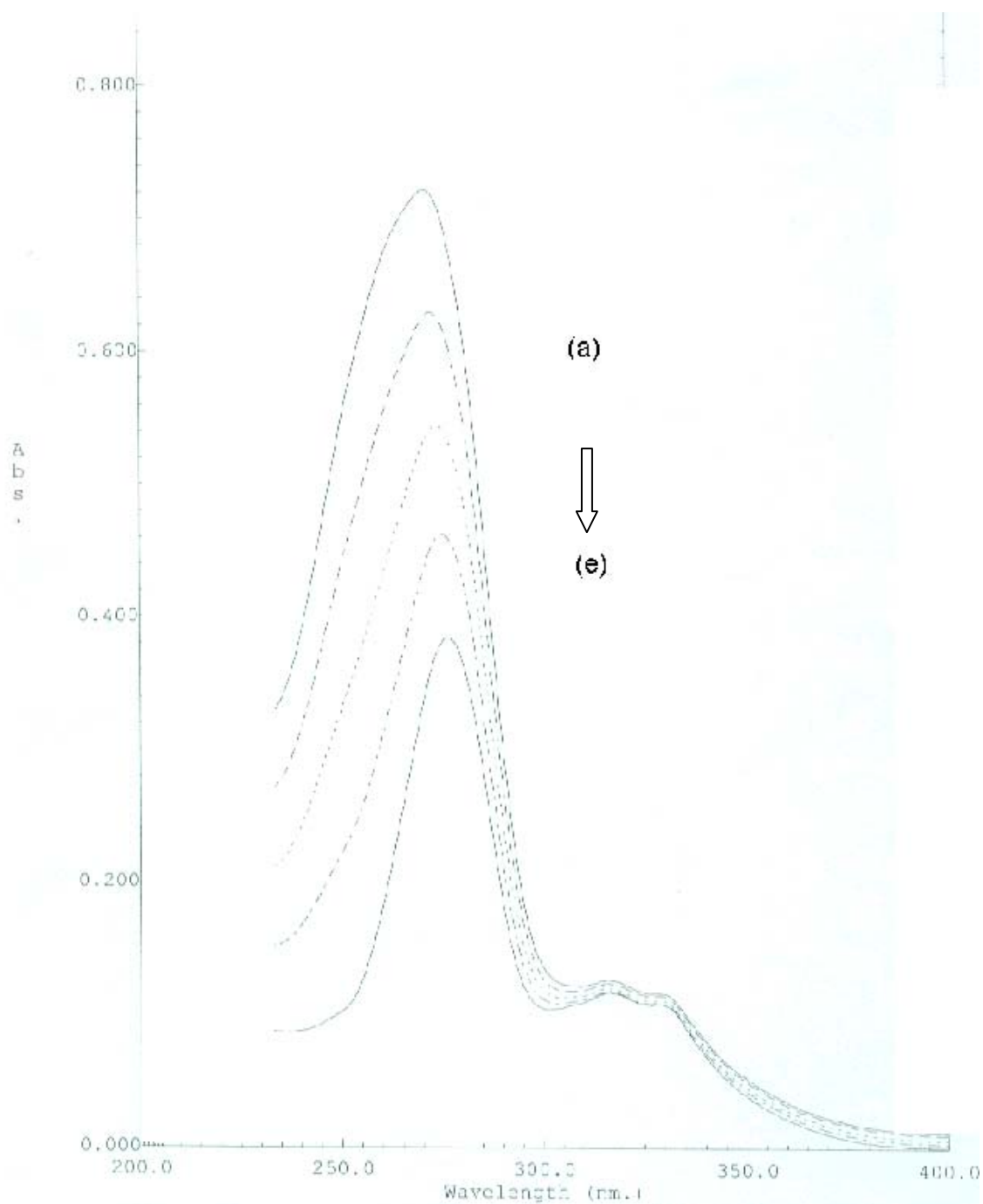


Figure (3): UV/Vis absorption spectra of acetate buffer solution (pH 5) containing 10 μM ENR in the presence of DNA (μM): (a) 0.00; (b) 10.0; (c) 20.0; (d) 30.0; (e) 40.0

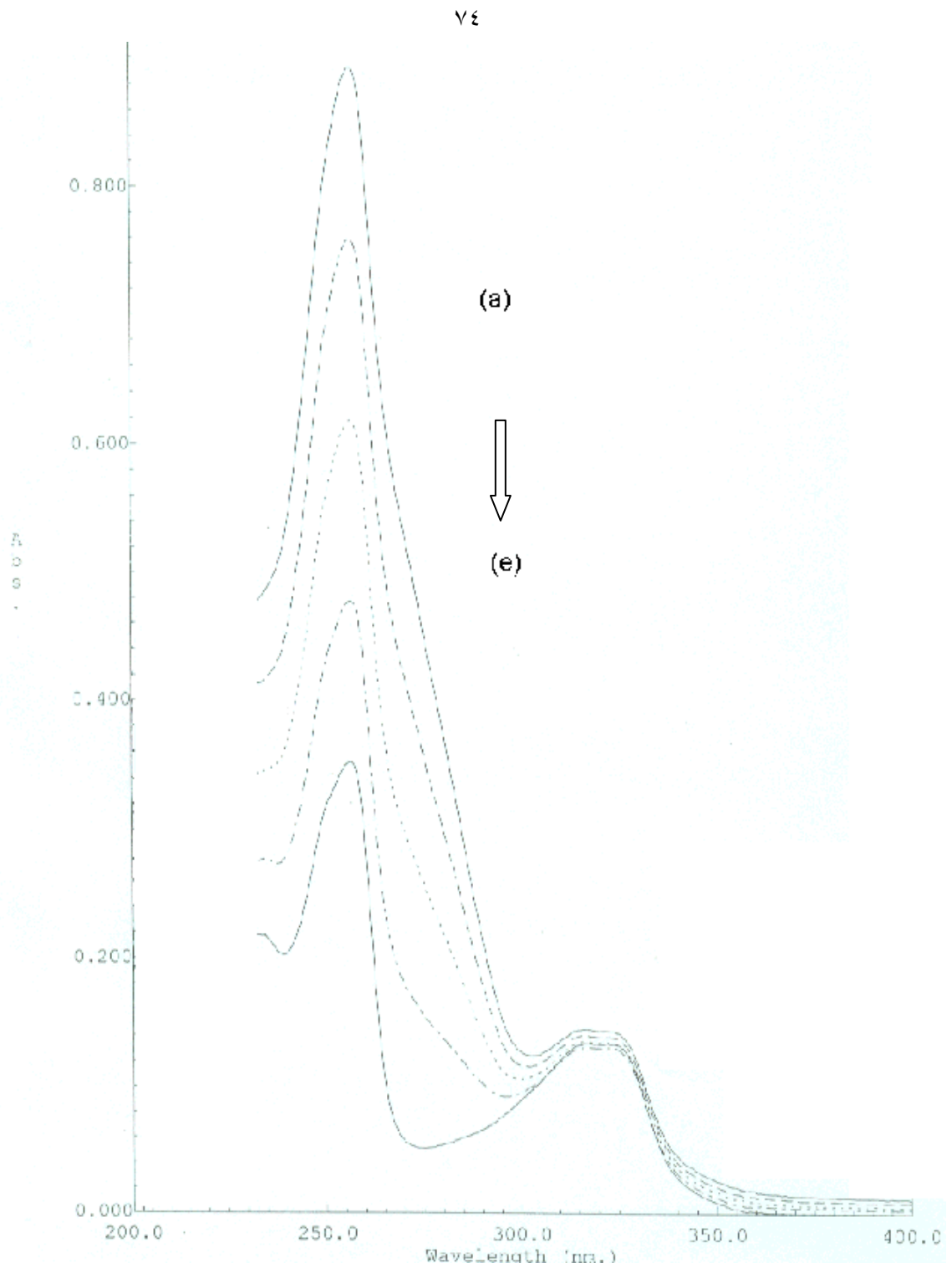


Figure (4): UV/Vis absorption spectra of acetate buffer solution (pH 5) containing 10 μM NAL in the presence of DNA (μM): (a) 0.00; (b) 10.0; (c) 20.0; (d) 30.0; (e) 40.0

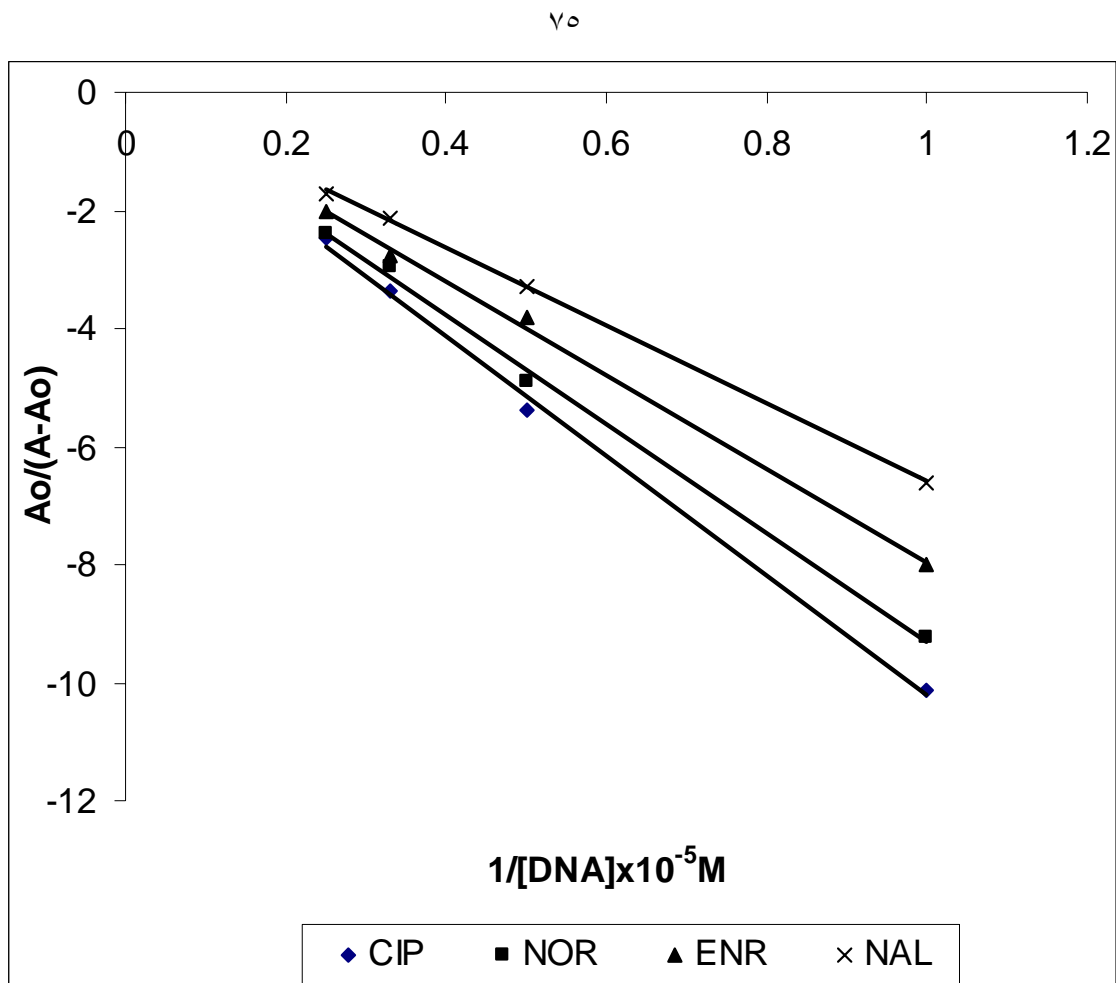


Figure (5): Plot of $A_0/(A-A_0)$ vs. $1/[DNA]$
 $[Q] = 5 \times 10^{-6} \text{ M}$ in acetate buffer solution (pH 5) containing 10.0-50.0 μM DNA

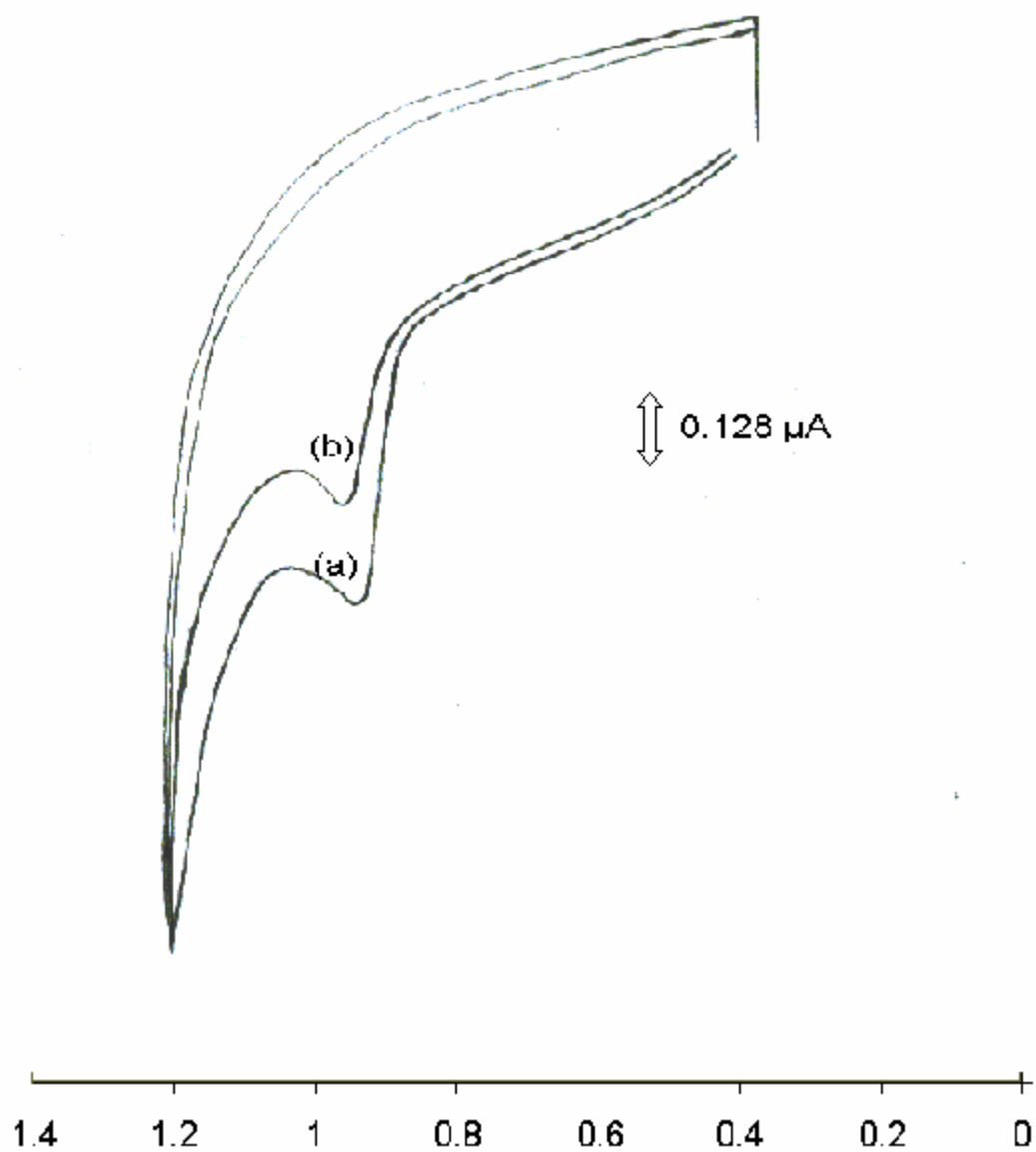


Figure (6): Cyclic voltammograms of acetate buffer solution (pH 5) containing $3 \times 10^{-5} \text{ M}$ CIP in the absence (a) and presence (b) of $1.2 \times 10^{-3} \text{ M}$ DNA. Scan rate: 100mV/s. Initial potential: +0.3 V.

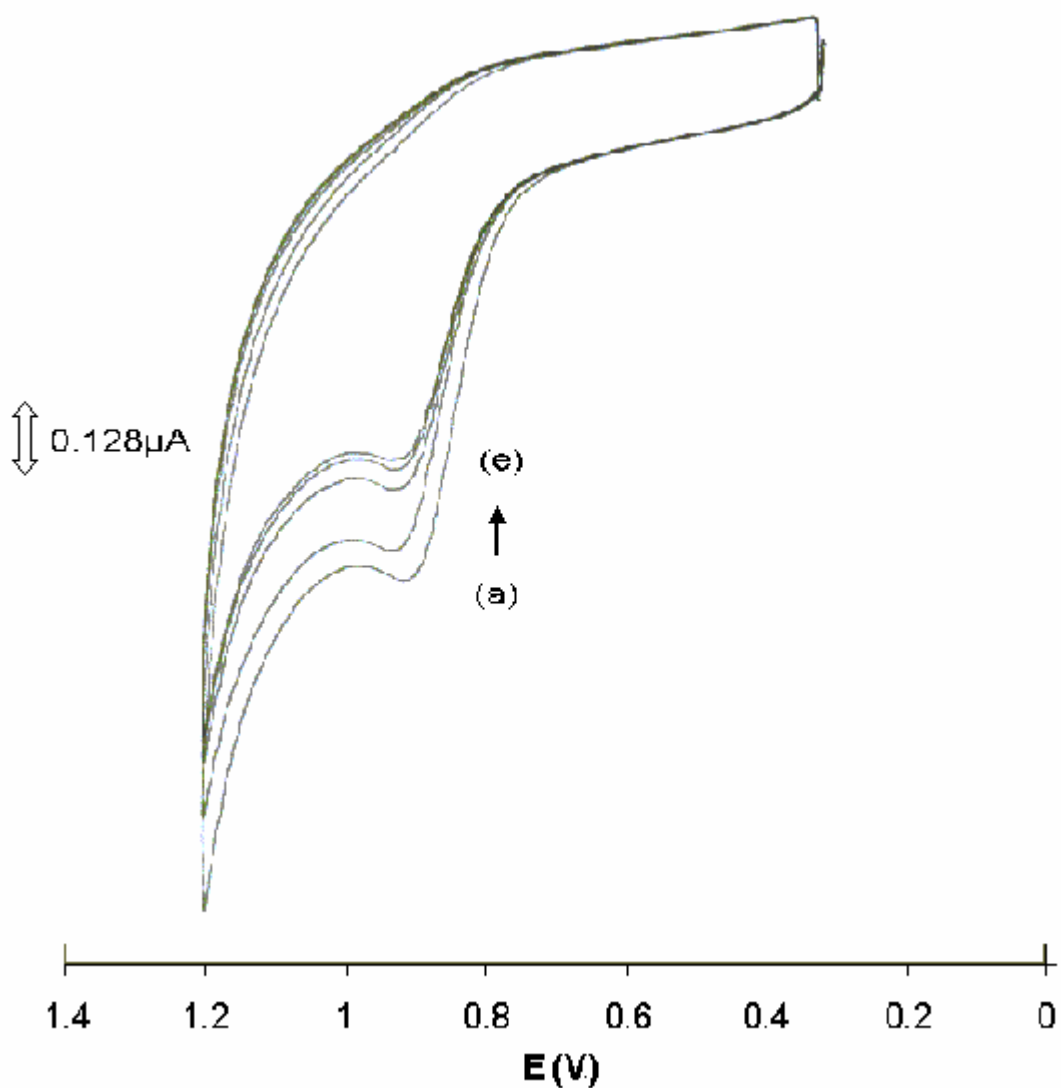


Figure (7): Cyclic voltammograms of acetate buffer solution (pH 5) containing $3 \times 10^{-5} \text{ M}$ NOR in the absence (a) and presence of; (b) $1.5 \times 10^{-4} \text{ M}$; (c) $6 \times 10^{-4} \text{ M}$; (d) $9 \times 10^{-4} \text{ M}$; (e) $1.2 \times 10^{-3} \text{ M}$ DNA. Scan rate: 100 mV/s . Initial potential: $+0.3 \text{ V}$.

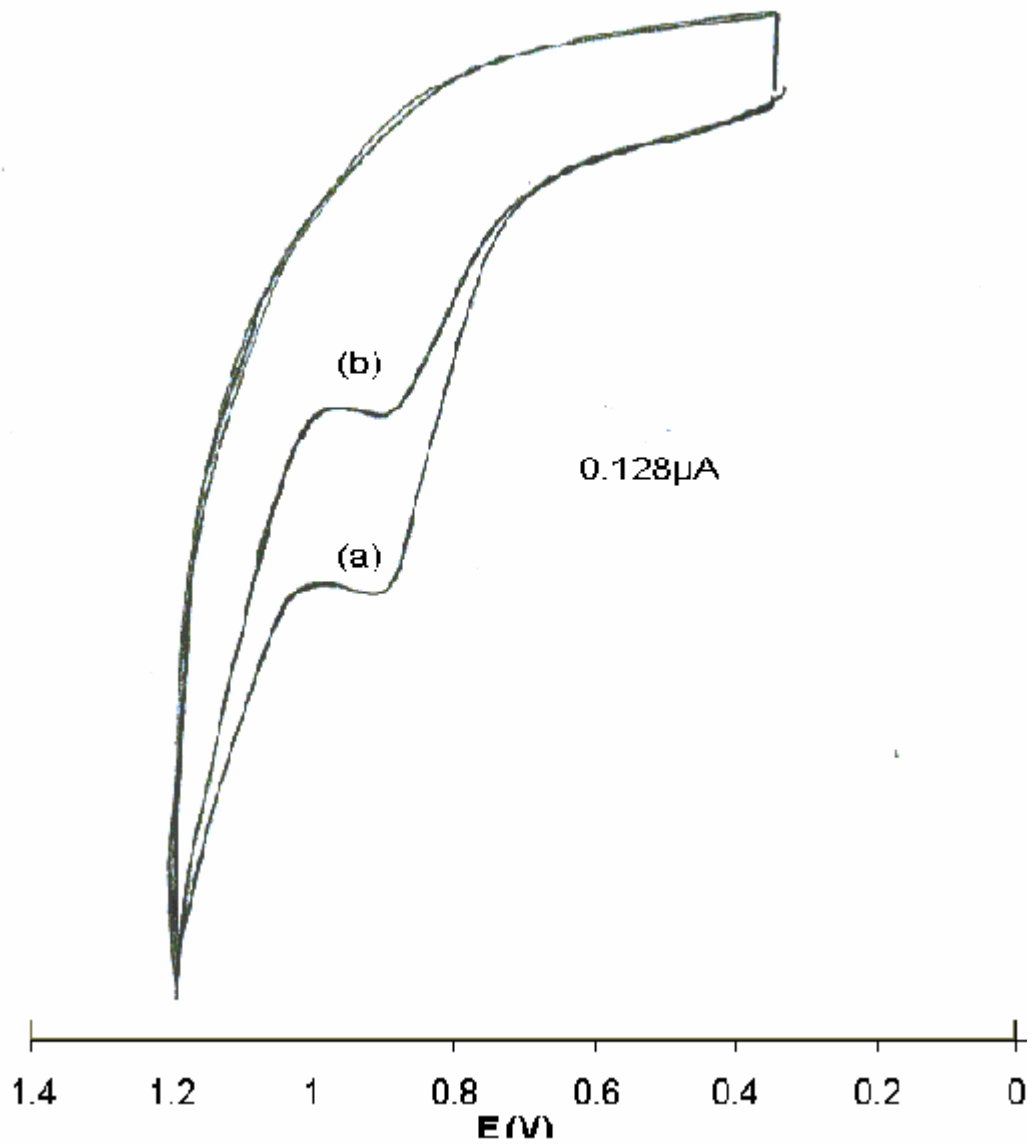


Figure (8): Cyclic voltammograms of acetate buffer solution (pH 5) containing $3 \times 10^{-5} \text{M}$ ENR in the absence (a) and presence (b) of $1.2 \times 10^{-3} \text{M}$ DNA. Scan rate: 100mV/s . Initial potential: $+0.3 \text{ V}$.

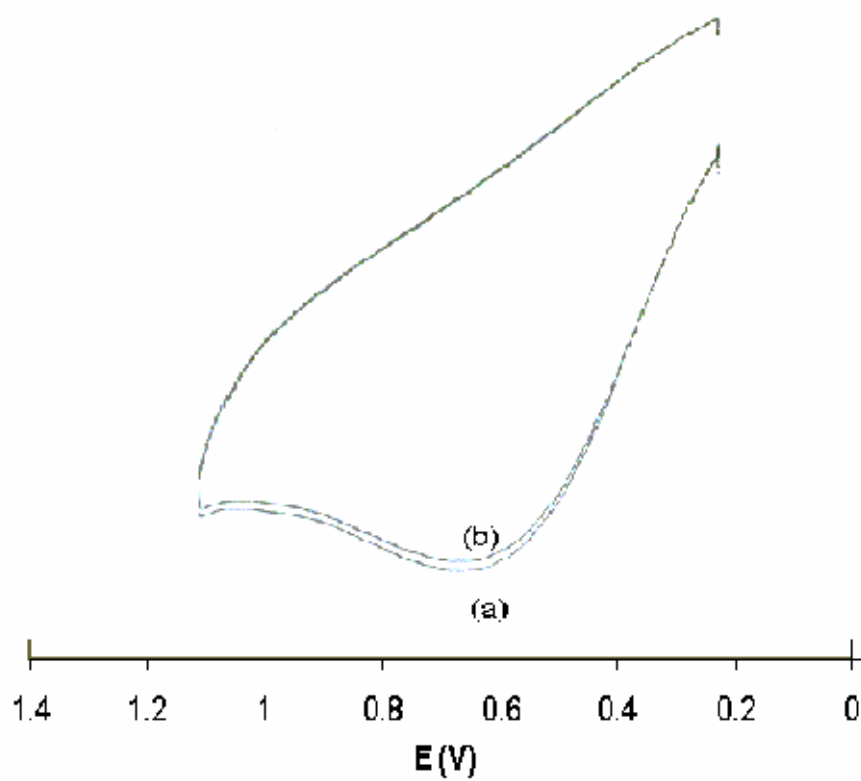


Figure (9): Cyclic voltammograms of $K_4Fe(CN)_6$ in the absence (a) and presence (b) of $1.2 \times 10^{-3} M$ DNA. Scan rate: 100mV/s. Initial potential: +0.2 V.

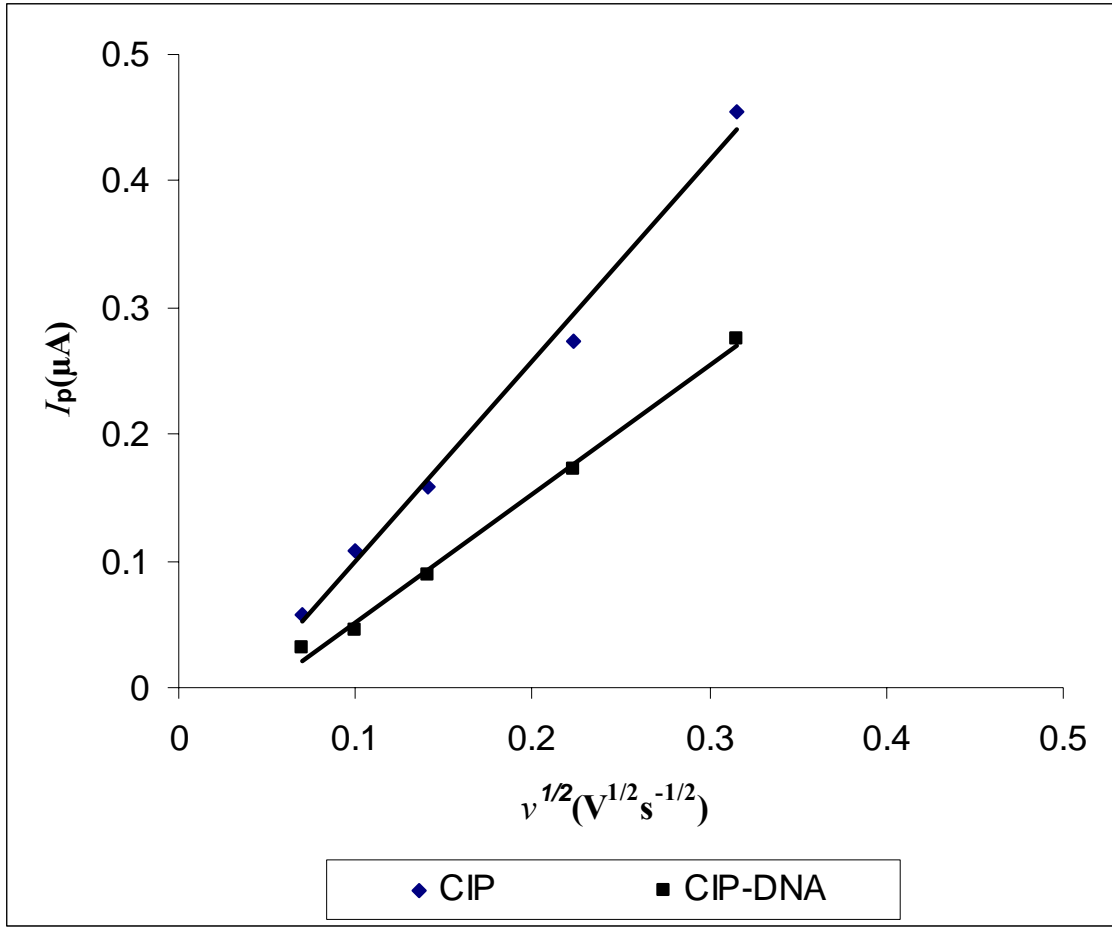


Figure (10): Plot of I_p vs $v^{1/2}$ of acetate buffer solution (pH 5) containing $3 \times 10^{-5} M$ CIP in the absence and presence of $1.6 \times 10^{-4} M$ DNA.

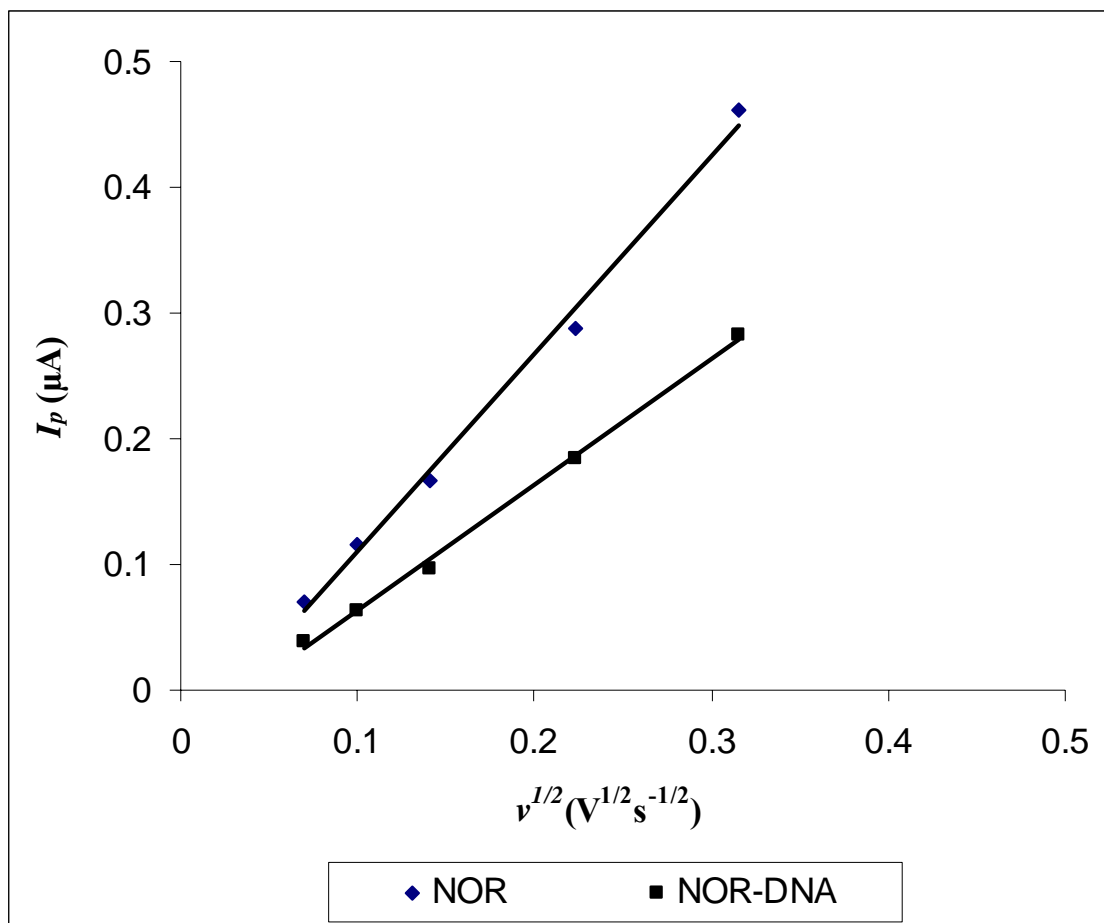


Figure (11): Plot of I_p vs $v^{1/2}$ of acetate buffer solution (pH 5) containing 3×10^{-5} M NOR in the absence and presence of 1.2×10^{-3} M DNA.

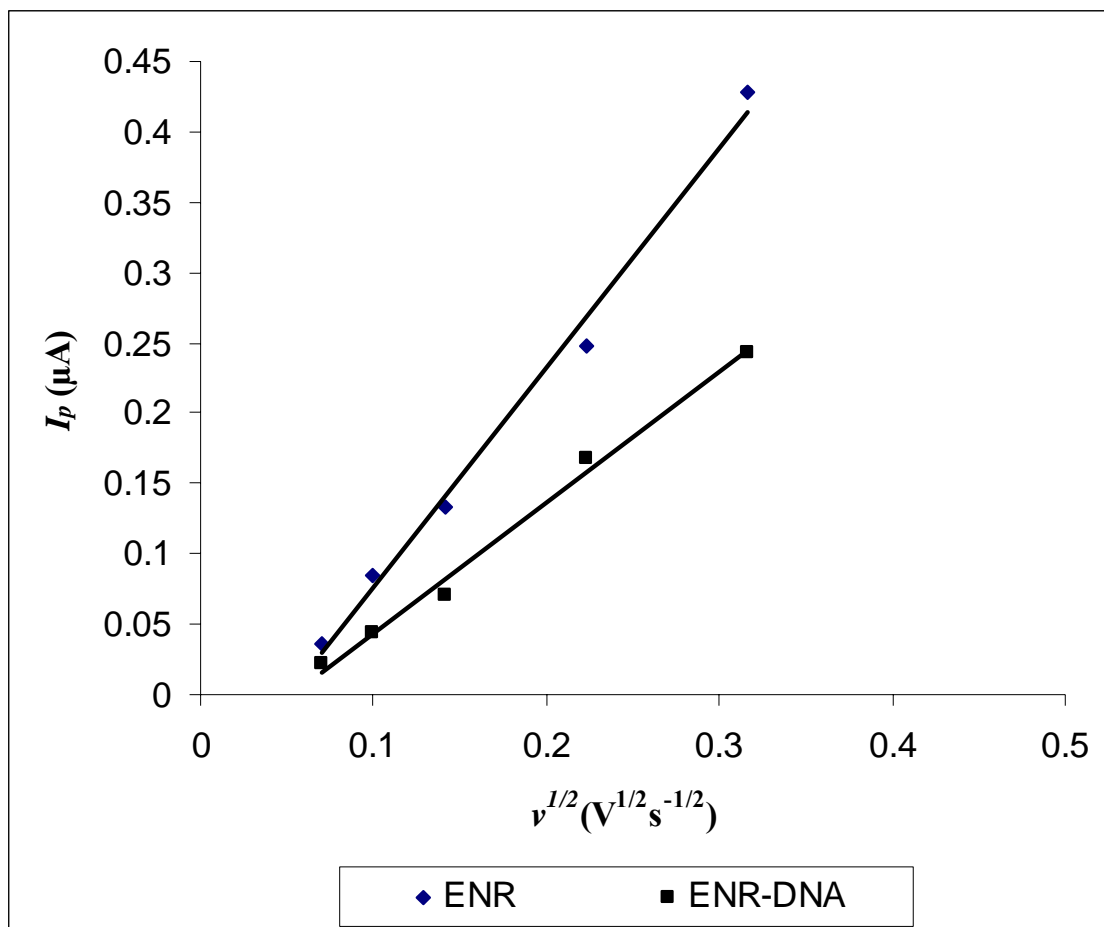


Figure (12): Plot of I_p vs $v^{1/2}$ of acetate buffer solution (pH 5) containing $3 \times 10^{-5} \text{M}$ ENR in the absence and presence of $1.2 \times 10^{-3} \text{M}$ DNA.

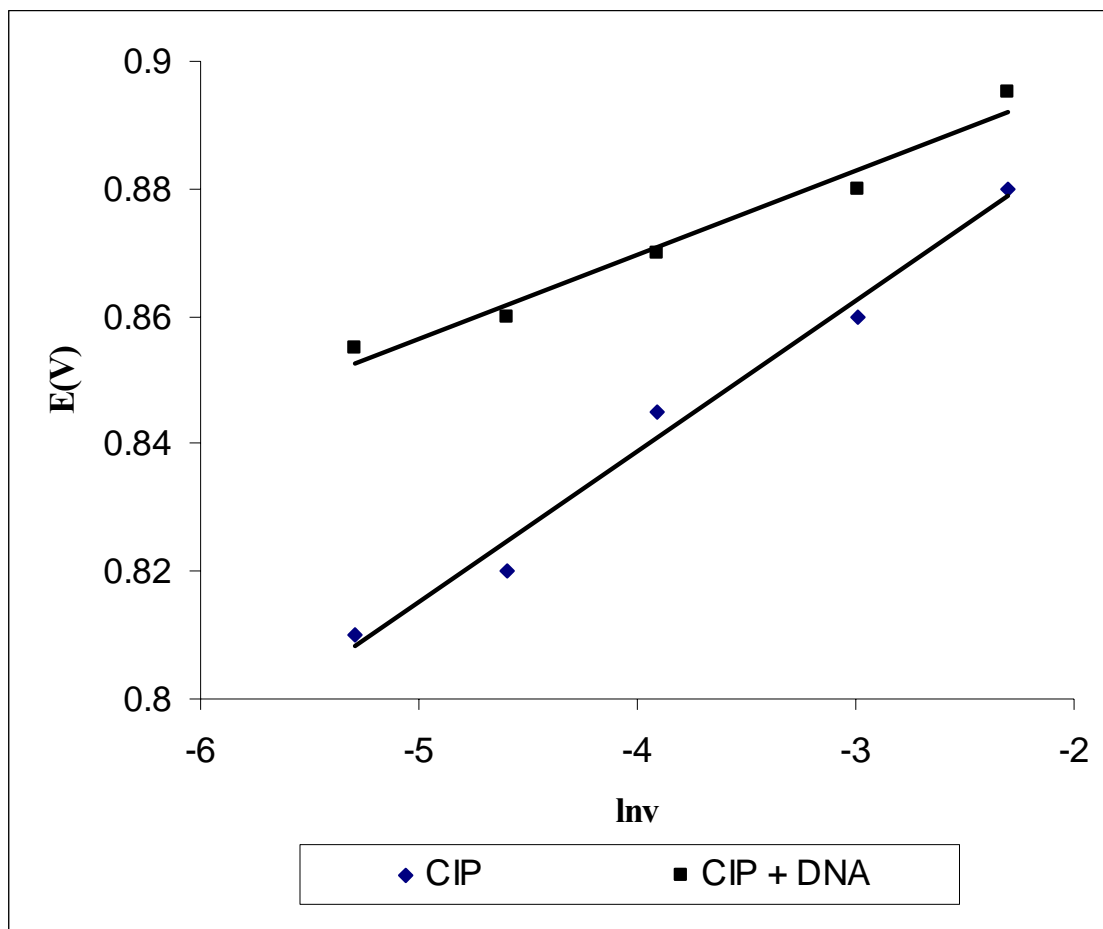


Figure (13): Plot of E_p vs $\ln v$ of acetate buffer solution (pH 5) containing 3×10^{-5} M CIP in the absence and presence of 1.2×10^{-3} M DNA.

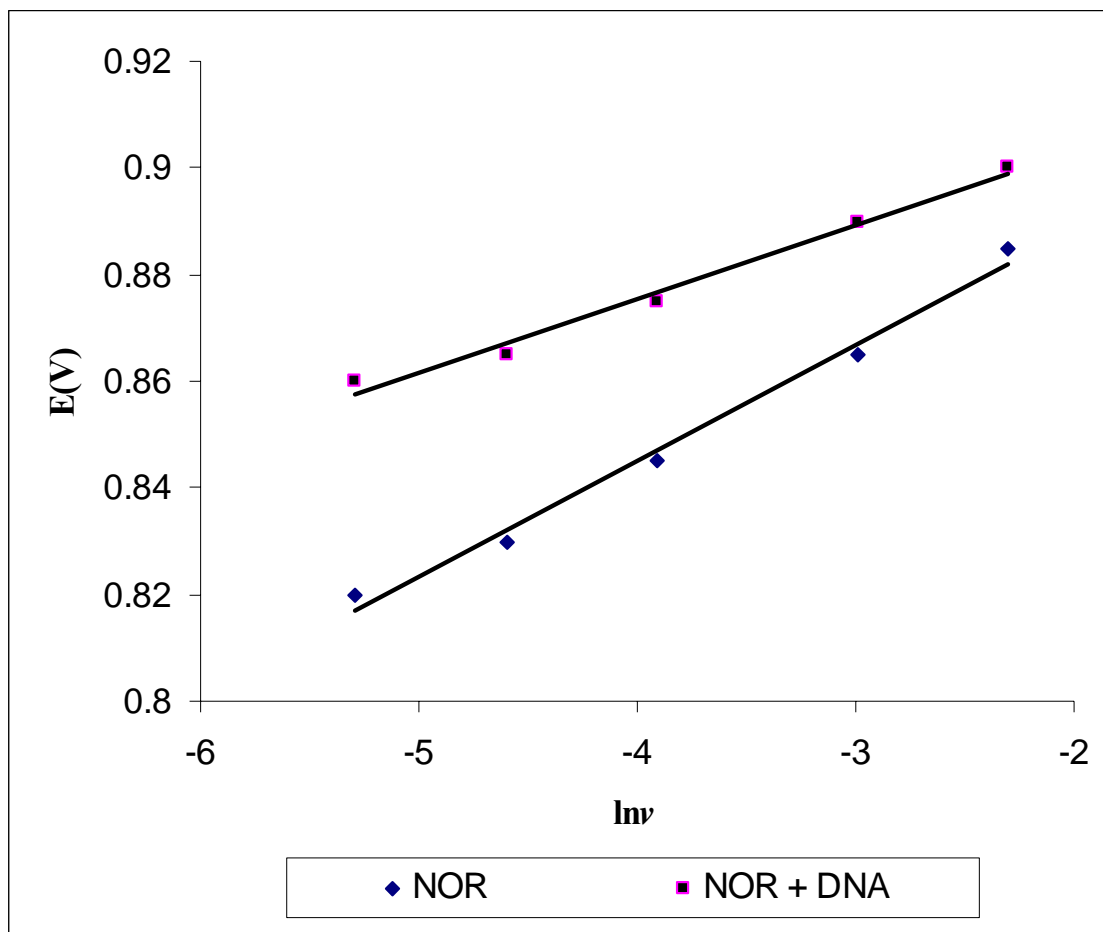


Figure (14): Plot of E_p vs $\ln v$ of acetate buffer solution (pH 5) containing 3×10^{-5} M NOR in the absence and presence of 1.2×10^{-3} M DNA.

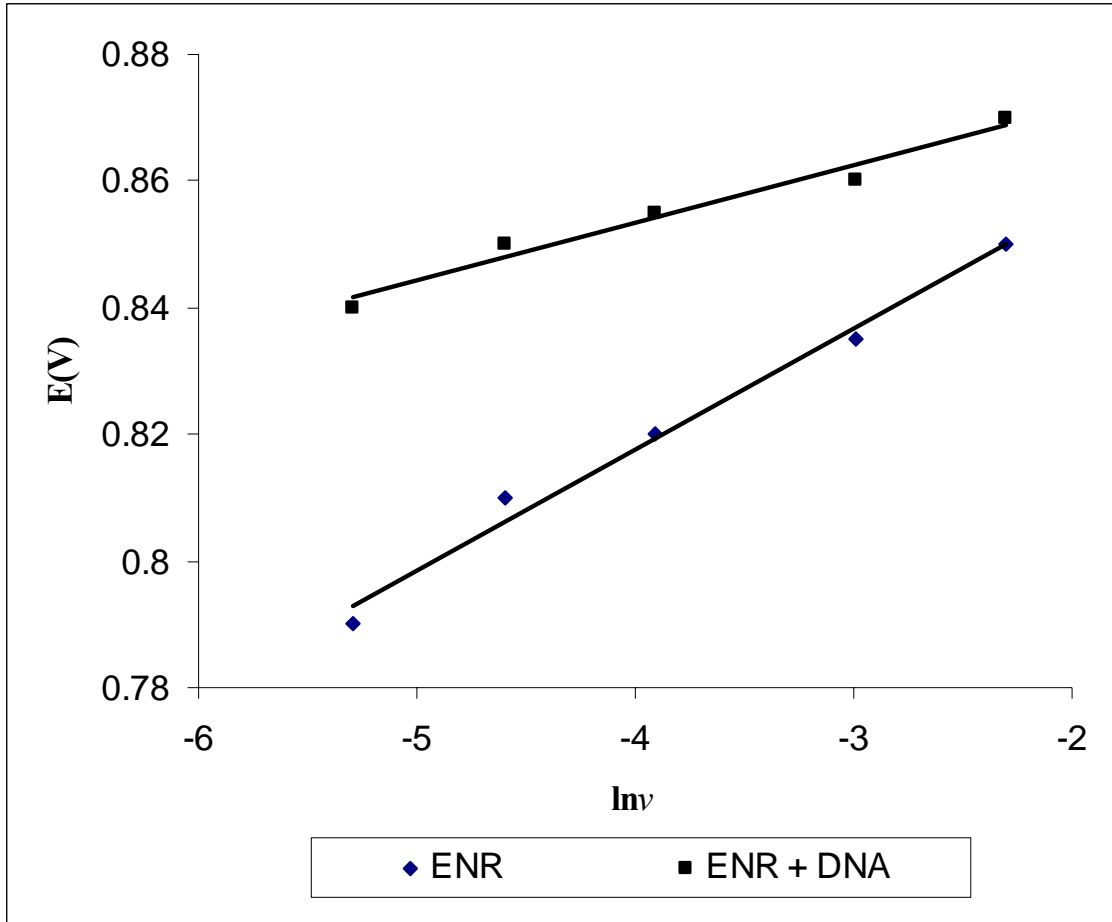


Figure (15): Plot of E_p vs $\ln v$ of acetate buffer solution (pH 5) containing 3×10^{-5} M ENR in the absence and presence of 1.2×10^{-3} M DNA.

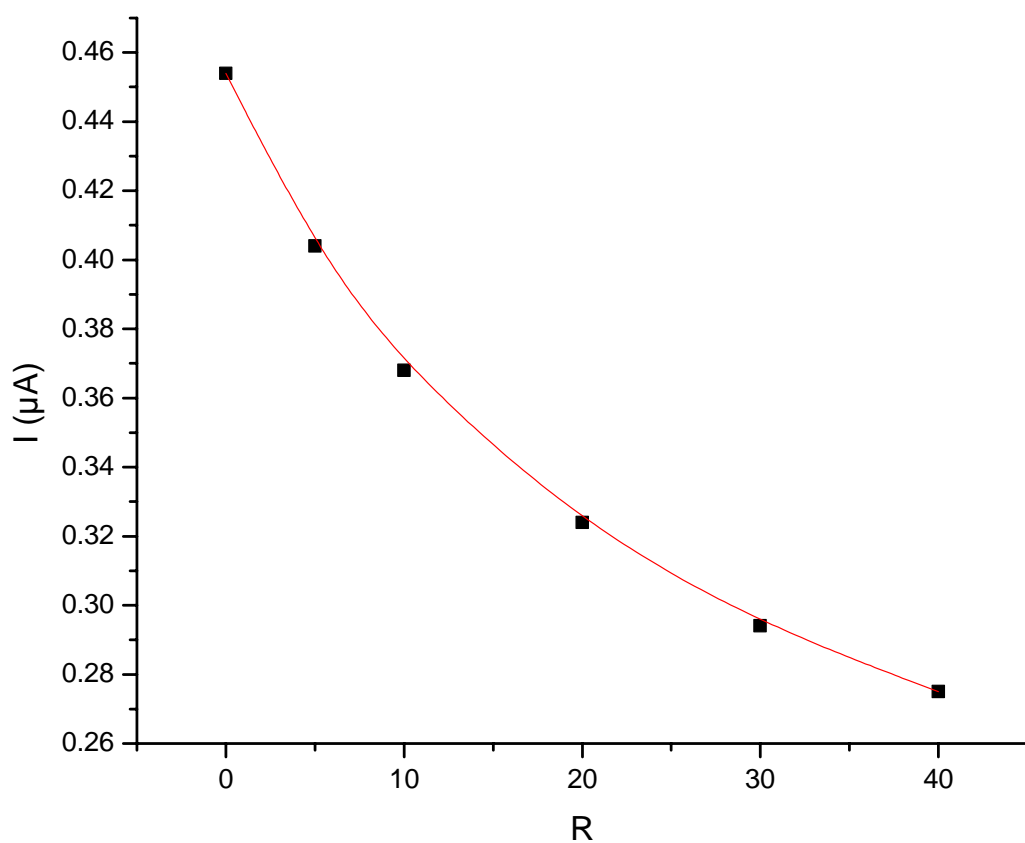


Figure (16): Binding curve of 3×10^5 M CIP with DNA acetate buffer solution (pH 5). Scan rate: 100mV/s.

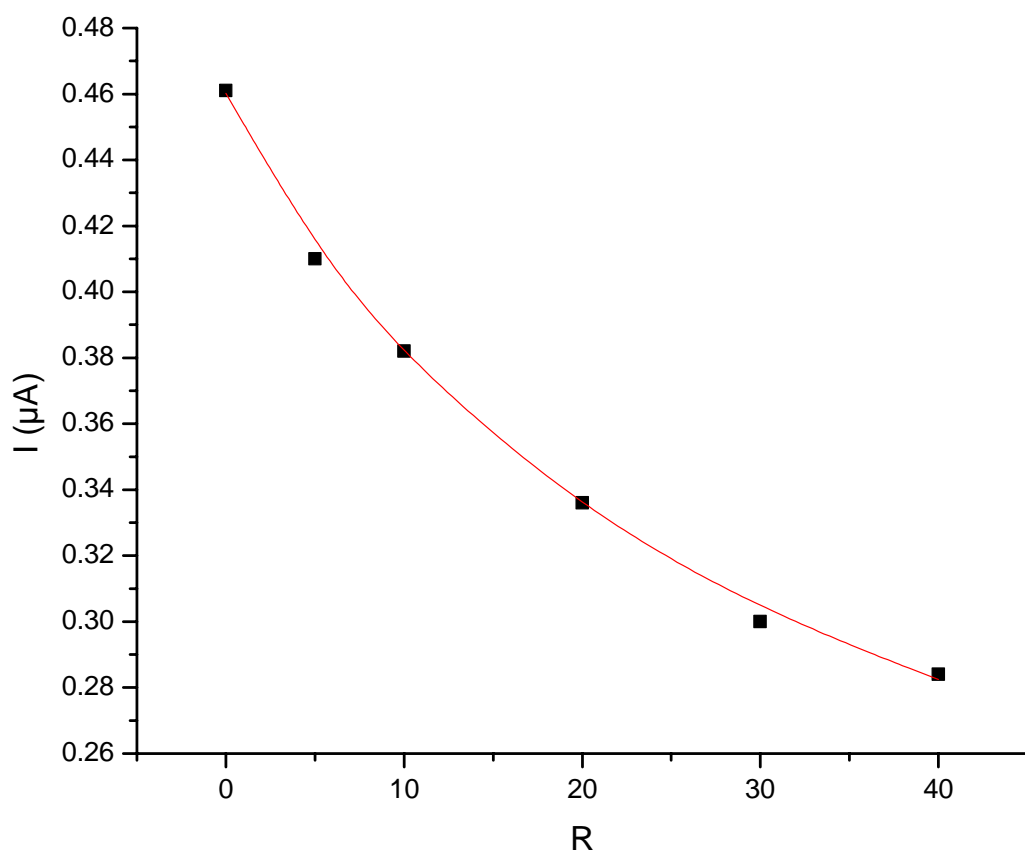


Figure (17): Binding curve of 3×10^5 M NOR with DNA in acetate buffer solution (pH 5). Scan rate: 100mV/s.

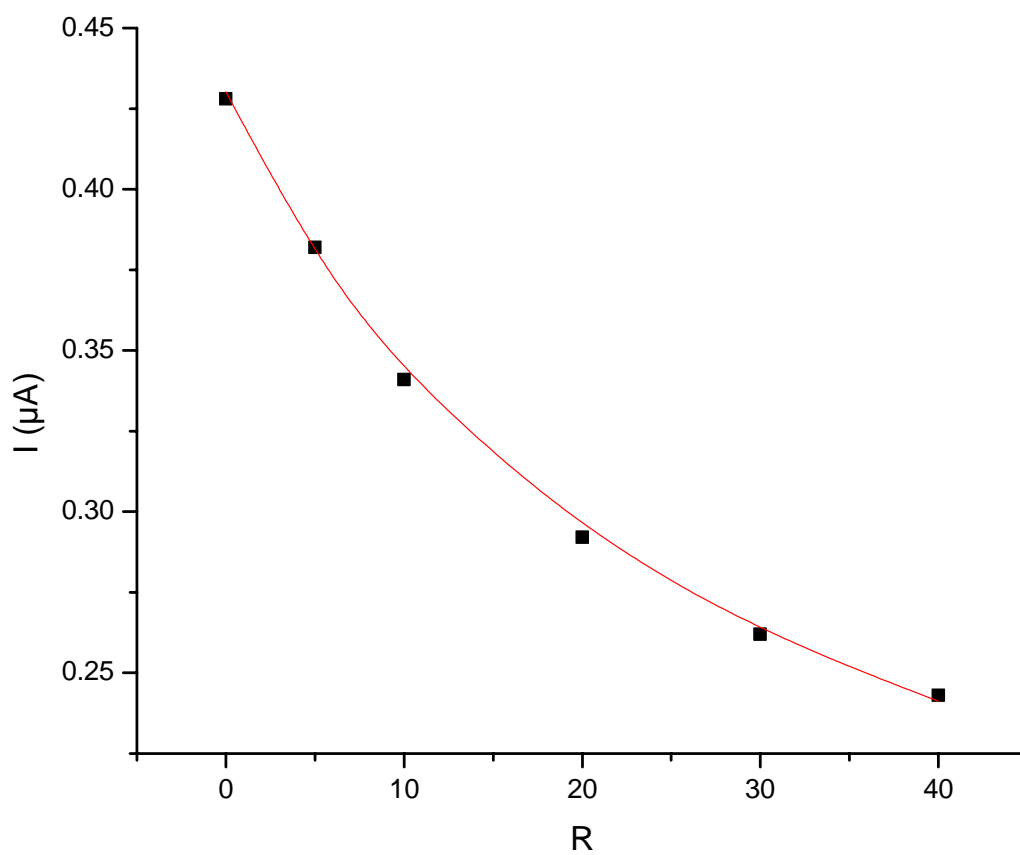


Figure (18): Binding curve of 3×10^5 M ENR with DNA in acetate buffer solution (0.2M, pH 5). Scan rate: 100mV/s.

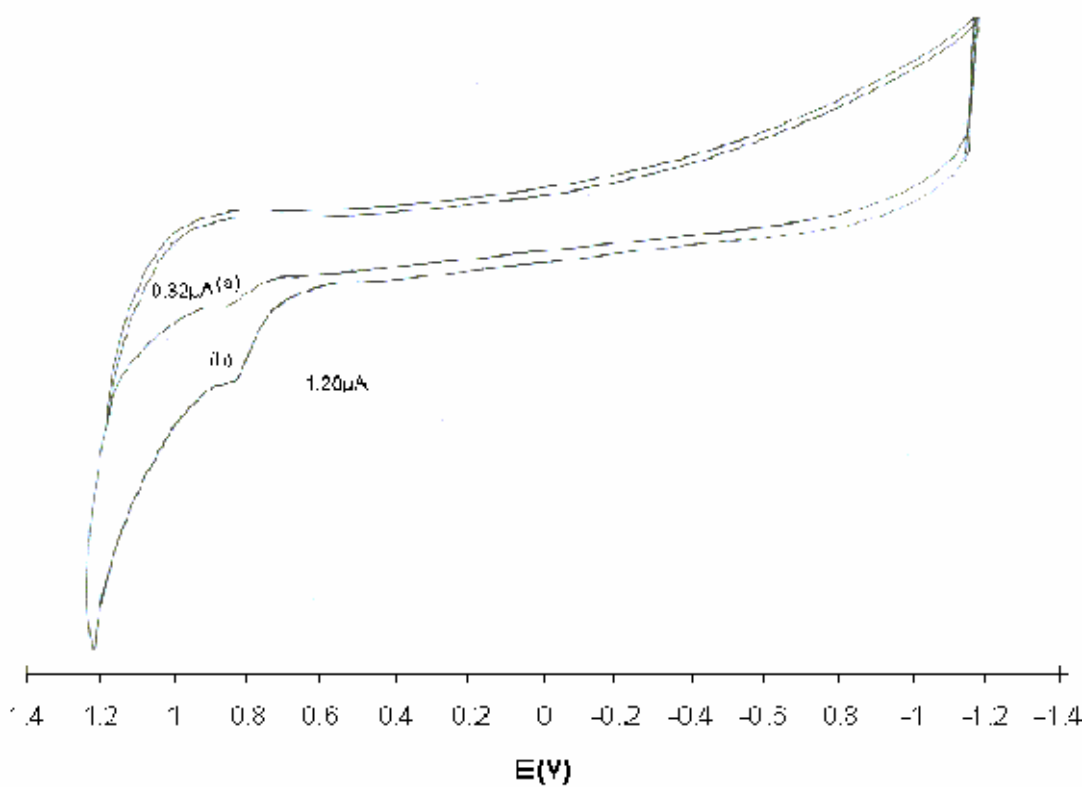


Figure (19): Cyclic voltammograms of $1 \times 10^{-5} \text{ M}$ CIP in acetate buffer solution (pH 5) at: (a) bare GC electrode and (b) DNA-modified GC electrode. (Scan rate: 100 mV/s. Initial potential: +0.2 V. Accumulation time: 1.0 min).

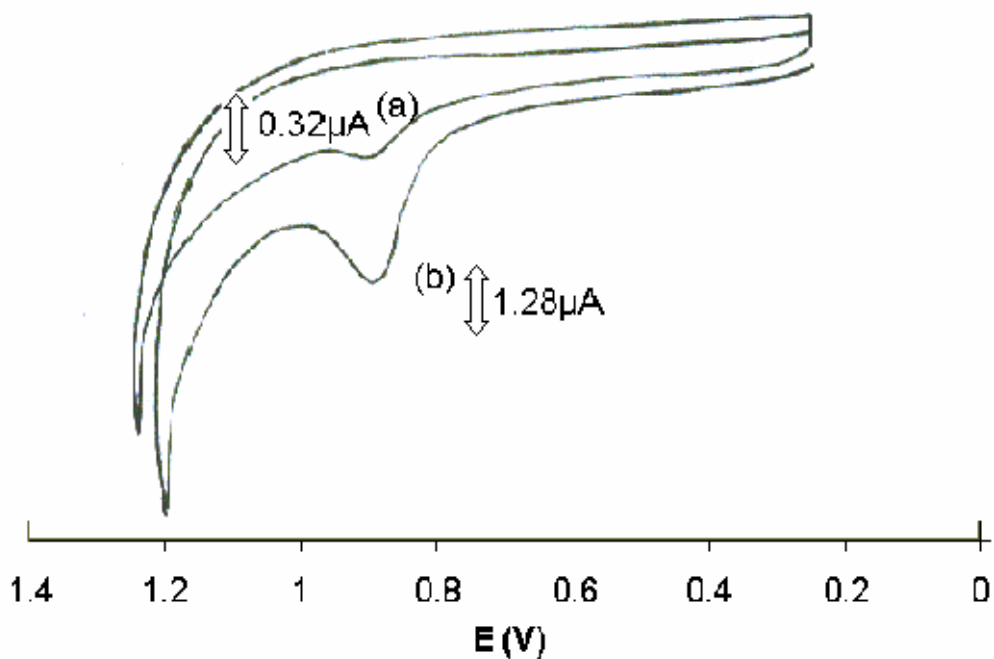


Figure (20): Cyclic voltammograms of $1 \times 10^{-5} \text{ M}$ NOR in acetate buffer solution (pH5) at: (a) bare GC electrode and (b) DNA-modified GC electrode. (Scan rate: 100 mV/s . Initial potential: $+0.2 \text{ V}$. Accumulation time: 1.0 min).

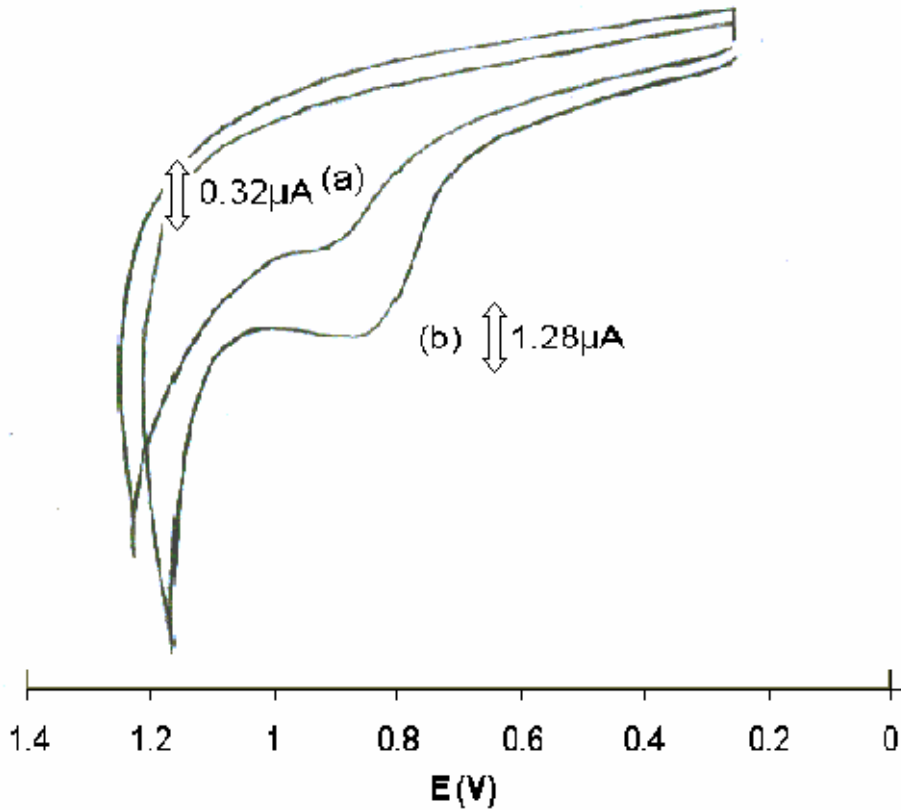


Figure (21): Cyclic voltammograms of $1 \times 10^{-5} \text{ M}$ ENR in acetate buffer solution (pH 5) at: (a) bare GC electrode and (b) DNA-modified GC electrode. (Scan rate: 100 mV/s . Initial potential: $+0.2 \text{ V}$. Accumulation time: 1.0 min).

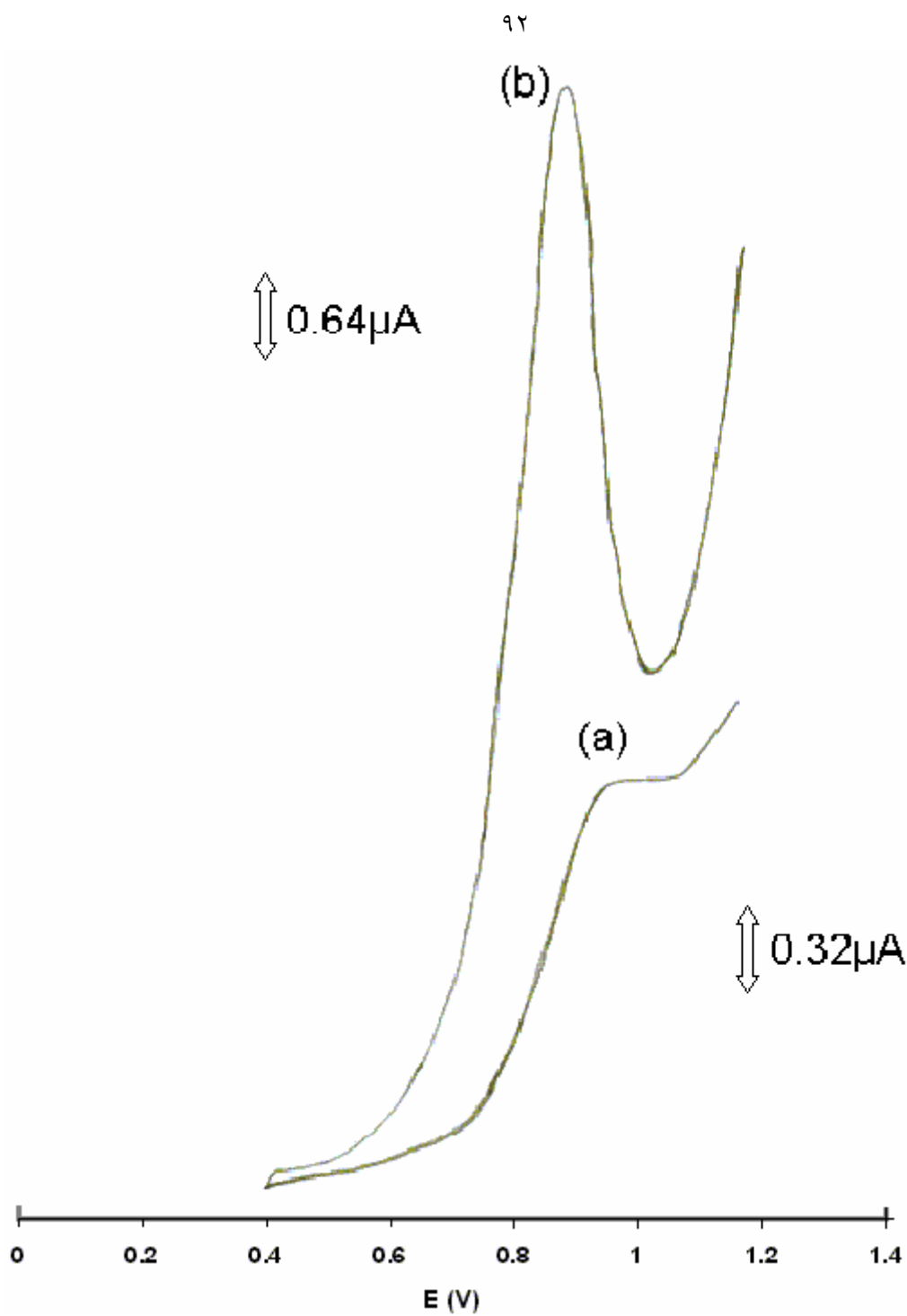


Figure (22): Differential-pulse anodic stripping voltammograms of 1×10^{-5} M CIP in acetate buffer solution (pH 5) at (a) bare GC electrode and (b) DNA-modified GC electrode. (Scan rate: 10 mV/s. Initial potential: +0.4 V. Accumulation time: 1.0 min).

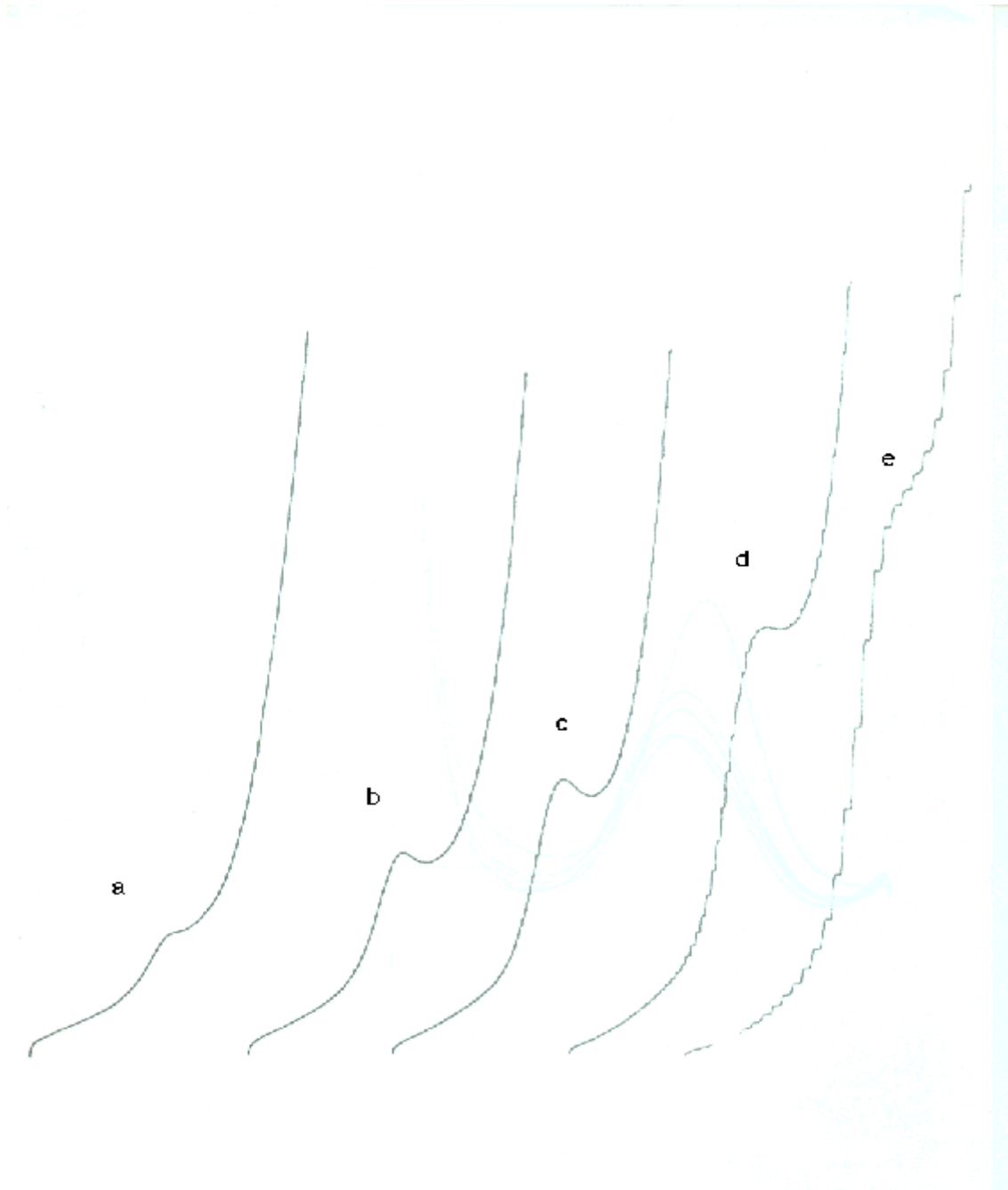


Figure (23): Differential-pulse anodic stripping voltammograms of 1×10^{-6} M CIP in acetate buffer solution (pH 5) at DNA-modified GC electrode at different scan rates (mV/s): (a) 5 (b) 10 (c) 20 (d) 50 (e) 100. (Initial potential: +0.4 V. Accumulation time: 1.0 min).

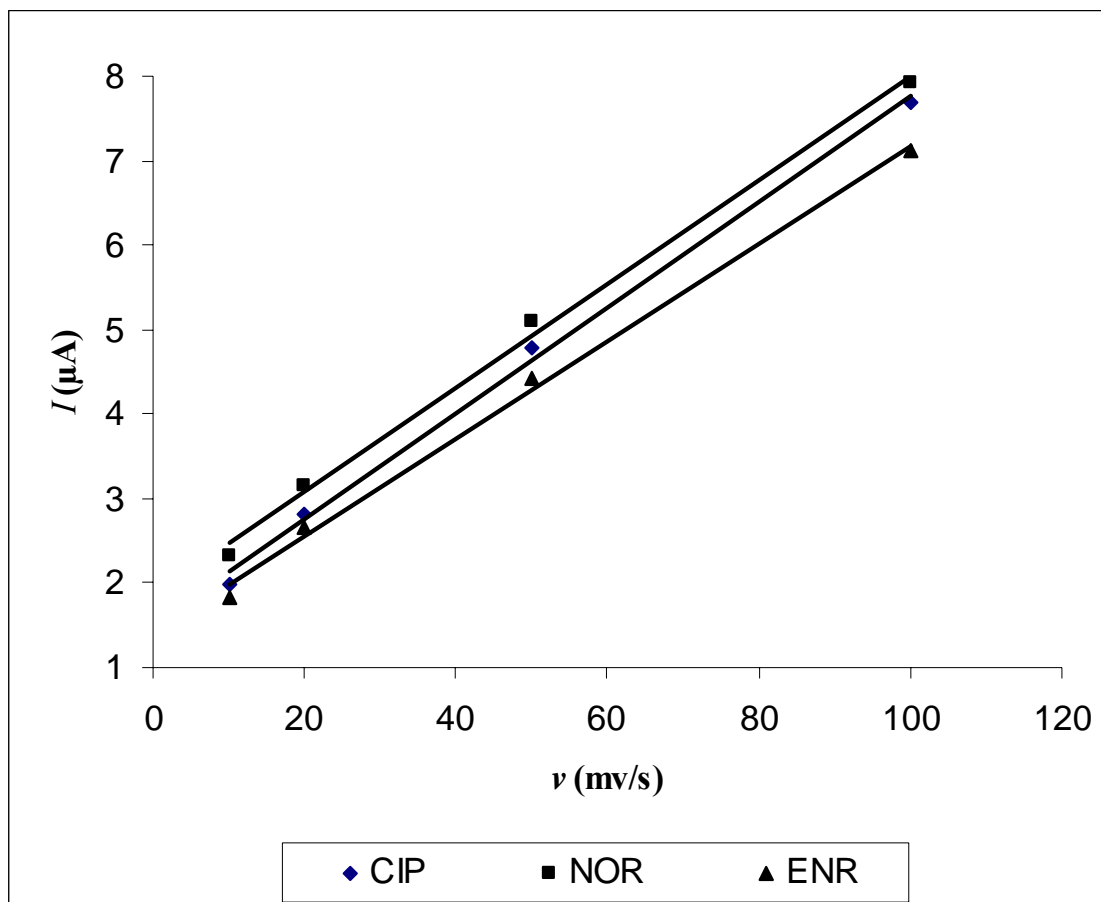


Figure (24): Effect of scan rate on the DPASV peak currents of $1 \times 10^{-6} \text{M}$ drug in acetate buffer solution (pH 5) at DNA-modified GC electrode. (Initial potential: +0.4 V. Accumulation potential: 1.0 min).

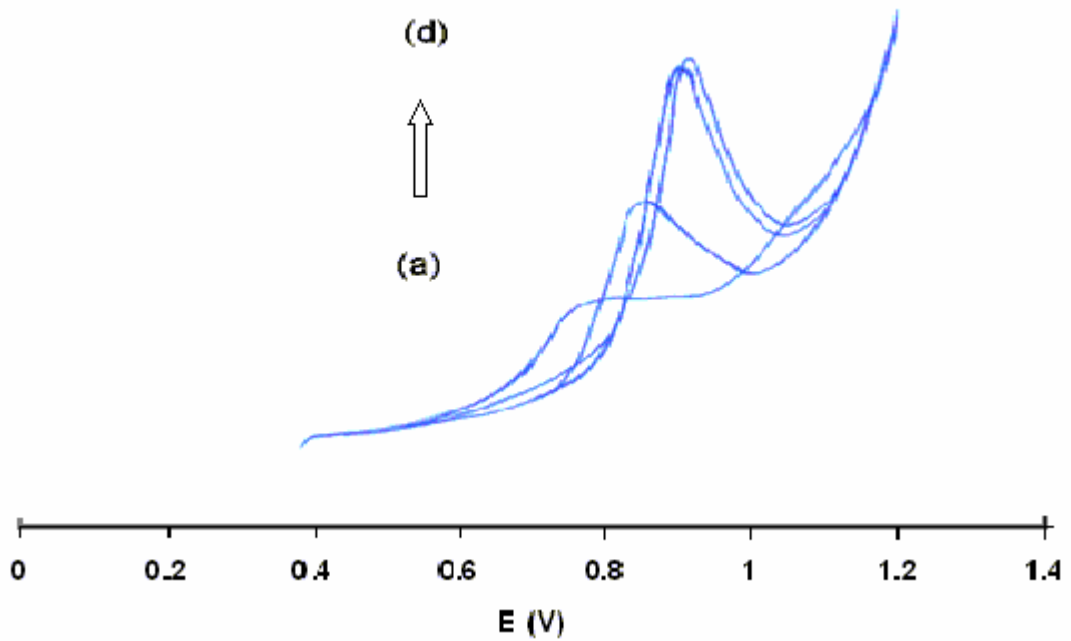


Figure (25): Differential - pulse anodic stripping voltammograms of 1×10^{-5} M CIP at DNA-modified GC electrode in acetate buffer solutions of different pH values: (a) pH 9, (b) pH 7, (c) pH 5, (d) pH 3.5. (Scan rate: 10 mV/s. Accumulation time: 1.0 min. Initial potential: + 0.4 V).

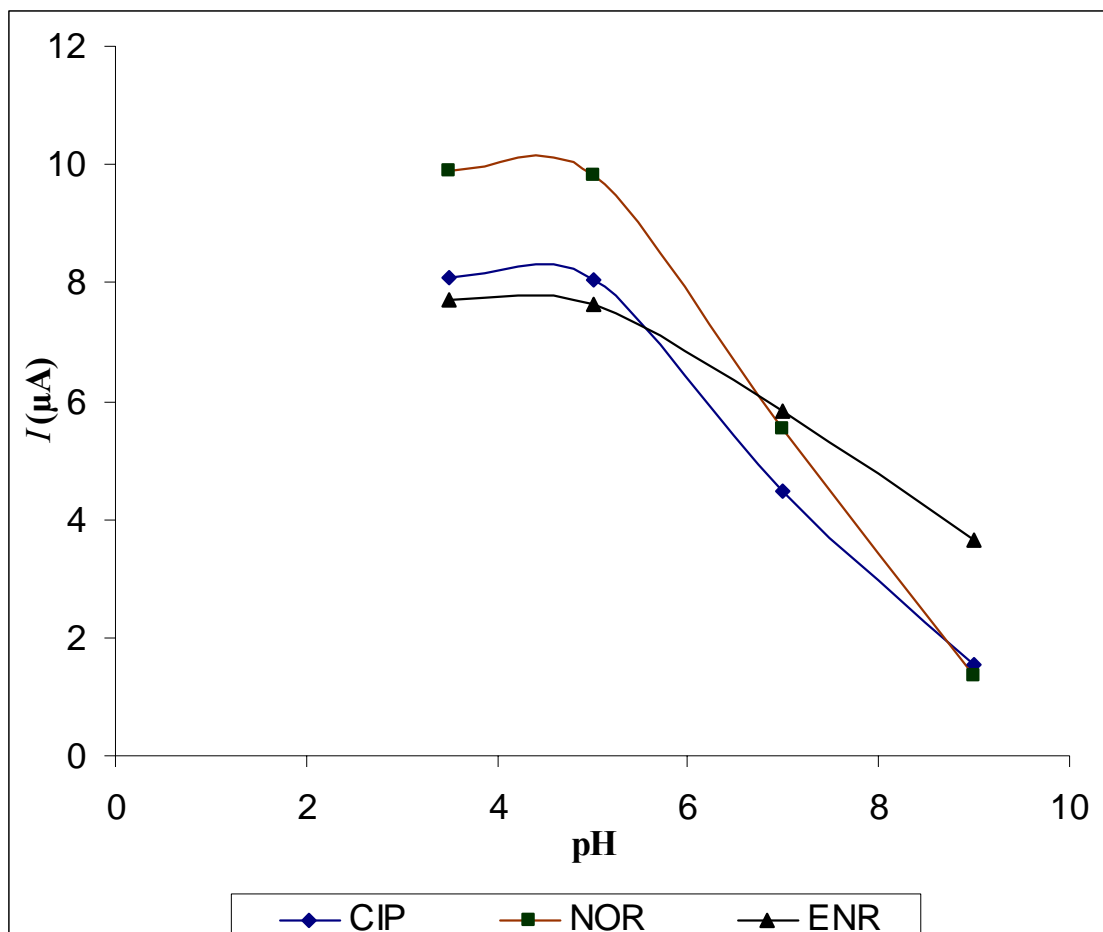


Figure (26): Effect of pH on the DPASV peak currents of $1 \times 10^{-5} \text{M}$ drug in acetate buffer solution at DNA-modified GC electrode. (Scan rate: 10 mV/s. Initial potential: +0.2 V. Accumulation potential: 1.0 min).

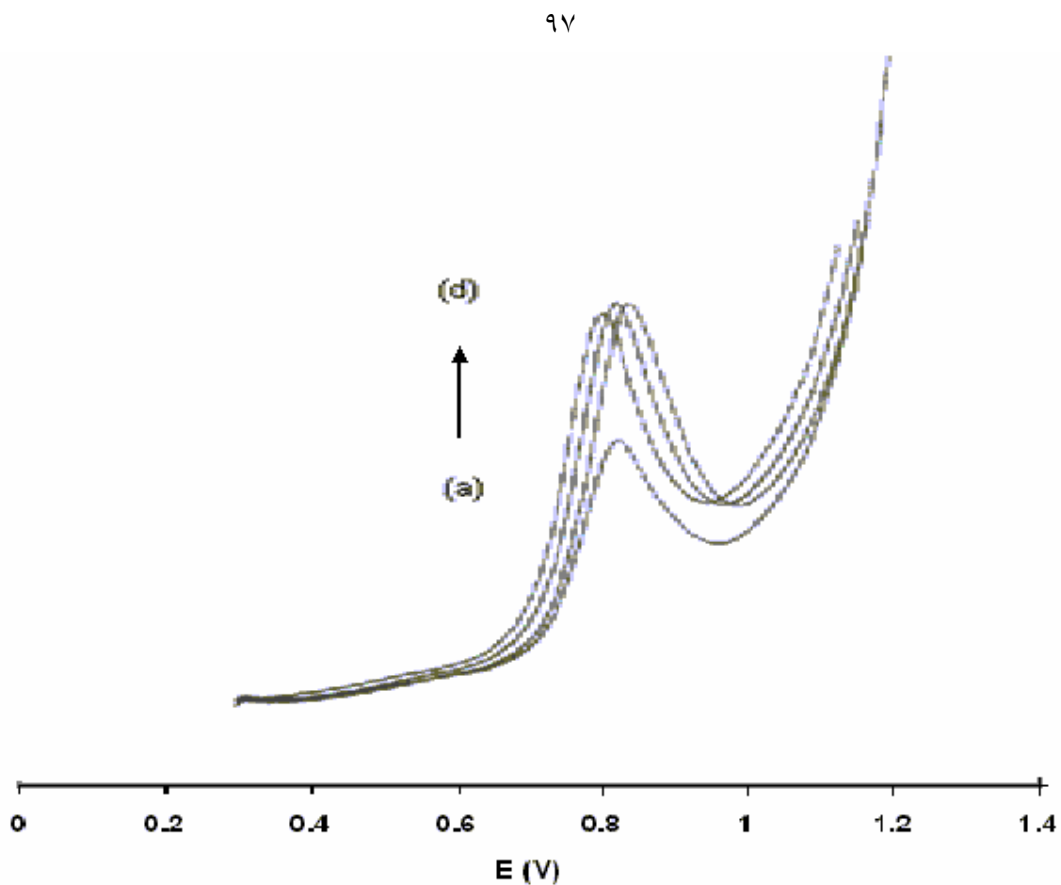


Figure (27): Differential-pulse anodic stripping voltammograms of 1×10^{-5} M CIP at DNA-modified GC electrode in acetate buffer solution (pH 5) at different accumulation times (s): (a) 15, (b) 30, (c) 60, (d) 120. (Scan rate: 10 mV/s. Initial potential: +0.3 V).

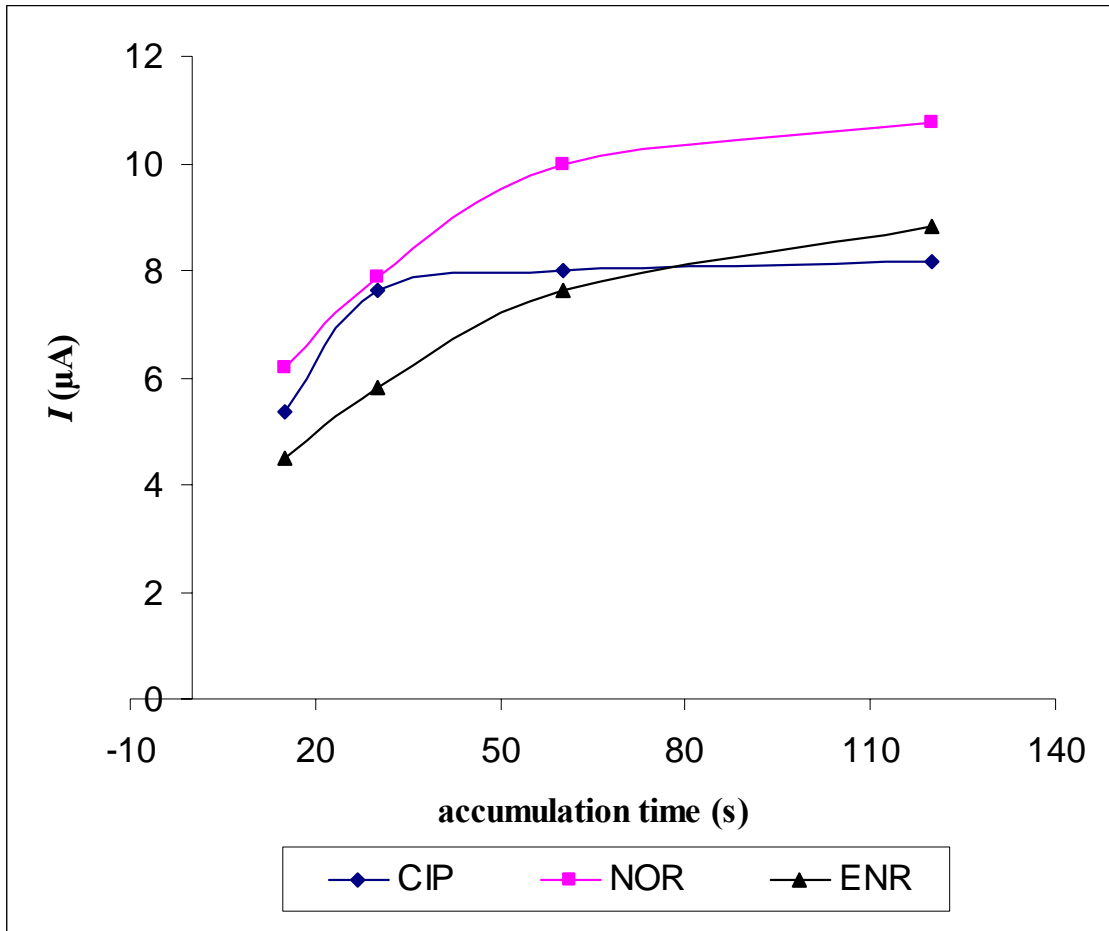


Figure (28): Effect of accumulation time on the DPASV peak currents of $1 \times 10^{-5} \text{M}$ drug in acetate buffer solution (pH 5) at DNA-modified GC electrode. (Scan rate: 10 mV/s. Initial potential: +0.2 V).

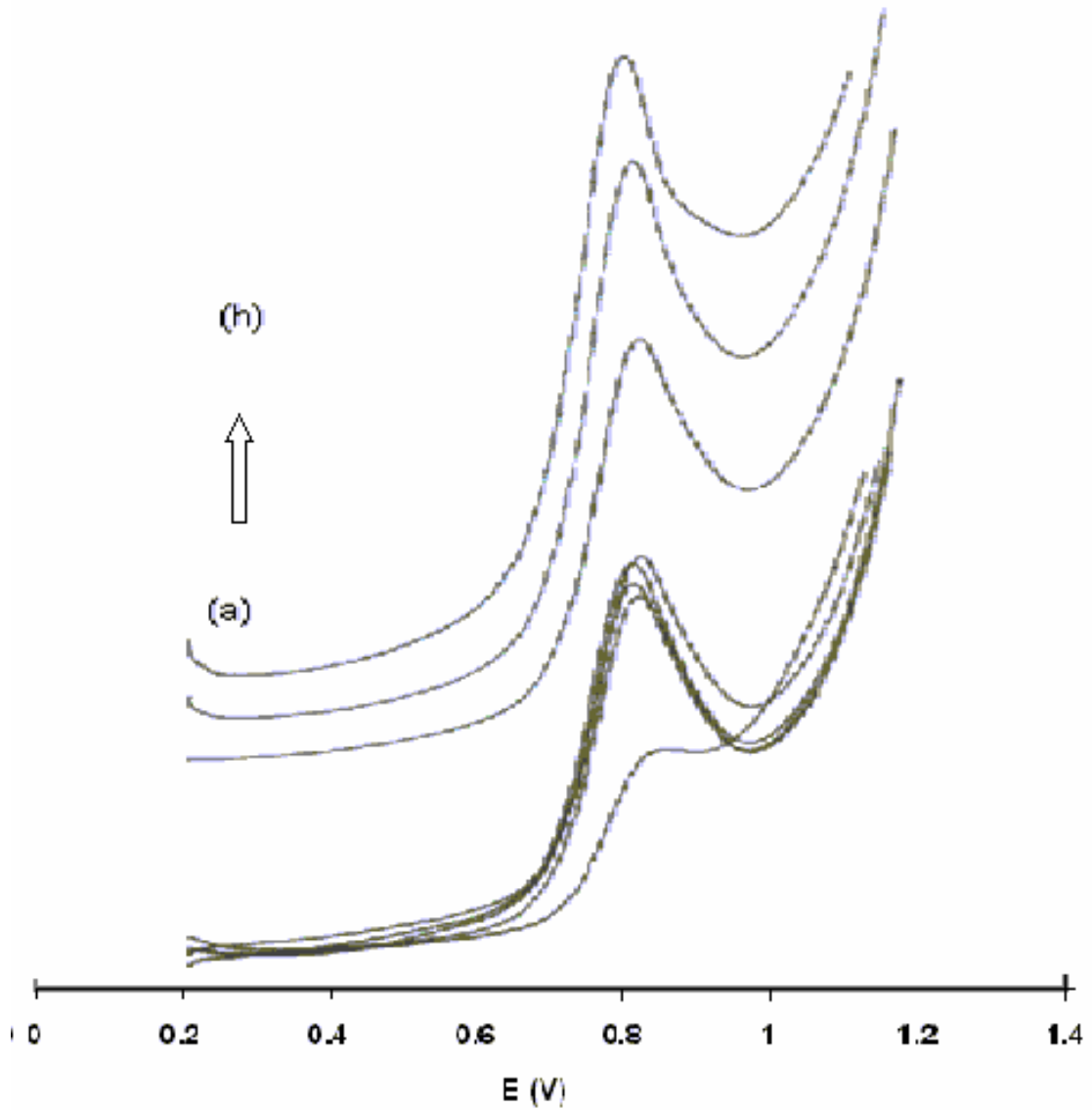


Figure (29): Differential-pulse anodic stripping voltammograms of 1×10^{-5} M CIP at DNA-modified GC electrode in acetate buffer solution (pH 5) at different accumulation potentials (V): (a) +0.8, (b) +0.6, (c) +0.4, (d) +0.2, (e) 0.0, (f) -0.2, (g) -0.4, (h) -0.6 . (Scan rate: 10 mV/s. Initial potential: +0.2 V. Accumulation time: 30s).

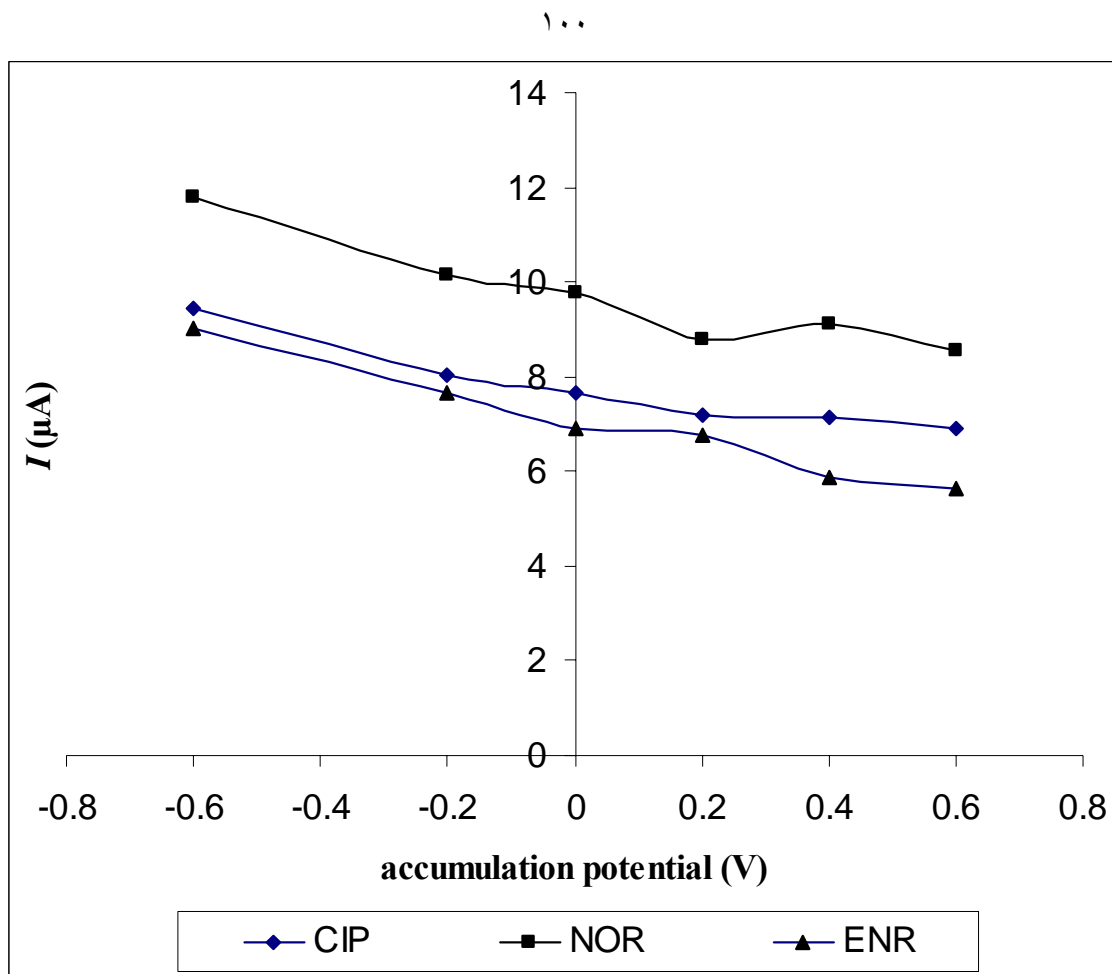


Figure (30): Effect of accumulation potential on the DPASV peak currents of $1 \times 10^{-5} \text{M}$ drug in acetate buffer solution (pH 5) at DNA-modified GC electrode. (Scan rate: 10 mV/s. Initial potential: +0.2 V. Accumulation time: 30s).

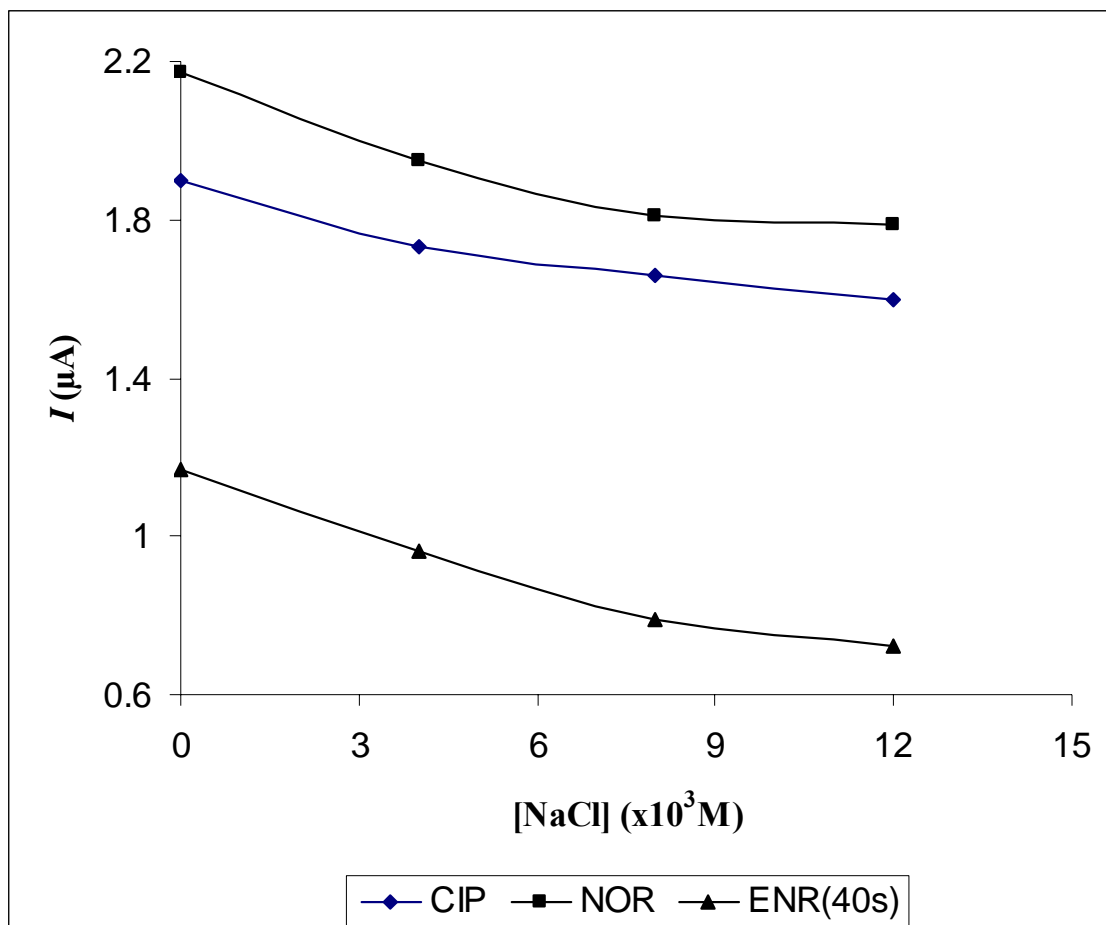


Figure (31): Effect of ionic strength on the DPASV peak currents of $1 \times 10^{-6} \text{M}$ drug in acetate buffer solution (pH 5) at DNA-modified GC electrode. (Scan rate: 10 mV/s. Initial potential: +0.4 V. Accumulation time: 60s for CIP and NOR and 40s for ENR).

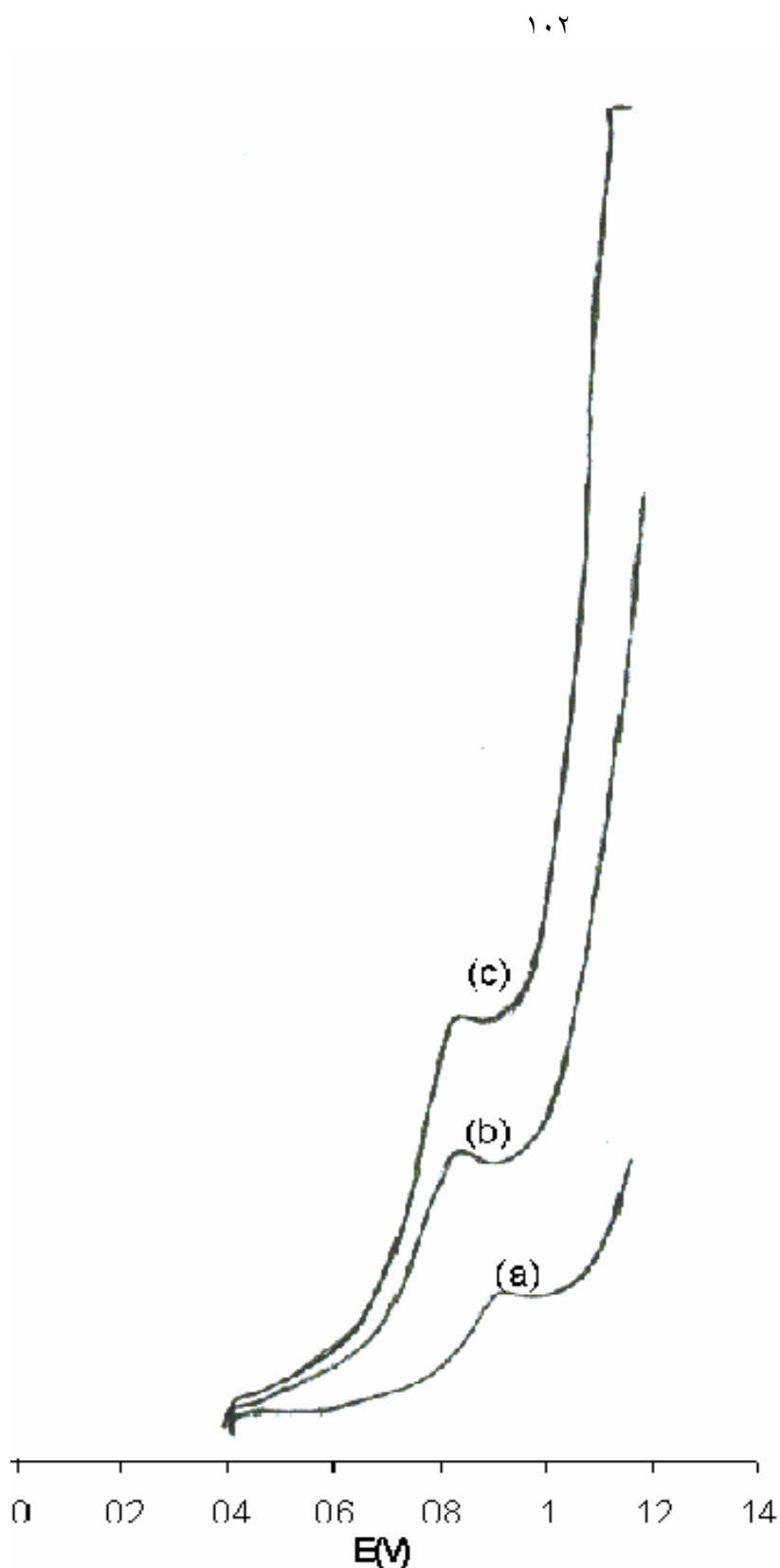


Figure (32): Differential-pulse anodic stripping voltammograms of 1×10^{-6} M CIP at DNA-modified GC electrode in acetate buffer solution (pH 5) at different pulse amplitudes (mV): (a) 25, (b) 50, (c) 100. (Scan rate: 10 mV/s. Initial potential: +0.4 V. Accumulation time: 30 s).

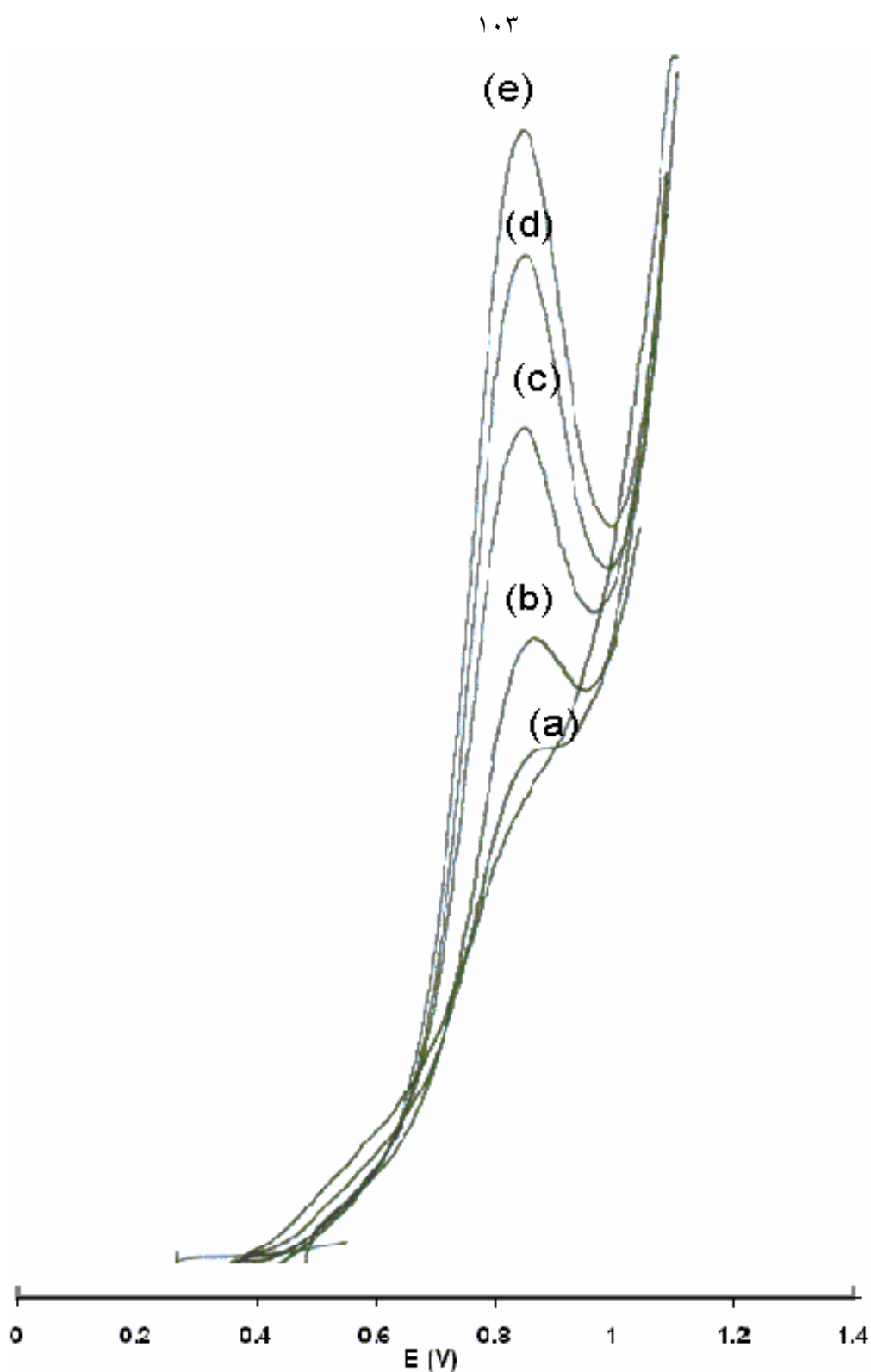


Figure (33): Differential-pulse anodic stripping voltammograms of different concentrations (μM) of CIP at DNA-modified GC electrode in acetate buffer solution (pH 5): (a) 1.0, (b) 2.0, (c) 3.0, (d) 4.0, (e) 5.0. (Scan rate: 10 mV/s. Initial potential: +0.4 V. Accumulation time: 30s).

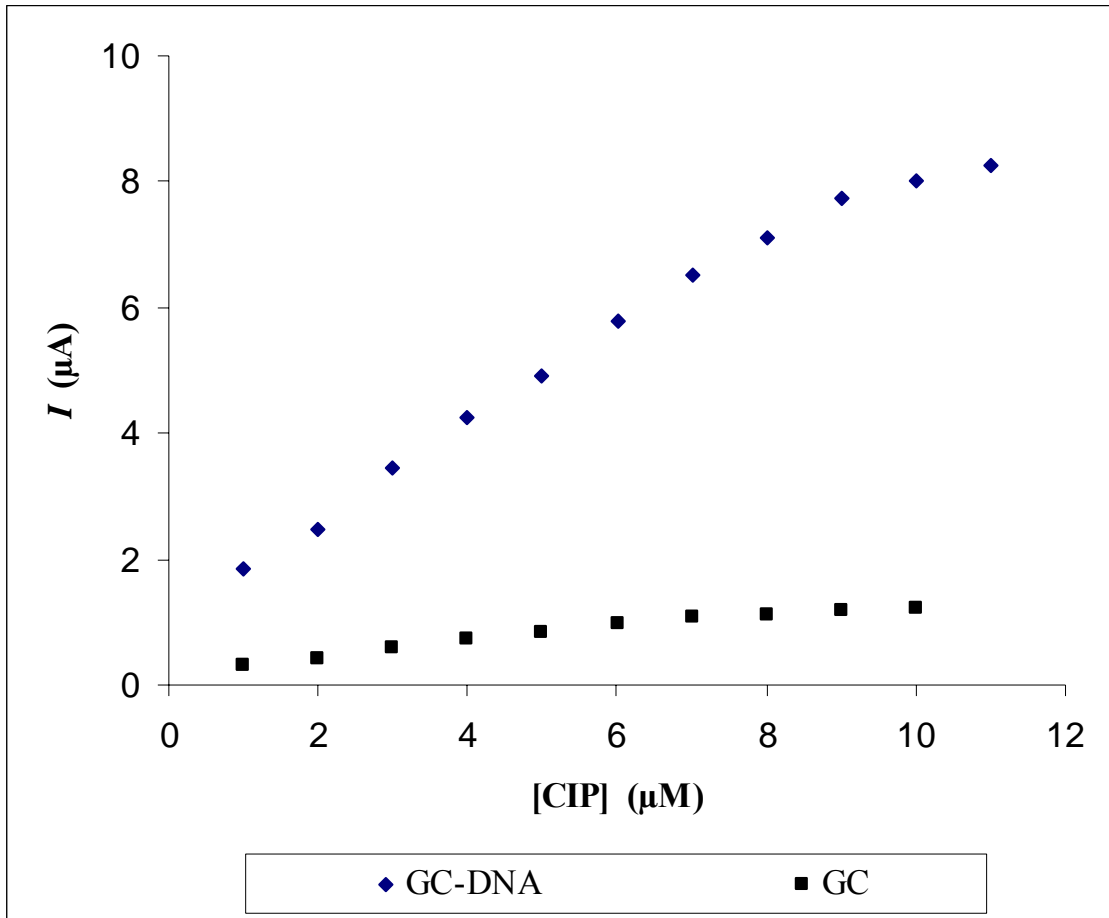


Figure (34): Effect of CIP concentration on the DPASV peak currents in acetate buffer solution (pH 4) at bare and DNA-modified GC electrode. (Scan rate: 10 mV/s. Initial potential: +0.4 V. Accumulation time: 60s).

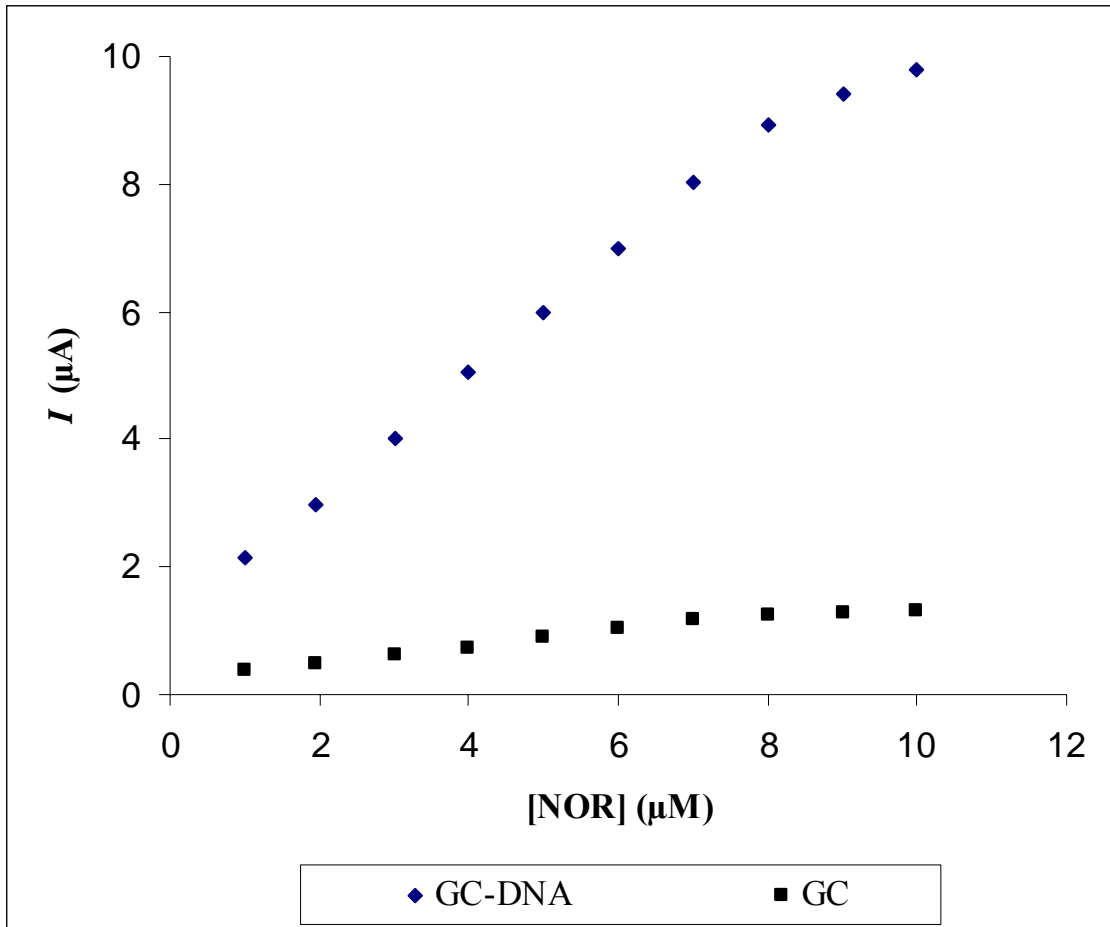


Figure (35): Effect of NOR concentration on the DPASV peak currents in acetate buffer solution (pH 4) at DNA-modified GC electrode. (Scan rate: 10 mV/s. Initial potential: +0.4 V. Accumulation time: 60s).

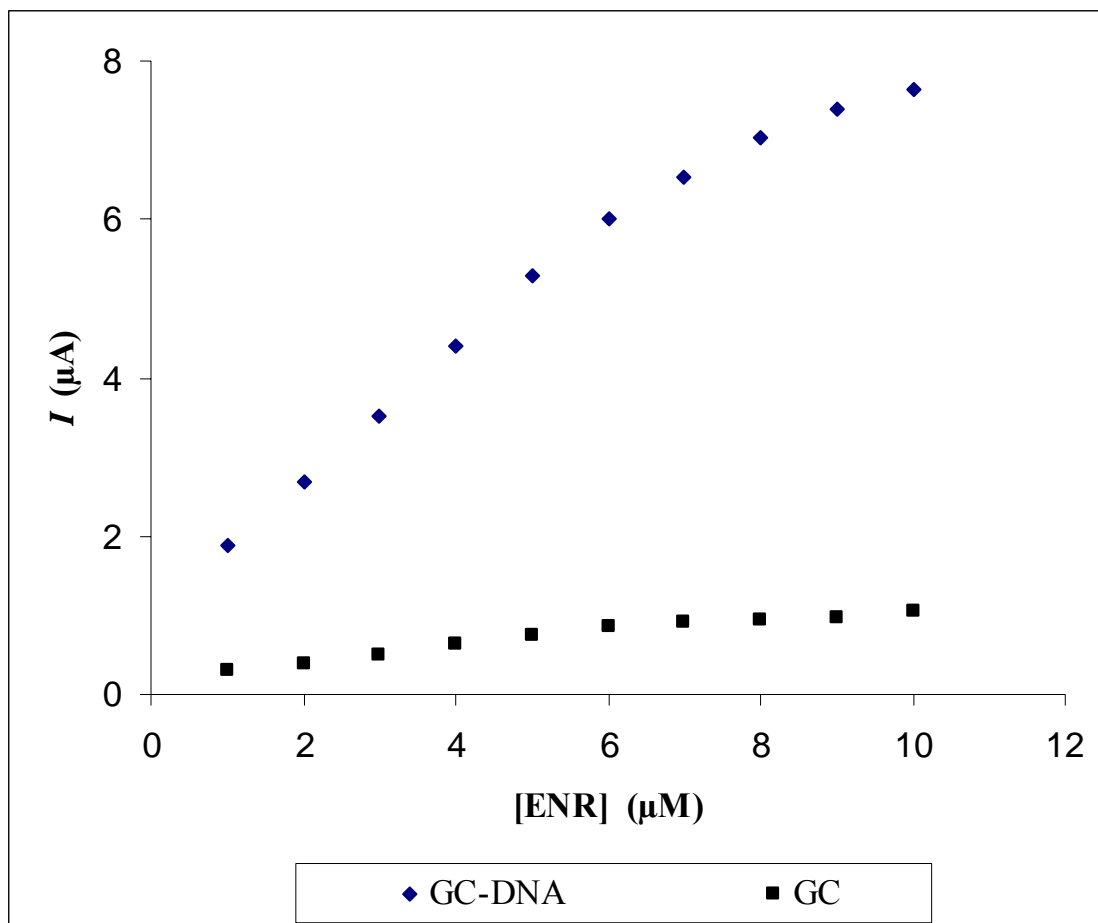


Figure (36): Effect of ENR concentration on the DPASV peak currents in acetate buffer solution (pH 4) at DNA-modified GC electrode. (Scan rate: 10 mV/s. Initial potential: +0.4 V. Accumulation time: 60s).

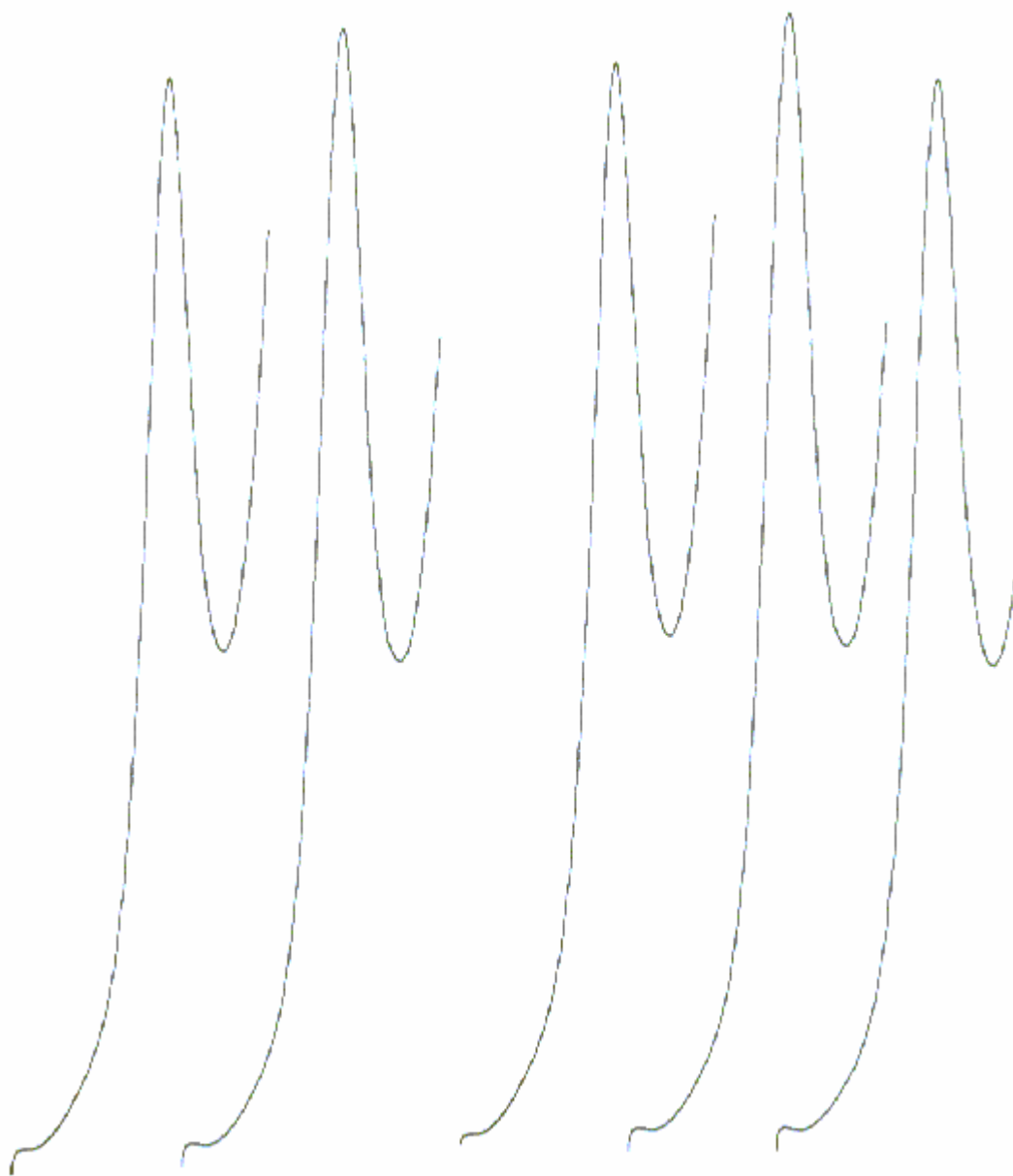


Figure (37): Differential-pulse anodic stripping voltammograms of different samples of Ciprocare tablet solution. (Scan rate: 10 mV/s. Initial potential: +0.4 V. Accumulation time: 60s).

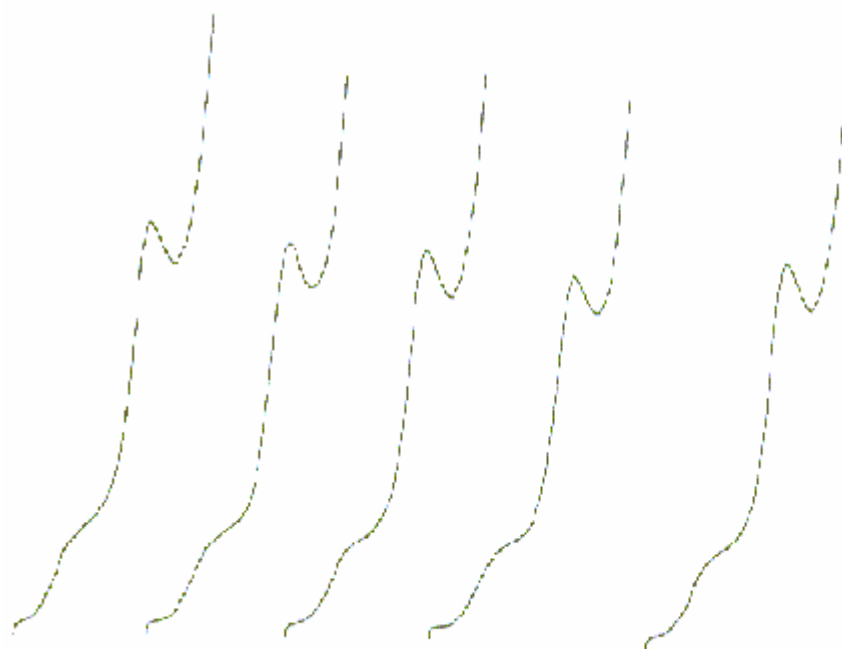
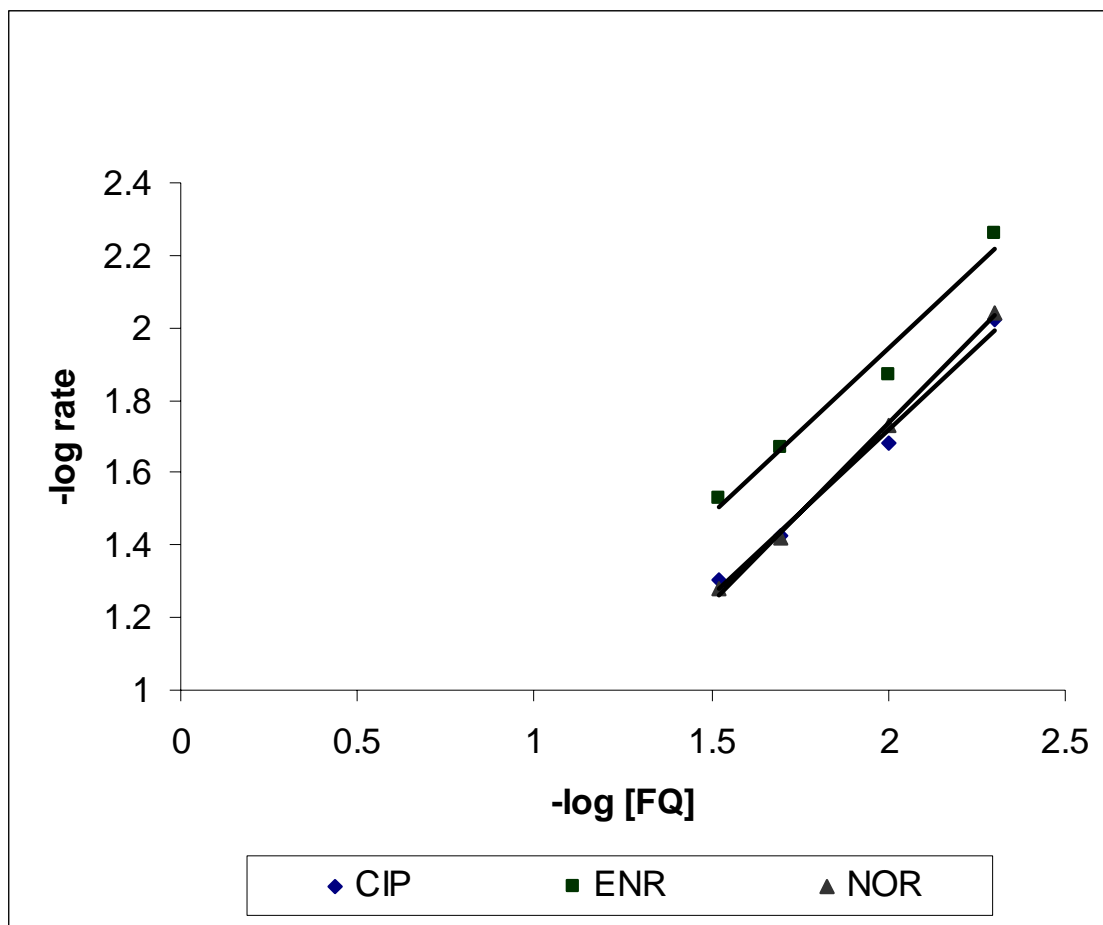
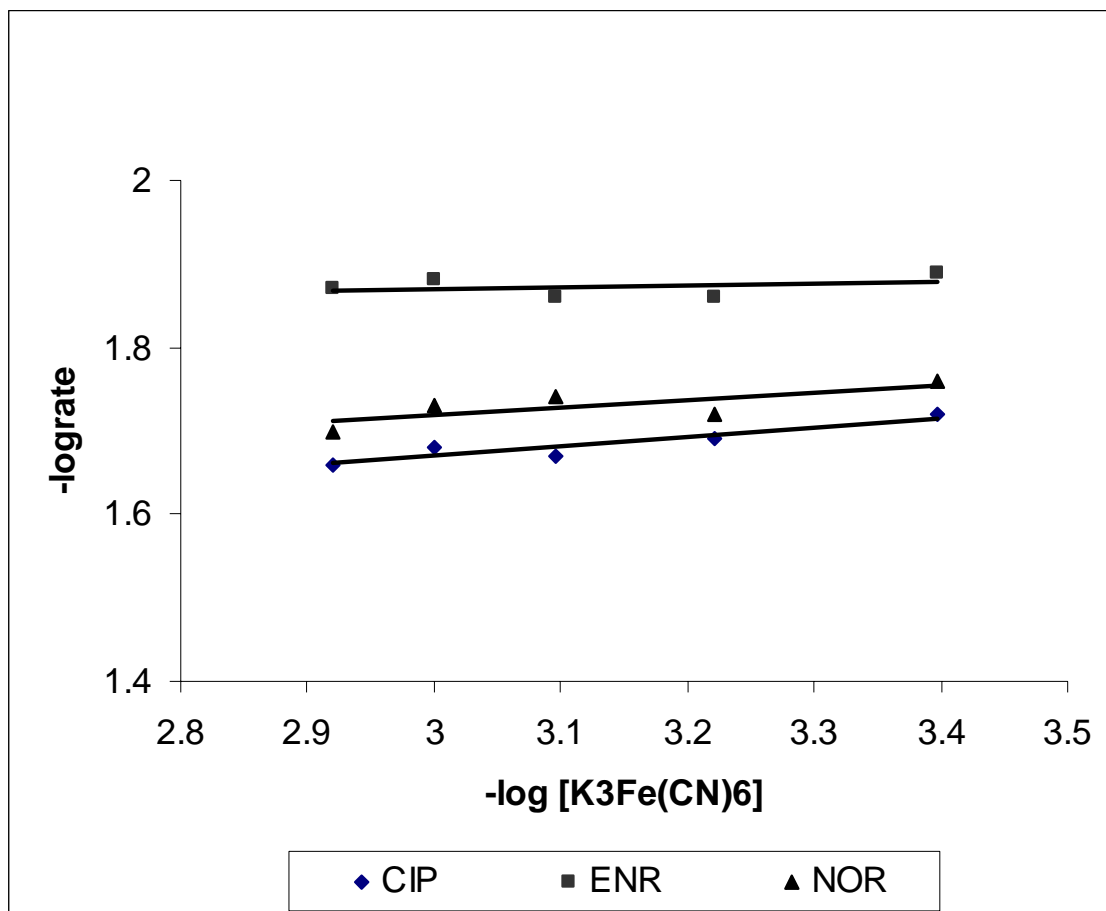


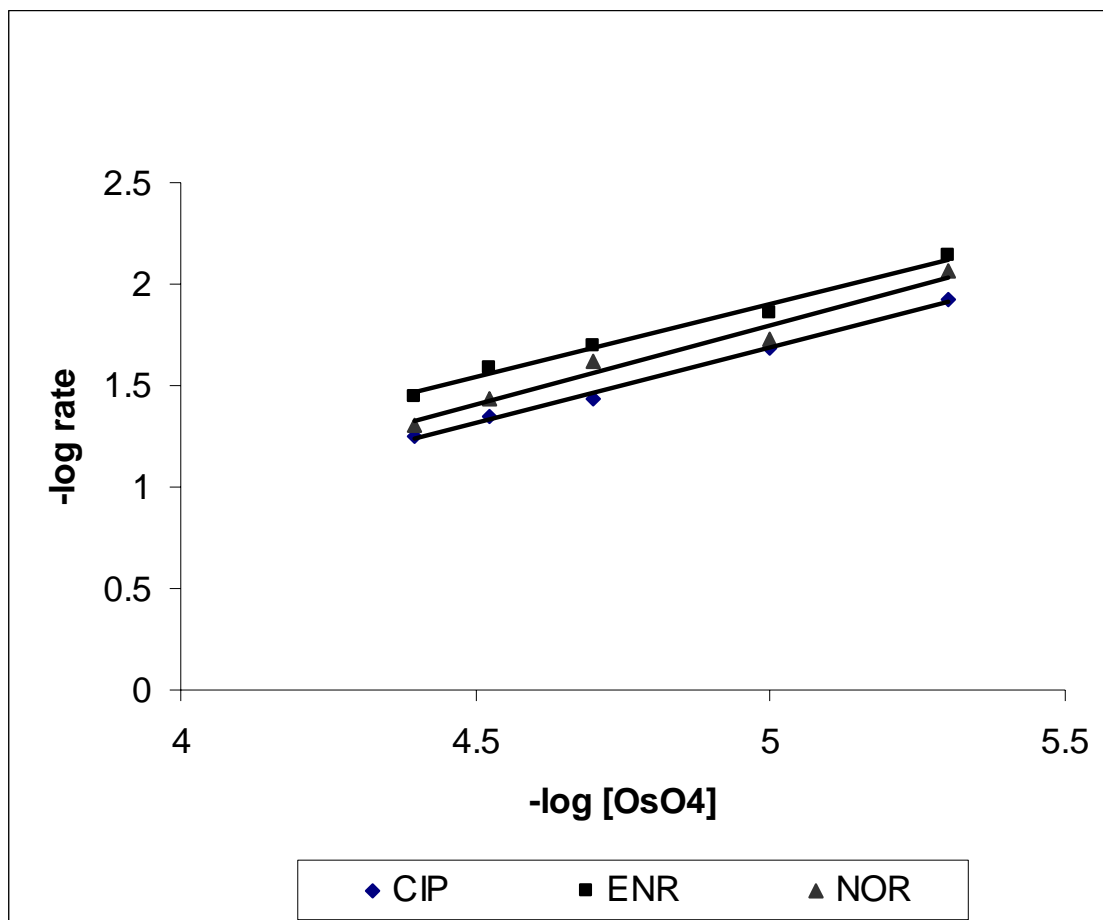
Figure (38): Differential-pulse anodic stripping voltammograms of urine samples spiked with CIP. (Scan rate: 10 mV/s. Initial potential: +0.4 V. Accumulation time: 60s).



Figure(39): Effect of FQ concentration on reaction rate:
Plots of $-\log \text{rate}$ vs. $-\log [\text{FQ}]$, $[\text{K}_3\text{Fe}(\text{CN})_6] = 1 \times 10^{-3}\text{M}$, $[\text{OsO}_4] = 1 \times 10^{-5}\text{M}$, $[\text{OH}^-] = 0.1\text{M}$, temperature = 25°C , $\mu = 0.15$



Figure(40): Effect of $K_3Fe(CN)_6$ concentration on reaction rate:
 Plots of $-\log$ rate vs. $-\log [K_3Fe(CN)_6]$, $[FQ] = 0.01M$, $[OsO_4] = 1 \times 10^{-5}M$, $[OH^-] = 0.1M$, temperature = $25^\circ C$, $\mu = 0.15$



Figure(41): Effect of OsO_4 concentration on reaction rate:
Plots of $-\log \text{rate}$ vs. $-\log [\text{OsO}_4]$, $[\text{FQ}] = 0.01\text{M}$, $[\text{K}_3\text{Fe}(\text{CN})_6] = 1 \times 10^{-3}\text{M}$, $[\text{OH}^-] = 0.1\text{M}$, temperature = 25°C , $\mu = 0.15$

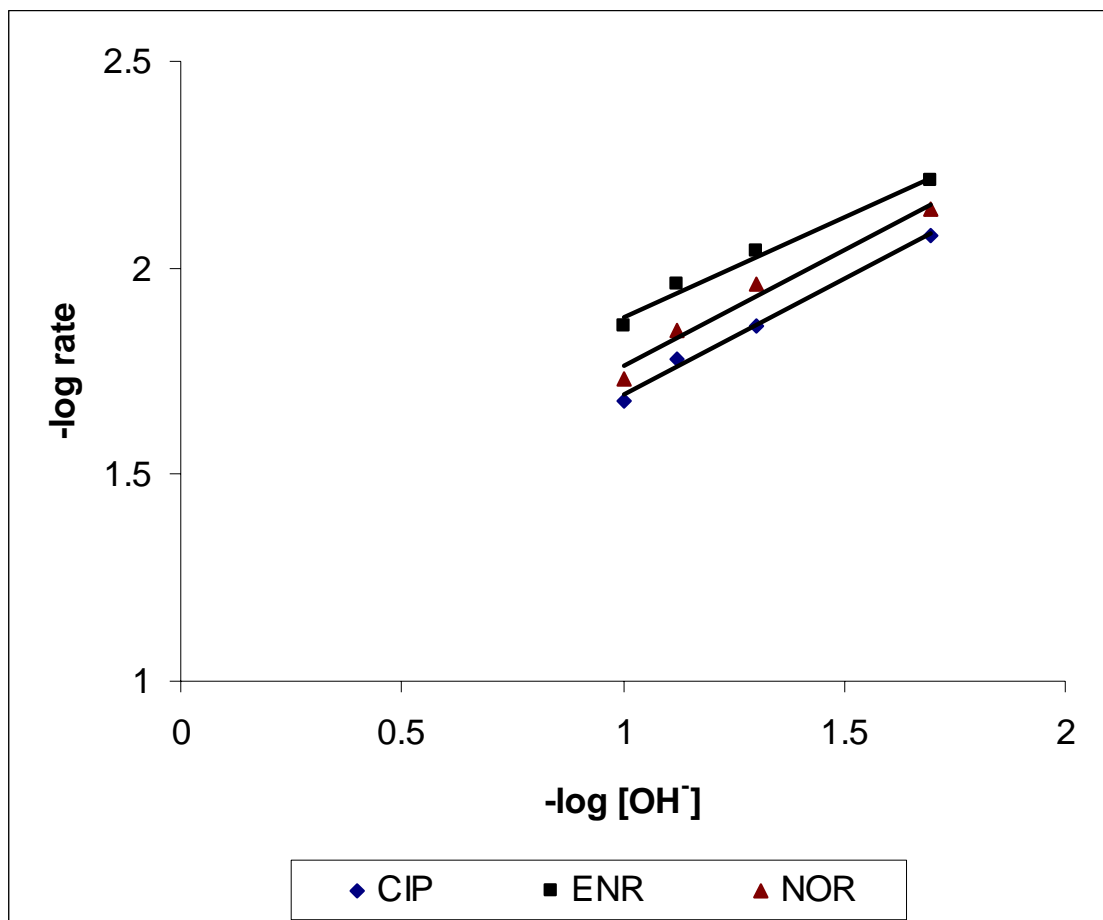
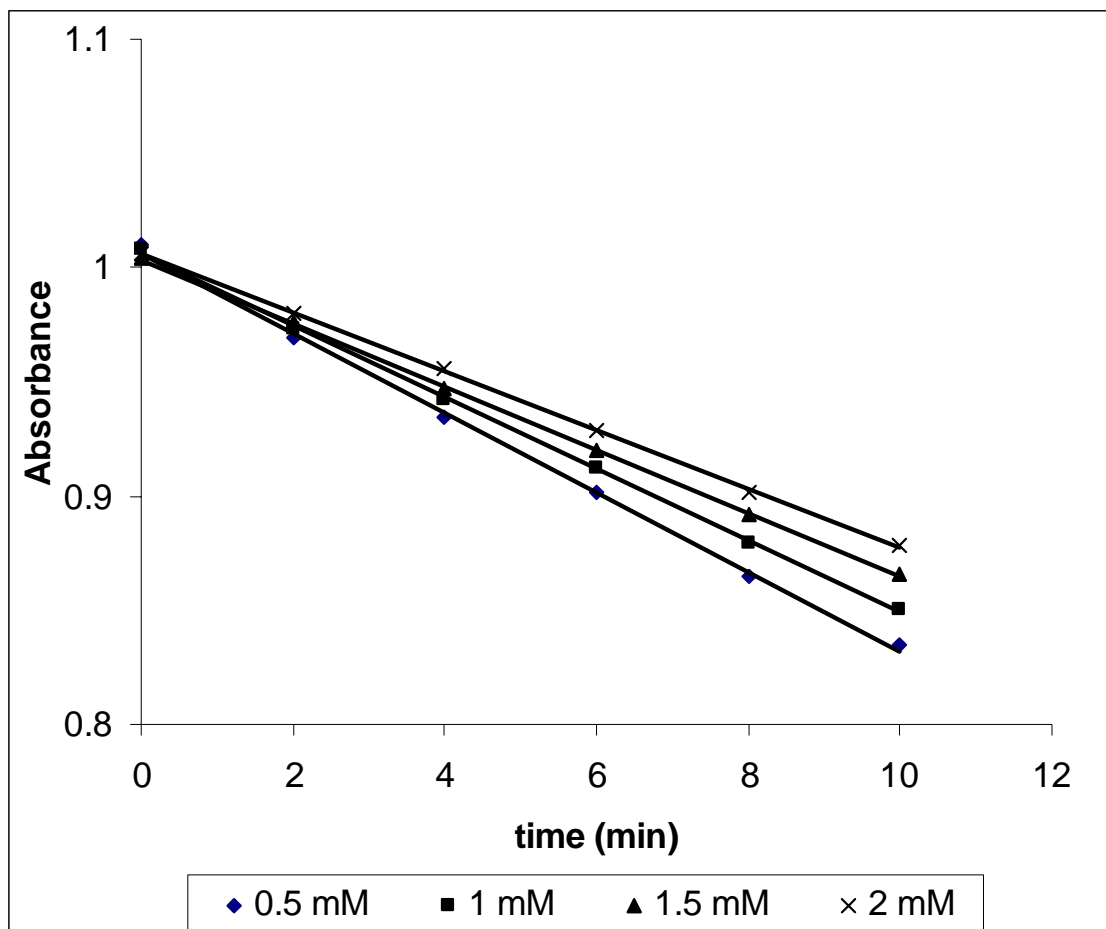
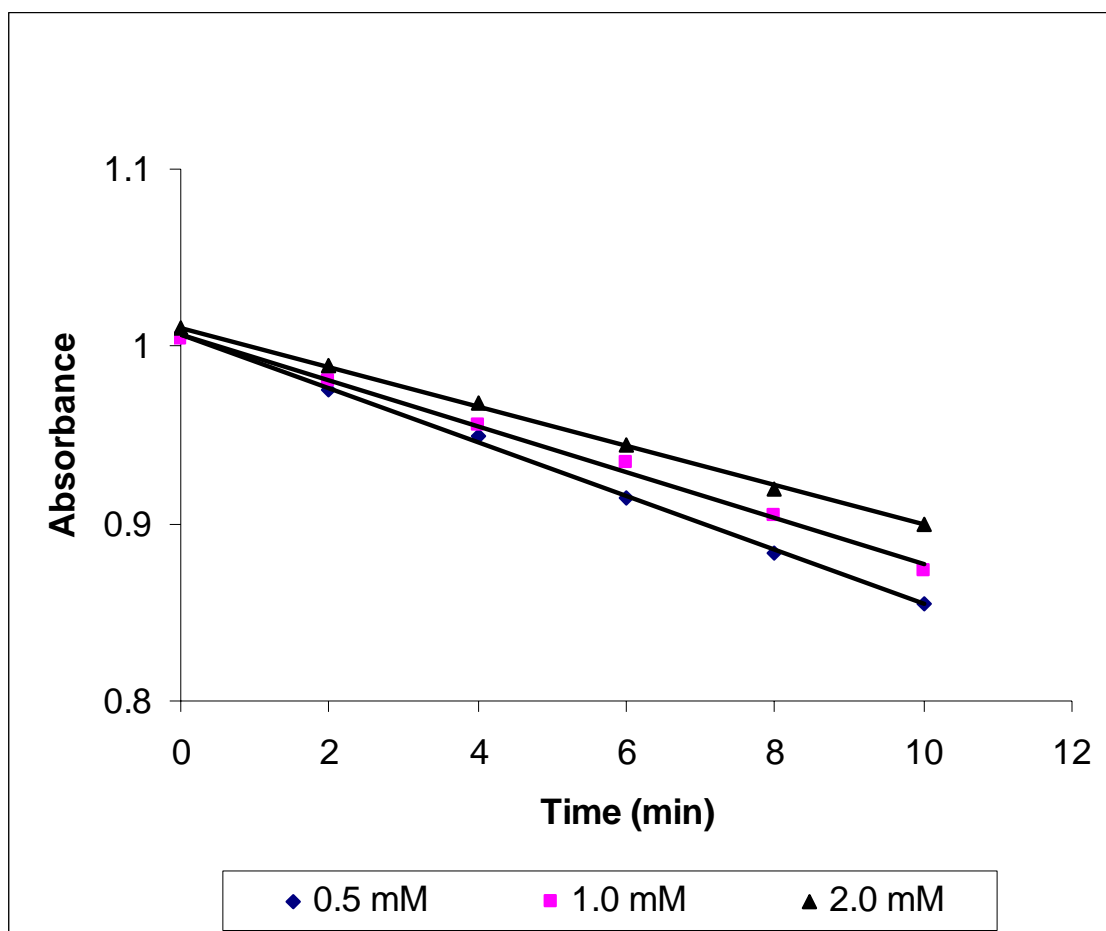


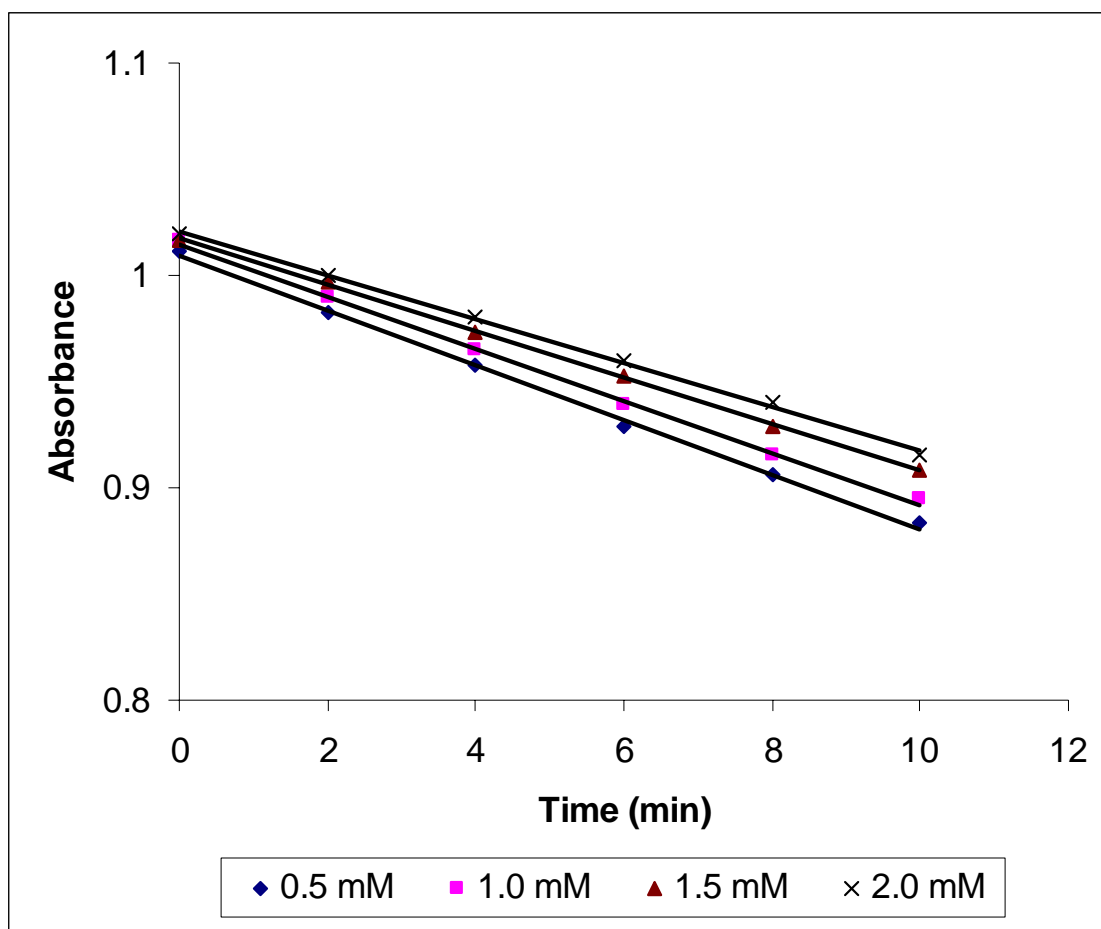
Figure (42): Effect of hydroxide ion concentration on reaction rate:
Plots of $-\log \text{rate}$ vs. $-\log [\text{OH}^-]$, $[\text{FQ}] = 0.01\text{M}$, $[\text{K}_3\text{Fe}(\text{CN})_6] = 1 \times 10^{-3}\text{M}$,
 $[\text{OsO}_4] = 1 \times 10^{-5}\text{M}$, temperature = 25°C , $\mu = 0.15$



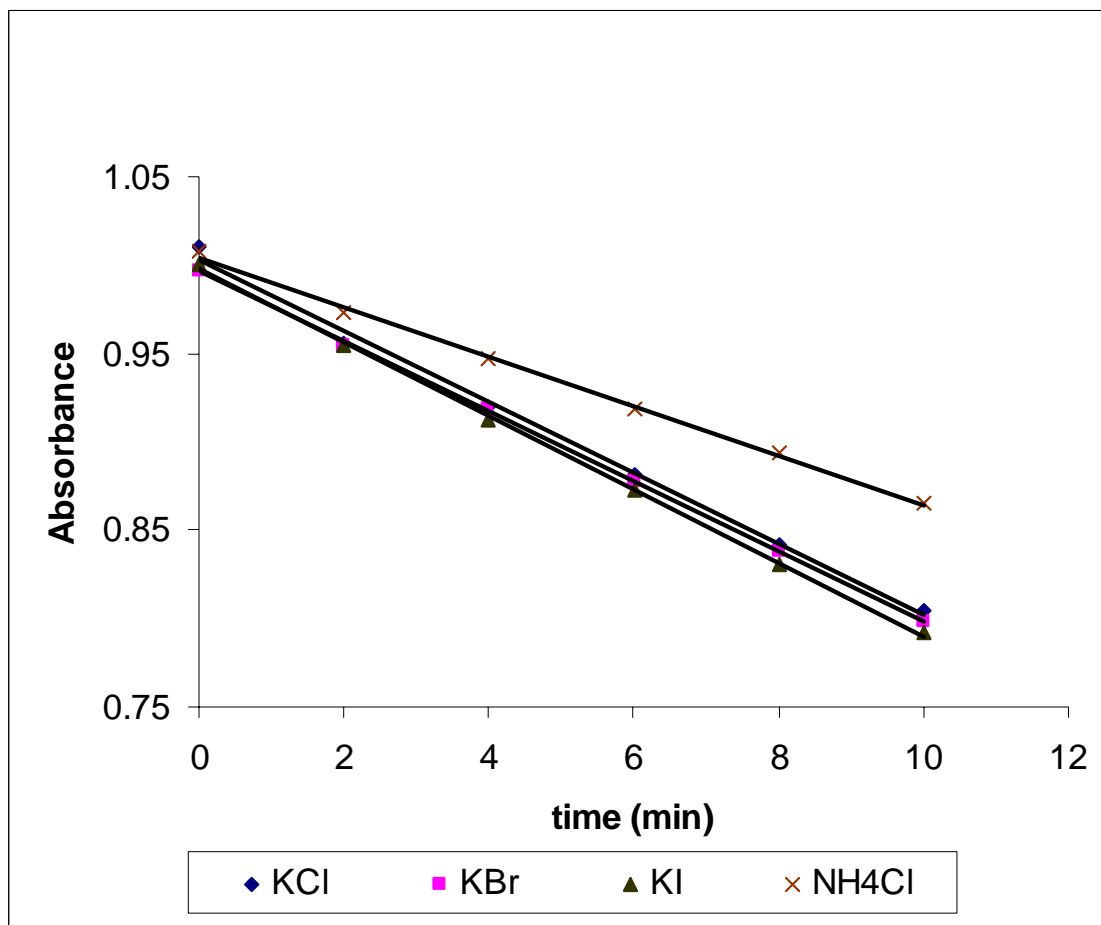
Figure(43): Effect of added $K_4Fe(CN)_6$ on ciprofloxacin reaction rate:
[CIP]=0.01M, $[K_3Fe(CN)_6]=1 \times 10^{-3}M$, $[OsO_4]=1 \times 10^{-5}M$, $[OH^-]=0.1M$,
temperature = $25^\circ C$, $\mu = 0.15$



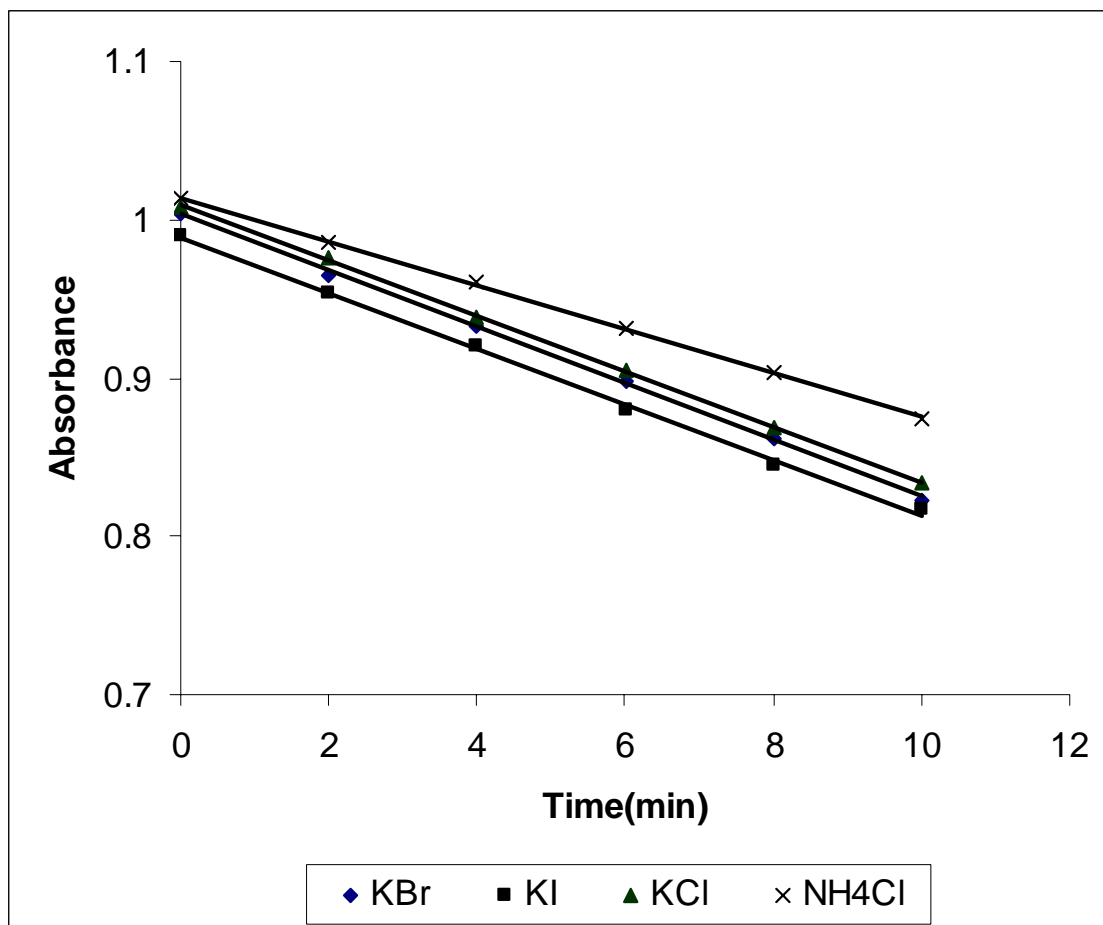
Figure(44): Effect of added $K_4Fe(CN)_6$ on norfloxacin reaction rate:
[NOR] = 0.01M, $[K_3Fe(CN)_6] = 1 \times 10^{-3}M$, $[OsO_4] = 1 \times 10^{-5}M$, $[OH^-] = 0.1M$, temperature = $25^\circ C$, $\mu = 0.15$



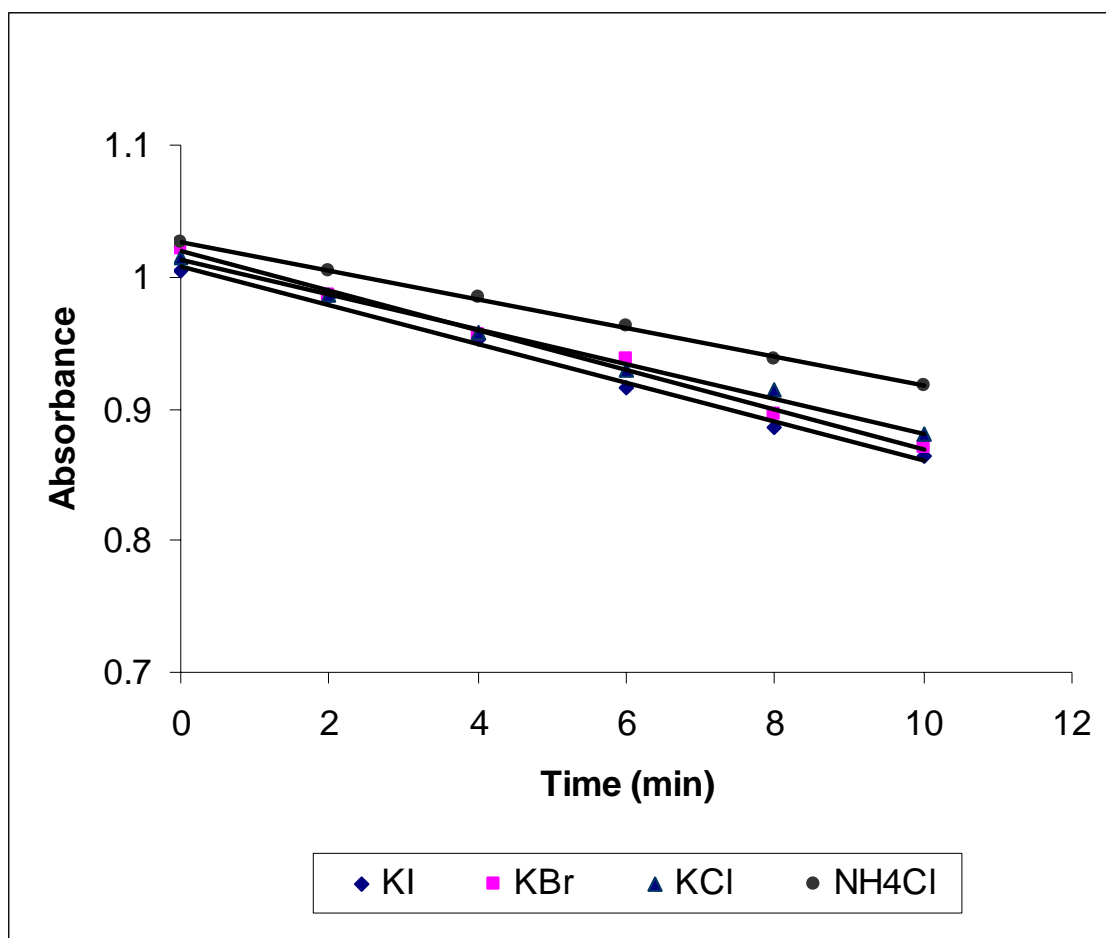
Figure(45): Effect of added $K_4Fe(CN)_6$ on enrofloxacin reaction rate:
[ENR] = 0.01M, $[K_3Fe(CN)_6] = 1 \times 10^{-3}M$, $[OsO_4] = 1 \times 10^{-5}M$, $[OH^-] = 0.1M$
temperature = 25°C, $\mu = 0.15$



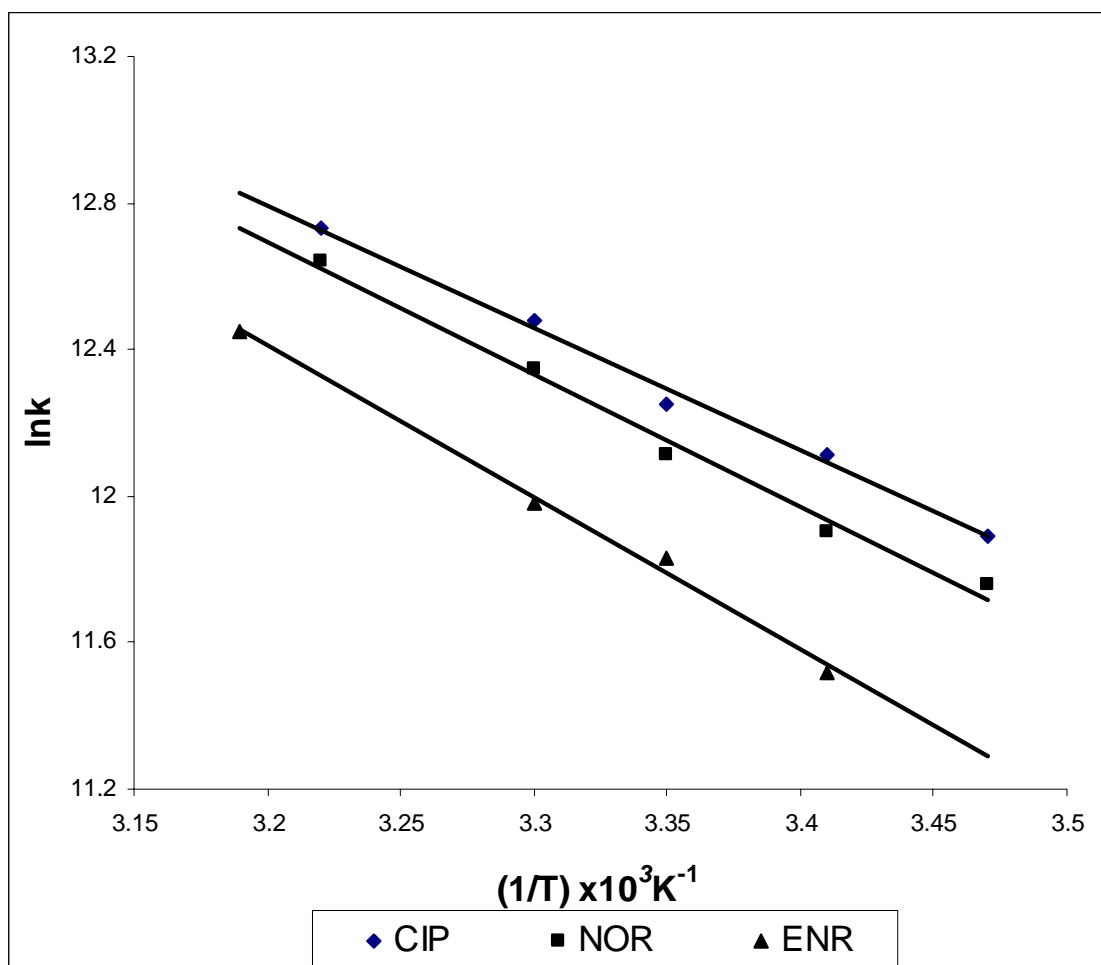
Figure(46): Effect of added salt on ciprofloxacin reaction rate:
[CIP] = 0.01M, [K₃Fe(CN)₆] = 1x10⁻³M, [OsO₄] = 1x10⁻⁵M, [OH⁻] = 0.1M
temperature = 25°C, μ = 0.15



Figure(47): Effect of added salt on norfloxacin reaction rate:
[NOR] = 0.01M, $[K_3Fe(CN)_6] = 1 \times 10^{-3}M$, $[OsO_4] = 1 \times 10^{-5}M$, $[OH^-] = 0.1M$
temperature = 25°C, $\mu = 0.15$



Figure(48): Effect added of salt on enrofloxacin reaction rate:
[ENR] = 0.01M, [K₃Fe(CN)₆] = 1x10⁻³M, [OsO₄] = 1x10⁻⁵M, [OH⁻] = 0.1M temperature = 25°C, $\mu = 0.15$



Figure(49): Effect of temperature on reaction rate:
 Plot of $\ln k$ vs. $1/T$, $[ENR] = 0.01M$, $[K_3Fe(CN)_6] = 1 \times 10^{-3}M$, $[OsO_4] = 1 \times 10^{-5}M$, $[OH^-] = 0.1M, \mu = 0.15$

REFERENCES

REFERENCES

1. G. Y. Leshner et al., '1,8-Naphthyridine derivatives: A new class of chemotherapeutic reagents', *J. Med. Pharm. Chem.*, **5** (1962) 1063 – 1065.
2. R. Gleckman, S. Alvares, and D. W. Joubert, 'Drug therapy reviews: Nalidixic acid' *Am. J. Hosp. Pharm.* **36** (1979) 1071.
3. G. C. Crumplin, 'The involvement of DNA topoisomerases in DNA repair and mutagenesis', *Carcinogenesis* **2** (1981) 157.
4. E. W. McChensey et al., 'Absorption, excretion, and metabolism of a new antimicrobial agent, nalidixic acid', *Toxicol. Appl. Pharmacol.* **6** (1964) 292.
5. D. T. W. Chu, P. B. Fernandes, in: B. Testa (Ed.), *Advances in Drug Research*, **vol.21**, London, Academic Press, 1991, pp39-144.
6. H. Koga et al., 'Structure-activity relationships of antibacterial 6,7- and 7,8- disubstituted 1-alkyl-1,4-dihydro-4-oxoquinolone-3-carboxylic acids', *J. Med. Chem.*, **23** (1980) 1358 – 1363.
7. J. E. F. Reynolds (Ed.), *Martindale, The Extra Pharmacopeia*, **30th ed.**, The Pharmaceutical Press, London, 1993, pp145-147.
8. H. C. Neu, 'Resistance of ciprofloxacin appearing during therapy', *Am. J. Med.* **87** (1989) 28 - 31.
9. J. Steward et al., 'Treatment of murine pneumonic *Francisella tularensis* infection with gatifloxacin, moxifloxacin, or ciprofloxacin', *Curr. Med. Chem.*, (2006) in press.

10. S. L. Gorbach, K. W. Nelson, in: A. P. R. Wilson, R. N. Gruneberg (Eds.), *Ciprofloxacin: 10 Years of Clinical Experience*, Maxim Medical, Oxford, 1997.
11. T. Skauge, I. Turel, and E. Sletten, 'Interaction between ciprofloxacin and DNA mediated by Mg^{2+} ions', *Inorg. Chim. Acta*, **339** (2002) 239-247.
12. A. J. Angel et al., 'Sensitive determination of ciprofloxacin and norfloxacin in biological fluids using an enzymatic rotating biosensor', *Biosens. Bioelectron.*, (2006) in press.
13. W. Michaela et al., 'Urinary bactericidal activity and pharmacokinetics of enrofloxacin versus norfloxacin and ciprofloxacin in healthy volunteers after a single oral dose', *Int. J. Antimicrob. Agents*, **10** (1998) 31 - 38.
14. A. Navalon et al., 'Determination of antibacterial enrofloxacin by differential-pulse adsorptive stripping voltammetry', *Anal. Chim. Acta*, **454** (2002) 83 -51.
15. M. Gellert et al., 'DNA gyrase: an enzyme that introduces super helical turns into DNA', *Proc. Natl. Acad. Sci., USA* **73** (1976) 3872 - 3876.
16. L. L. Shen, and D. T. W. Chu, 'A study of two procedures of HIV – 1 isolation from whole blood cultures', *Curr. Pharm. Des.*, **2** (1996) 195 - 2000.
17. L. L. Shen, and A. G. Pernet, 'Mechanism of inhibition of DNA gyrase by analogues of nalidixic acid: The target of the drugs in DNA', *Proc. Natl. Acad. Sci. USA* **82** (1985) 307 - 311.

18. S. C. Kampranis, and A. Maxwell, 'The DNA gyrase – quinolone complex. ATP hydrolysis and the mechanism of DNA cleavage', *J. Biol. Chem.*, **273** (1998) 22615 - 22626.
19. G. Palu et al., 'Quinolone binding to DNA is mediated by magnesium ions', *Proc. Natl. Acad. Sci. USA* **89** (1992) 9671 - 9675.
20. S. Lecomte et al., 'Effect of magnesium complexation by fluoroquinolones on their antibacterial properties', *Antimicrob. Agents Chemother.*, **38** (1994) 2810 - 2816.
21. S. Lecomte, N. J. Moreau, and M. T. Chenon, 'NMR investigation of pefloxacin – cation – DNA interactions: the essential role of Mg^{2+} ', *Int. J. Pharm.* **164** (1998) 57 - 65.
22. J. Y. Fan et al., 'Self – assembly of a quinobenzoxazine – Mg^{2+} complex on DNA: a new paradigm for the structure of a drug DNA complex and implications for the structure of the quinolone bacterial gyrase – DNA complex', *J. Med. Chem.*, **38** (1995) 408 - 424.
23. A. Radi, M. A. El-Ries, and S. Kandil. 'Electrochemical study of the interaction of levofloxacin with DNA', *Anal. Chim. Acta*, **459** (2003) 61 - 67.
24. B. G. Katzung, *Basic and Clinical Pharmacology*, **8th ed.**, Lange Medical Books, Mc Graw-Hill, (2001), pp797.
25. A. Hartmann et al., 'Identification of fluoroquinolone antibiotics as the main source of umuC genotoxicity in native hospital wastewater', *Environ. Toxicol. Chem.* **17** (1998) 377-382.
26. E. M. Golet et al., 'Trace determination of fluoroquinolone antibacterial agents in urban wastewater by solid - phase extraction

- and liquid chromatography with fluorescence detection', *Anal. Chem.*, **73** (2001) 3632-3638.
27. E. M. Golet, A. C. Alder, and W. Giger, 'Environmental exposure and risk assessment of fluoroquinolone antibacterial agents in wastewater and river water of the Glatt Valley watershed, Switzerland', *Environ. Sci. Technol.*, **36** (2002) 3645-3651.
 28. D. W. Kolpin et al., 'Pharmaceuticals, hormones, and other organic wastewater contaminants in U.S. streams, 1999 – 2000: A national reconnaissance', *Environ. Sci. Technol.*, **36** (2002) 1202-1211.
 29. A. Hartmann et al., 'Primary DNA damage but not mutagenicity correlates with ciprofloxacin concentrations in German hospital wastewater', *Arch. Environ. Contam. Toxicol.*, **36** (1999) 115-119.
 30. D. A. Volmer, B. Mansoori, and S. J. Locke, 'Study of 4 – quinolone antibiotics in biological samples by short – column liquid chromatography coupled with electrospray ionization tandem mass spectroscopy', *Anal. Chem.*, **69** (1997) 4143-4155.
 31. M. R. Al-Ghazali, S. F. Jazrawi, and Z. A. Al-Doori, 'Antibiotic resistance among pollution indicator bacteria isolated from Al – Khair River, Baghdad', *Water Research*, **22** (1998) 641-644.
 32. S. F. Jazrawi, Z. A. Al-Doori, and T. A. Haddad, 'Antibiotic resistant coliform and fecal coliform bacteria in drinking water', *Water, Air, and Soil Pollution*, **39** (1998) 377-382.
 33. A. Al-Almad, F. D. Daschner, and K. Kümmerer, 'Biodegradability of cefotiam, ciprofloxacin, meropenem, pencyllinG, and sulfamethoxazole and inhibition of wastewater bacteria', *Arch. Environ. Contam. Toxicol.*, **37** (1999) 158-163.

34. K. Kümmerer, A. Al-Ahmad, and V. Mersch-Sundermann, 'Biodegradability of some antibiotics, elimination of the genotoxicity and affection of wastewater bacteria in a simple test', *Chemosphere*, **40** (2000) 701-710.
35. J. R. Marengo et al., 'Biodegradation of ^{14}C – sarafloxacin hydrochloride, a fluoroquinolone antimicrobial by Phanerochaete Chrysosporium', *J. Scientific. Ind. Res.*, **60** (2001) 121-130.
36. H. G. Wetzstein et al., 'Degradation of ciprofloxacin by basidiomycetes and identification of metabolites generated by the brown rot fungus *Gleophyllum striatum*', *Appl. Environ. Microbiol.*, **65** (1999) 1556-1563.
37. G. Phillips, B. E. Johnson, and J. Ferguson, 'The loss of antibiotic activity of ciprofloxacin by photodegradation', *J. Antimicrob. Chemother.*, **26** (1990) 783-789.
38. J. Burhenne, M. Ludwig, and M. Spiteller, 'Polar photodegradation products of quinolones determined by HPLC/MS/MS', *Chemosphere*, **38** (1999) 1279-1286.
39. E. Fasani, M. Rampi, and A. Albini, 'Photochemistry of some fluoroquinolones: effect of pH and chloride ion', *J. Chem. Soc., Perkin Transactions 2: Physical Organic Chemistry*, **9** (1999) 1901-1907.
40. E. Fasani et al., 'Unexpected photoreactions of some 7-amino-6-fluoroquinolones in phosphate buffer', *Europ. J. Org. Chem.*, **2** (2001) 391-397.
41. M. Mella, E. Fasani, and A. Albini, 'Photochemistry of 1-cyclopropyl-6-fluoro-1,4-dihydro-4-oxo-7-(piperazin-1-yl) quinoline-3-carboxylic

- acid (ciprofloxacin) in aqueous solutions', *Helvetica Chim. Acta*, **8** (2001) 2508-2519.
42. A. Nowara, J. Burhenne, and M. Spiteller, 'Binding of fluoroquinolone carboxylic acid derivatives to clay minerals', *J. Agric. Food Chem.*, **45** (1997) 1459-1463.
 43. H. C. H. Lützhøft et al., '1-Octanol/water distribution coefficient of oxolinic acid: influence of pH and its relation to the interaction with dissolved organic carbon', *Chemosphere*, **40** (2000) 711-714.
 44. J. Tolls, 'Sorption of veterinary pharmaceuticals in soils; A review', *J. Environ. Sci. Technol.*, **35** (2001) 3397-3406.
 45. H. C. H. Lützhøft, 'Influence of pH and other modifying factors on the distribution behavior of 4-quinolones to solid phases humic acids studied by "negligible-depletion" SPME-HPLC', *Environ. Sci. Technol.*, **34** (2000) 4989-4994.
 46. Y. W. Sun et al., 'Pefloxacin and ciprofloxacin increase UVA-induced edema and immune suppression', *Photodermatol. Photoimmunol. Photomed.*, **17** (2001) 172-177.
 47. J. Ferguson, and B. E. Johnson, 'Retinoid associated phototoxicity and photosensitivity', *Pharmacology and Therapeutics*, **40** (1989) 123 - 135.
 48. A. R. Saniabaldi et al, 'Impairment of phagocytic cell respiratory by UVA in the presence of fluoroquinolones: an oxygen-dependent phototoxic damage to cell surface microvilli', *J. Photochem. Photobiol. B: Biol.*, **33** (1996) 137-142.

49. N. Umezawa et al., 'Participation of reactive oxygen species in phototoxicity induced by quinolone antibacterial agents', *Arch. Biochem. Biophys.*, **342** (1997) 275-281.
50. G. Quedraogo et al., 'Lysosomes are sites of fluoroquinolone photosensitization in human skin fibroblast: a microspectrofluorometric approach', *Photochem. Photobiol.*, **70** (1999) 123-129.
51. J. A. Parrish et al., 'Dermatological and ocular examination in rabbits chronically photosensitized with methoxsalen', *J. Invest. Dermatol.*, **73** (1979) 250-255.
52. G. Klecak, F. Urbach, and H. Urwyler, 'Fluoroquinolone antibacterials enhance UVA-induced skin tumors', *J. Photochem. Photobiol. B: Biol.*, **37** (1997) 174-181.
53. M. Makinem, P. D. Forbes, and F. Steinback, 'Quinolone antibacterials: a new class of photochemical carcinogens', *J. Photochem. Photobiol. B: Biol.*, **37** (1997) 182-187.
54. Y. Tokura et al., 'Photohaptenic properties of fluoroquinolones', *Photochem. Photobiol.*, **64** (1996) 838-844.
55. T. Horio et al., 'Phototoxicity and photoallergenicity of quinolones in guinea pigs', *J. Dermatol. Sci.*, **7** (1994) 130-135.
56. Y. Ni, Y. Wang, and S. Kokot, 'Simultaneous determination of three fluoroquinolones by linear sweep stripping voltammetry with the aid of chemometrics', *Talanta*, **69** (2006) 216 – 225.
57. F. Belal, A. A. Al-Majed, and A. M. Al-Obaid, 'Methods of analysis of 4-quinolone antibacterials', *Talanta*, **50** (1999) 765-786.

58. A. M. Y. Jaber, and A. Lounici, 'Polarographic behavior and determination of norfloxacin in tablets', *Anal. Chim. Acta*, **291** (1994) 53 - 64.
59. A. M. Y. Jaber, and A. Lounici, 'Adsorptive differential-pulse stripping voltammetry of norfloxacin and its analytical applications', *Analyst*, **119** (1994) 2351 - 2357.
60. A. Tamer, 'Adsorptive stripping voltammetric determination of ofloxacinm', *Anal. Chim. Acta*, **231** (1990) 129 - 131.
61. G. Zhou, and J. Pan, 'Polarographic and voltammetric behavior of ofloxacin and its analytical applications', *Anal. Chim. Acta*, **307** (1995) 49-53.
62. M. Rizk et al., 'Differential-pulse polarographic determination of ofloxacin in pharmaceuticals and biological fluids', *Talanta*, **46** (1998) 83-89.
63. M. M. Ghoneim, A. Radi, and A. M. Beltagi, 'Determination of norfloxacin by square-wave adsorptive voltammetry on a glassy carbon electrode', *J. Pharm. Biomed. Anal.*, **25** (2001) 205 - 210.
64. P. O'Dea et al., 'Comparison of adsorptive stripping voltammetry at mercury and carbon paste electrodes for the determination of ciprofloxacin in urine', *Electroanalysis*, **3** (1991) 337 - 342.
65. M. Rizk et al., 'Voltammetric analysis of certain 4-quinolones in pharmaceuticals and biological fluids', *J. Pharm. Biomed. Anal.*, **24** (2000) 211 - 218.
66. A. Navalon et al., 'Determination of the antibacterial enrofloxacin by differential-pulse adsorptive stripping voltammetry', *Anal. Chim. Acta*, **454** (2002) 83 - 91.

67. W. J. Van Oort et al., 'Polarographic reduction and determination of nalidixic acid', *Anal. Chim. Acta*, **149** (1983) 175 - 191.
68. M. S. Ibrahim, I. S. Shehatta, and M. R. Sultan, 'Cathodic adsorptive stripping voltammetric determination of nalidixic acid in pharmaceuticals, human urine, and serum', *Talanta*, **56** (2002) 471-479.
69. A. Radi, and Z. El-Sharif, 'Determination of levofloxacin in human urine by adsorptive square-wave anodic stripping voltammetry on a glassy carbon electrode', *Talanta*, **58** (2002) 319-324.
70. V. Kapetanovic et al., 'Voltammetric methods for analytical determination of fleroxacin in Quinodis[®] tablets', *J. Pharm. Biomed. Anal.*, **22** (2000) 925-932.
71. N. Erk, 'Voltammetric behavior and determination of moxifloxacin in pharmaceutical products and human plasma', *Anal. Bioanal. Chem.*, **378** (2004) 1351.
72. J. L. Vilchez et al., 'Determination of the antibacterial trovafloxacin by differential-pulse adsorptive stripping voltammetry', *J. Pharm. Biomed. Anal.*, **31** (2003) 465-471.
73. J. L. Vilchez et al., 'Differential-pulse adsorptive stripping voltammetric determination of the antibacterial lomefloxacin', *J. Pharm. Biomed. Anal.*, **26** (2001) 23-29.
74. J. L. Beltran et al., 'Determination of quinolone antimicrobial agents in strongly overlapped peaks from capillary electrophoresis using multivariate calibration methods', *Anal. Chim. Acta*, **501** (2004) 137-141.

75. M. Hernandez, F. Borrul, and M. Calull, 'Determination of quinolones in plasma samples by capillary electrophoresis using solid phase extraction', *J. Chromatogr. B*, **742** (2000) 255 - 265.
76. K. D. Altria, *Analysis of Pharmaceuticals by Capillary Electrophoresis*. Vieweg Publication, 1998.
77. R. Kuhn, S. Hoffstetter-Kuhn, *Capillary Electrophoresis: Principles and Practice*, Springer, Berlin, 1993.
78. J. G. Moller et al., 'Capillary electrophoresis with laser-induced fluorescence: a routine method to determine moxifloxacin in human body fluids in very small sample volumes', *J. Chromatogr. B*, **716** (1998) 325-334.
79. R. A. Wallingford, and A. G. Ewing, 'Retention of ionic and non ionic catechols in capillary zone electrophoresis with micellar solutions', *J. Chromatogr.*, **441** (1988) 299 - 309.
80. G. Chen, L. Zhang, and Y. Zhu 'Determination of glucoside and sugars in Moutan cortex by capillary electrophoresis with electrochemical detection', *J. Pharm. Biomed. Anal.*, **41** (2006) 129 – 134..
81. P. Gebauer, and P. Bocek, 'Recent progress in capillary isotachopheresis', *Electrophoresis*, **21** (2000) 3898 - 3904.
82. Z. K. Shihabi, 'Stacking in capillary zone electrophoresis', *J. Chromatogr. A*, **902** (2000) 107 - 117.
83. L. Krivankova, and P. Bocek, 'Synergism of capillary isotachopheresis and capillary zone electrophoresis', *J. Chromatogr. B*, **689** (1997) 13 - 34.

84. L. Krivankova, and P. Gebauer, 'Theory, practice, and new techniques in CZE. Some practical aspects of utilizing the on-line combination of isotachopheresis and capillary zone electrophoresis', *J. Chromatogr. A*, **716** (1995) 35 - 48.
85. T. Perez-Ruiz et al., 'Separation and simultaneous determination of quinolone antibiotics by capillary zone electrophoresis', *Chromatographia*, **94** (1999) 419 - 423.
86. K. H. Bannefeld, H. Stass, and G. Blasche, 'Capillary electrophoresis with laser-induced fluorescence detection, an adequate alternative to high-performance liquid chromatography, for the determination of ciprofloxacin and its metabolite desethyleneciprofloxacin in human plasma', *J. Chromatogr. B*, **692** (1997) 453 - 459.
87. C. K. Holtzapple, S. A. Buckley, and L. H. Stanker, 'Immunsorbents coupled on-line with liquid chromatography for the determination of fluoroquinolones in chicken liver', *J. Agric. Food. Chem.*, **47** (1999) 2963 - 2968.
88. B. Hamel et al., 'Reversed-phase high-performance liquid chromatographic determination of enoxacin and 4-oxo-enoxacin in human plasma and prostatic tissue. Application to a pharmacokinetic study', *J. Chromatogr. A*, **812** (1998) 369 - 379.
89. T. Perez-Ruiz et al., 'Separation and simultaneous determination of nalidixic acid, hydroxyl nalidixic acid, and carboxy nalidixic acid in serum and urine by micellar electrokinetic capillary chromatography', *J. Chromatogr.*, **B 724** (1999) 319 -324.
90. M. G. Khaled, *High Performance Capillary Electrophoresis*, Wiley-Inter Science, New York, 1998.

91. P. G. Gigosos et al., 'Determination of quinolones in animal tissues and eggs by high-performance liquid chromatography with photodiode-array detection', *J. Chromatogr. A*, **871** (2000) 31 - 36.
92. N. J. Reinhoud, U. R. Tjaden, and J. Vander Greef, 'Automated isotachophoretic analyte focusing for capillary zone electrophoresis in a single capillary using hydrodynamics back-pressure', *J. Chromatogr.*, **641** (1993) 155 - 162.
93. A. Rogstad, V. Hormazabal, and M. Yndestad, 'Extraction and high-performance liquid chromatographic determination of enrofloxacin in fish serum and tissues', *J. Liq. Chromatogr.*, **14** (1991) 521 - 531.
94. J. Manceau et al., 'Simultaneous determination of enrofloxacin and ciprofloxacin in animal biological fluids by high-performance liquid chromatography. Application to pharmacokinetic studies in pig and rabbit', *J. Chromatogr. B*, **726** (1999) 175 - 184.
95. M. Hernandez et al., 'Determination of ciprofloxacin, enrofloxacin, and flumequine in pig plasma samples by capillary isotachopheresis-capillary zone electrophoresis', *J. Chromatogr. B*, **772** (2002) 163-172.
96. C. E. Lin et al., 'Electrophoretic behavior and pKa determination of quinolones with a piperazinyl substituent by capillary zone electrophoresis', *J. Chromatogr. A*, **1051** (2004) 283-290.
97. H. Roseboom et al., 'Rapid gas chromatographic method for the determination of nalidixic acid in plasma', *J. Chromatogr. B: Biomed. Sci. Appl.*, **13** (1979) 92 - 95.

98. H. L. Wu, T. Nakagawa, and T. Uno, 'Gas chromatographic determination of nalidixic acid in tablets', *J. Chromatogr.*, **157** (1978) 297 – 302.
99. K. J. Wang et al., 'Derivatization-gas chromatographic analysis of cinoxacin in capsules as its pentafluorobenzyl derivative', *J. Chromatogr.*, **360** (1986) 443 - 448.
100. R. H. Bishara, and I. M. Jakovljevic, 'Thin-layer chromatography of cinoxacin and some related compounds', *J. Chromatogr. A*, **116** (1976) 485 - 489.
101. H. K. L. Hundt, and E. C. Barlow, 'Thin-layer chromatographic method for the quantitative analysis of nalidixic acid in human plasma', *J. Chromatogr. Biomed. Appl.*, **12** (1981) 165 - 172.
102. P. L. Wang, Y. L. Feng, and L. A. Chen, 'Simultaneous determination of norfloxacin, pefloxacin, and ciprofloxacin by TLC-fluorescence spectrodensimetry', *Microchem. J.*, **56** (1997) 229 - 235.
103. I. Choma et al, 'Determination of flumequine and doxycycline in milk by a simple thin-layer chromatographic method', *J. Chromatogr. B*, **734** (1999) 7-14.
104. L. A. Shervington et al., 'The simultaneous separation and determination of five quinolone antibiotics using isocratic reversed-phase HPLC: Application to stability studies on an ofloxacin tablet formulation', *J. Pharm. Biomed. Anal.*, **93** (2005) 769-775.
105. J. C. Yorke, and P. Froc, 'Quantitation of nine quinolones in chicken tissues by high-performance liquid chromatography with fluorescence detection', *J. Chromatogr. A*, **882** (2000) 63-77.

106. C.K. Holtzapple, S. A. Buckley, and L. H. Stanker, 'Determination of fluoroquinolones in serum using an on-line clean-up column coupled to high-performance immuno affinity reversed-phase liquid chromatography', *J. Chromatogr. B*, **754** (2001) 1-9.
107. M. J. Schneider, and D. J. Donoghue, 'Multiresidue analysis of fluoroquinolone antibiotics in chicken tissue using liquid chromatography-fluorescence-multiple mass spectrometry', *J. Chromatogr. B*, **780** (2002) 83-92.
108. A. Zotou, and N. Miltiadou, 'Sensitive liquid chromatographic determination of ciprofloxacin in pharmaceutical preparations and biological fluids with fluorescence detection', *J. Pharm. Biomed. Anal.*, **28** (2002) 559-568.
109. M. J. Schneider, and D. J. Donoghue, 'Multiresidue determination of fluoroquinolone antibiotics in eggs using liquid chromatography-fluorescence-mass spectrometry', *Anal. Chim. Acta*, **483** (2003) 39-49.
110. M. Ramos et al., 'Simple and sensitive determination of five quinolones in food by liquid chromatography with fluorescence detection', *J. Chromatogr. B*, **789** (2003) 373-381.
111. E. Turiel, G. Bordin, and A. R. Rodriguez, 'Trace enrichment of (fluoro) quinolone antibiotics in surface waters by solid-phase extraction and their determination by liquid chromatography-ultraviolet detection', *J. Chromatogr. A*, **1008** (2003) 145-155.
112. H. Liang, M. B. Kays, and K. M. Sowinski, 'Separation of levofloxacin, ciprofloxacin, gatifloxacin, moxifloxacin, trovafloxacin, and cinoxacin by high-performance liquid chromatography: application to levofloxacin determination in human plasma', *J. Chromatogr. B*, **772** (2002) 53-63.

113. M. Ferdig et al., 'Improved capillary electrophoretic separation of nine (fluoro) quinolones with fluorescence detection for biological and environmental samples', *J. Chromatogr. A*, **1074** (2004) 305-311.
114. A. Montero et al., 'Detection of antimicrobial agents by a specific microbiological method (Eclipse 100[®]) for ewe milk', *Small Ruminant Research*, **57** (2005) 229-237.
115. S. Z. Al Khateeb, S. A. Abdel Razek, and M. M. Amer, 'Stability-indicating methods for the spectrophotometric determination of norfloxacin', *J. Pharm. Biomed. Anal.*, **17** (1998) 829 – 840.
116. P. Parimoo, C. V. N. Prasad, and R. Vineeth, 'Simultaneous quantitative determination of metronidazole and nalidixic acid in tablets by difference spectroscopy', *Gene*, **242** (2000) 105 - 114.
117. M. J. Stankov et al., 'Determination of fleroxacin in human serum and dosage forms by derivative uv-spectrophotometry', *J. Pharm. Biomed. Anal.*, **19** (1999) 501 – 510.
118. F. Eldin, O. Suliman, and S. M. Sultan, 'Sequential-injection technique employed for stoichiometric studies, optimization and quantitative determination of some fluoroquinolone antibiotics complexed with iron (III) in sulfuric acid media', *Talanta*, **43** (1996) 559 - 568.
119. L. Fratini, and E. E. S. Schapoval, 'Ciprofloxacin determination by visible light spectroscopy using iron (III) nitrate', *Int. J. Pharm.*, **127** (1996) 279 - 282.
120. H. N. Alkaysi et al., 'Chemical and micribiological investigation of metal ion interaction with norfloxacin', *Int. J. Pharmaceutics*, **87** (1992) 73–77.

- 121.** S. Mostafa, M. El-Sadek, and E. Awad Allah, 'Spectrophotometric determination of ciprofloxacin, enrofloxacin, and pefloxacin through charge transfer complex formation', *J. Pharm. Biomed. Anal.*, **27** (2002) 133 - 142.
- 122.** Z. Bilgic, S. Tosunoglu, N. Buyuktimkin, 'Two new spectrophotometric methods for ciprofloxacin', *Acta Pharm. Turk.*, **33** (1991) 19 - 22.
- 123.** J. A. Ocana, 'Spectrofluorimetric determination of moxifloxacin in tablets, human urine and serum', *Analyst*, **125** (2000) 2322 - 2325.
- 124.** J. A. Ocana et al., 'Spectrofluorimetric determination of levofloxacin in tablets, human urine and serum', *Talanta*, **52** (2000) 1149 - 1156
- 125.** J. A. M. Pulgarin, A. A. Molina, and P. F. Lopez, 'Direct determination of nalidixic acid in urine by matrix isopotential synchronous fluorescence spectrometry', *Talanta*, **43** (1996) 431 - 438.
- 126.** P. T. Djurdjevic, M. Jelkic-Stankov, and D. Stankov, 'Fluorescence reaction and complexation equilibria between norfloxacin and aluminum (III) ion in chloride medium', *Anal. Chim. Acta*, **300** (1995) 253 - 259.
- 127.** T. Perez-Ruiz et al., 'Determination of norfloxacin in real samples by different spectrofluorimetric techniques', *Analyst*, **122** (1997) 705 - 708.
- 128.** M. Rizk et al., 'Spectrofluorimetric analysis of certain 4-quinolones in pharmaceuticals and biological fluids', *Pharmaceutica Acta Helvetiae*, **74** (2000) 371 - 377.
- 129.** J. A. Ocana, M. Callejon, and F. J. Barra

130. gani, 'Terbium-sensitized luminescence determination of levofloxacin in tablets, human urine and serum', , *Analyst*, **125** (2000) 1851 – 1854.
131. J. A. Hernandez-Arteseros, R. Compano, and M. D. Prat, 'Determination of ciprofloxacin and enrofloxacin in edible animal tissues by terbium-sensitized luminescence', *Analyst*, **123** (1998) 2729- -2732.
132. S. V. Beltyukova et al., 'Use of sensitized luminescence of lanthanides in analysis of drugs', *J. Pharm. Biomed. Anal.*, **18** (1998) 263 – 266.
133. M. E. El-Kommos et al., 'Spectrofluorometric determination of certain quinolone antibacterials using metal chelation', *Talanta*, **60** (2003) 1033 -1050.
134. L. M. Du, H. Y. Yao, and M. Fu, 'Spectrofluorometric studt of charge-transfer complexation of certain fluoroquinolones with 7,7,8,8,-tetracyanoquinodimethane', *Spectrochimica Acta*, **A 61** (2005) 281 - 286.
135. S. Rauf et al., 'Electrochemical approach of anticancer drugs-DNA interaction', *J. Pharm. Biomed. Anal.*, **37** (2005) 205 - 217.
136. H. Heli, S. Z. Bathaie, and M. F. Mousavi, 'An electrochemical study of neutral red-DNA interaction', *Electrochimica Acta*, **51** (2005) 1108 – 1116.
137. E. F. Gale et al., 'The molecular basis of antibiotic action', Wiley, London, (1981).
138. S. J. Lippard, and J. M. Berg, 'Principles of bioinorganic chemistry', University Science Books, Clifornia, (1994).
139. D. E. Graves, and L. M. Vela, *Curr. Org. Chem.*, **4** (2000) 915.

140. K. R. Fox, M. J. Waring, 'DNA structural variations produced by actinomycin and distamycin as revealed by DNAase I footprinting', *Nucl. Acids Res.*, **12** (1984) 9271 - 9285.
141. K. Sandstorm et al., '¹H NMR studies of selective interactions of norfloxacin with double-stranded DNA', *Biochem. Biophys. Res. Comm.*, **304** (2003) 55 - 59.
142. S. Lecomte, N. J. Moreau, and M. T. Chenon, 'NMR investigation of pefloxacin -cation-DNA interactions: the essential role of Mg²⁺ ', *Int. J. Pharm.*, **164** (1998) 57 - 65.
143. L. Oehlers, C. L. Mazzitelli, and J. S. Brodbelt, 'Evaluation of complexes of DNA duplexes and novel benzoxazoles or benzimidazoles by electrospray ionization spectrometry', *J. Am. Soc. Mass Spectrom.*, **15** (2004) 1593 - 1603.
144. M. Gopal, M. S. Shahabuddin, and S. R. Inamdar, 'Interaction between an 8-methoxypyrimido[4prime,5prime:4,5] thieno(2,3-b)quinoline-4-(3H)one antitumor drug and deoxyribonucleic acid', *Proc. Indian Acad. Sci.*, **114** (2002) 687 - 696.
145. H. Morjani et al., 'Molecular and cellular interaction between intoplicine, DNA, and topoisomerase II studied by surface-enhanced Raman scattering spectroscopy', *Cancer Res.*, **53** (1993) 4784 - 4790.
146. J. M. Le Gal, H. Morjani, and M. Manfait, 'Ultrastructural appraisal of the multidrug resistance in K562 and LR73 cell lines from Fourier transform infrared spectroscopy', *Cancer Res.*, **53** (1993) 3681 - 3686.
147. Y. He, G. W. Song, and Q. C. Zou, 'Spectra analysis of interaction between poly ((2-methylacryloxyethyl) dimethyl butylammonium

- bromide) and nucleic acids', *Sensors and Actuators*, **B 106** (2005) 325 - 330.
- 148.** S. Nafisi et al., 'Interaction of antitumor drug $\text{Sn}(\text{CH}_3)_2\text{Cl}_2$ with DNA and RNA', *J. Mol. Struct.*, **750** (2005) 23 - 28.
- 149.** J. Caldwell, and P. A. Collman, 'A mmolecular mechanical study of netropsin-DNA interactions', *Biopolymers*, **25** (1986) 249 - 266.
- 150.** P. Cieplak et al., 'Free energy calculation on base specificity of drug-DNA interactions: Application to daunomycin and acridine intercalation into DNA', *Biopolymers*, **29** (1990) 717-727.
- 151.** B. Llorente, F. Leclerc, and R. Cedergren, 'Using SAR and QSAR analysis to model the activity and structure of the quinolone-DNA complex', *Bioorg. Medicin. Chem.*, **4** (1996) 61 - 71.
- 152.** L. N. Ji, X. H. Zou, and J. G. Liu, 'Shape and enantioselective interaction of Ru (II) / Co (III) polypyridyl complexes with DNA', *Coord. Chem. Rev.*, **216-217** (2001) 513 - 536.
- 153.** W. D. McFadyen et al., 'The interaction of substituted and rigidly linked diquinolones with DNA', *Biochim. Biophys. Acta*, **1048** (1990) 50 - 58.
- 154.** N. H. H. Heegaard, and R. T. Kennedy, 'Antigen-antibody interactions in capillary electrophoresis', *J. Chromatogr. B*, **768** (2002) 93 - 103.
- 155.** G. Kemp, 'Capillary electrophoresis: A versatile family of analytical techniques', *Biotechnol. Biochem.*, **27** (1998) 9 - 17.
- 156.** X. He et al., 'Interaction between netropsin and double-stranded DNA in capillary zone electrophoresis and affinity capillary electrophoresis', *J. Chromatogr. A*, **982** (2002) 285 - 291.

157. K. Akdi et al., 'Effect of Tris and Hepes buffers on the interaction palladium-diaminopropane complex with DNA', *J. Inorg. Biochem.*, **99** (2005) 1360 - 1368.
158. K. Morohashi et al., 'Identification of a drug target motif: An anti-tumor drug NK109 interacts with a PNxxxxP', *Biochem. Pharmacol.*, **70** (2005) 37 - 46.
159. M. H. D. Thi et al., 'Molecular basis of gyrase poisoning by the addiction toxin CcdB', *J. Mol. Biol.*, **348** (2005) 1091 - 1102.
160. S. C. Kampranis, A. J. Howells, and A. Maxwell, 'The interaction of DNA gyrase with bacterial toxin CcdB: evidence for the existence of two gyrase-CcdB complexes', *J. Mol. Biol.*, **293** (1999) 733 - 744.
161. C. Bailly et al., 'Drug-DNA sequence-dependent interactions analyzed by electric linear dichroism', *J. Mol. Recognit.*, **5** (1992) 155 - 171.
162. P. Colson, C. Bailly, and C. Houssier, 'Electric linear dichroism as a new tool to study sequence preference in drug binding to DNA', *Biophys. Chem.*, **58** (1996) 125 - 140.
163. M. Eriksson, and B. Norden, 'Linear and circular dichroism of drug-nucleic acid complexes', *Meth. Enzymol.*, **340** (2001) 68 - 98.
164. C. Bailly et al., 'The binding mode of drugs to the TAR RNA of HIV-1 studied by electric linear dichroism', *Nucl. Acids Res.*, **24** (1996) 1460 - 1464.
165. C. Bailly, P. Colson, and C. Houssier, 'The orientation of norfloxacin bound to double stranded-DNA', *Biochem. Biophys. Res. Commun.*, **243** (1998) 844 - 848.

166. G. S. Son et al., 'Base specific complex formation of norfloxacin with DNA', *Biophys. Chem.*, **74** (1998) 225 - 236.
167. E. Palecek, 'Past, present, and future of nucleic acids electrochemistry', *Talanta*, **56** (2002) 809 - 819.
168. A. F. Collings, and F. Caruso, 'Biosensors: recent development', *Rep. Prog. Phys.*, **60** (1997) 1397 - 1445.
169. J. E. Pearson, A. Gill, and P. Vadgama, 'Analytical aspects of biosensors', *Annu. Clin. Biochem.*, **37** (2000) 119 - 145.
170. J. Wang, 'From DNA biosensors to gene chips', *Nucl. Acids Res.*, **28** (2000) 3011 - 3016.
171. J. J. Gooding, 'Electrochemical DNA hybridization biosensors', *Electrolysis*, **14** (2002) 1149 - 1156.
172. J. R. Dimmock et al., 'Mannich bases of phenolic azobenzenes possessing cytotoxic activity', *J. Med. Chem.*, **7** (1997) 583 - 594.
173. J. R. Dimmock et al., 'Cytotoxic activities of Mannich bases of chalcones and related compounds', *J. Med. Chem.*, **41** (1998) 1014 - 1026.
174. A. Ferancova et al., 'Association interaction and voltammetric determination of 1-aminopyrene and 1-hydroxypyrene at cyclodextrin and DNA based electrochemical sensors', *Bioelectrochemistry*, **67** (2005) 191 - 197.
175. B. Meric et al., 'Electrochemical biosensor for interaction of DNA with the alkylating agent 4,4'-dihydroxy chalcone based on guanine and adenine signals', *J. Pharm. Biomed. Anal.*, **30** (2002) 1339 - 1346.

176. J. Jasnowska et al., 'DNA sensor for o-dianisidine', *Bioelectrochemistry*, **64** (2004) 85 - 90.
177. S. T. Girousi, I. C. Gherghi, and M. K. Karava, 'DNA-modified carbon paste electrode applied to the study of interaction between Rifampicin and DNA in solution and at the electrode surface', *J. Pharm. Biomed. Anal.*, **36** (2004) 851 - 858.
178. A. Radi, M. A. El-Ries, and S. Kandil, 'Electrochemical study of the interaction of levofloxacin with DNA', *Anal. Chim. Acta*, **495** (2003) 61 - 67.
179. A. Erdem, and M. Ozsoz, 'Interaction of the anticancer drug epirubicin with DNA', *Anal. Chim. Acta*, **437** (2001) 107 - 114.
180. E. L. Debeer, A. E. Bottone, and E. E. Voest, 'Doxorubicin and mechanical performance of cardiac trabeculae after acute and chronic treatment', *Eur. J. Pharmacol.*, **415** (2001) 1 - 11.
181. S. Wang, T. Peng, and F. C. Yang, 'Investigation on the interaction of DNA and electroactive ligands using a rapid electrochemical method', *J. Biochem. Biophys. Meth.*, **55** (2003) 191 - 204.
182. M. A. La-Scalea et al., 'Voltammetric behavior of benznidazole at a DNA- electrochemical biosensor', *J. Pharm. Biomed. Anal.*, **29** (2002) 561 - 568.
183. A. M. Oliveira- Brett, and V. C. Diculescu, 'Electrochemical study of quercetin-DNA interactions Part II. In situ sensing with DNA biosensors', *Bioelectrochemistry*, **64** (2004) 143 - 150.
184. N. Diab, A. Abu-Zuhri, and W. Shuhmann, 'Sequential-injection stripping analysis of nifuroxime using DNA-modified carbon electrodes', *Bioelectrochemistry*, **61** (2003) 57 - 63.

- 185.** Z. Zhu, C. Li, and N. Q. Li, 'Electrochemical studies of quercitin interacting with DNA', *Microchem. J.*, **71** (2002) 57 - 63.
- 186.** A. M. Oliveira- Brett et al., 'Electrochemical detection of in situ adriamycin oxidative damage to DNA', *Talanta*, **56** (2002) 959 - 970.
- 187.** A. M. Oliveira- Brett et al., 'Electrochemical determination of carboplatin in serum using a DNA-modified glassy carbon electrode', *Electroanalysis*, **8** (1996) 992 - 995.
- 188.** A. M. Oliveira- Brett, and V. C. Diculescu, 'Electrochemical study of quercitin-DNA interactions: Part I. Analysis in incubated solutions. *Bioelectrochemistry*, **64** (2004) 133 - 141.
- 189.** H. C. M. Yau, H. L. Chan, and M. Yang, 'Electrochemical properties of DNA-interacting doxorubicin and methylene blue on n-hexadecyl mercaptan-doped 5'-thiol-labeled DNA-modified gold electrodes', *Biosens. Bioelectron.*, **18** (2003) 873 - 878.
- 190.** S. Y. Zhou et al., 'Cumulative and irreversible cardiac mitochondrial dysfunction induced by doxorubicin', *Cancer Res.*, **61** (2001) 771 - 777.
- 191.** H. M. Geller et al., 'Oxidative stress mediates neuronal damage and apoptosis in response to cytosine arabinoside', *J. Neurochem.* **78** (2001) 265 - 75.
- 192.** N. Zhang, X. Zhang, and Y. Zhao, 'Voltammetric study of the interaction ciprofloxacin-copper with nucleic acids and the determination of nucleic acids', *Talanta*, **62** (2004) 1041 - 1045.
- 193.** X. Chau et al., 'Voltammetric studies of the interaction of daunomycin anticancer drug with DNA and analytical applications', *Anal. Chim. Acta*, **373** (1998) 29 - 38.

194. H. Karadeniz et al., 'Disposable electrochemical biosensor for the detection of the interaction between DNA and lycorine based on guanine and adenine signals', *J. Pharm. Biomed. Anal.*, **33** (2003) 295 - 302.
195. J. Kang et al., 'Electrochemical investigation on interaction between DNA and quercetin and Eu-Qu₃ complex', *J. Inorg. Biochem.*, **98** (2004) 79 - 86.
196. X. Lin, X. Jiang, and L. Lu, 'DNA deposition on carbon electrodes under controlled dc potentials', *Biosens. Bioelectron.*, **20** (2005) 1709 - 1717.
197. J. R. de Souza, 'Zinc binding to Lambda phage DNA studied by voltammetric techniques', *J. Braz. Chem. Soc.*, **11** (2000) 398 - 404.
198. E. Laviron in: A. J. Bard (Ed.), *Electroanalytical Chemistry*, Dekker, N. Y., (1982) 53 - 157.
199. Z. Nagy in: R. E. White, J. O. M. Bockris, B. E. Conway (Eds.), *Modern Aspects of Electrochemistry*, Plenum, N. Y., (1990) 237 - 292.
200. A. M. Bond, *Modern Polarographic Methods In Analytical Chemistry*, Dekker, N. Y., (1980) 269 - 272.
201. J. Wang et al., 'Nucleic-acid immobilization, recognition and detection at chronopotentiometric DNA chips', *Biosens. Bioelectron.*, **12** (1997) 587 - 599.
202. A. M. Oliveira-Brett et al., 'Voltammetric behavior of nitromidazoles at a DNA-biosensor', *Electroanalysis*, **9** (1997) 1132 - 1137.

- 203.** A. M. Oliveira-Brett et al., 'Voltammetric behavior of mitoxantrone at a DNA-biosensor', *Biosens. Bioelectron.*, **13** (1998) 861 - 867.
- 204.** L. Li et al., 'Electrochemical investigation of DNA adsorbed on conducting polymer modified electrode', *Anal. Sci.*, **13** (1997) 305 - 310.
- 205.** D. W. Pang, and H. D. Abruna, 'Micromethod for the investigation of the interaction between DNA and redox-active molecules', *Anal. Chem.*, **70** (1998) 3162 - 3169.
- 206.** R. Palecek et al., 'Electrochemical biosensors for DNA hybridization and DNA damage', *Biosens. Bioelectron.*, **13** (1998) 621 - 628.
- 207.** M. I. Pividori, A. Merkoci, and S. Alegret, 'Electrochemical genosensor design: immobilization of oligonucleotides onto transducer surfaces and detection methods', *Biosens. Bioelectron.*, **15** (2000) 291 - 303.
- 208.** D. Laloo and K. M. Mahanti, 'Kinetics of oxidation of amino acids by alkaline hexacyanoferrate (III)', *J. Chem. Soc. Dalton Trans.* **1** (1990) 311 - 313.
- 209.** K. C. Gupta, R. Gupta, and U. Saxena, 'Kinetics and mechanism of oxidation of o-, m-, and p-hydroxy-acetophenones by hexacyanoferrate (III) in alkaline medium', *Indian. J. Chem. A* **28** (1989) 253 - 254.
- 210.** K. S. Sidhu, W. R. Bansal, and S. Kaur, 'Mechanistic features of hexacyanoferrate (III) oxidation of diphenylamine in alkaline medium', *Indian. J. Chem. A* **26** (1987) 740 - 748.

- 211.** G. Dasgupta and K. M. Mahanti, 'Kinetics of oxidation of unsubstituted and substituted diphenylamine by alkaline hexacyanoferrate (III)', *Indian. J. Chem.* **A 25** (1986) 958 – 959.
- 212.** G. Dasgupta and K. M. Mahanti, 'Kinetics of oxidation of anilines by alkaline hexacyanoferrate (III). Oxidation of N-alkyl side chains', *Bull. Soc. Chim. Fr.*, **4** (1986) 492 - 496.
- 213.** M. M. Al-Subu, 'Kinetics and mechanism of oxidation of diallylamine by alkaline hexacyanoferrate (III)', *An-Najah J. Res.*, **7** (1992) 37 - 44.
- 214.** K. M. Mahanti, 'A guide tour of electron transfere reactions', *J. Indian Chem. Soc.*, **66** (1989) 5 – 16.
- 215.** N. Nath and L. P. Singh, 'Kinetics and mechanism of ruthenium (III) catalysed oxidation of benzylamine by hexacyanoferrate (III) in alkaline medium', *J. Indian Chem. Soc.*, **62** (1985) 108 – 111.
- 216.** H. J. El-Aila, 'Kinetic study of cysteine oxidation by potassium hexacyanoferrate (III) in the presence of sodium dioctylsulfosuccinate', *Journal of Dispersion Science and Technology*, **25** (2004) 157 – 162.
- 217.** M. M. Al-Subu et al., 'Osmium (VIII)-catalyzed oxidation of some cyclic amines by potassium hexacyanoferrate (III) in alkaline medium. A kinetic and mechanistic study', *Chem. Heterocyclic compounds*, **4** (2003) 559 – 565.
- 218.** M. M. Al-Subu, 'Osmium (VIII)-catalyzed oxidation of pentamethylene sulfide', *Transition Met. Chem.* **28** (2003).
- 219.** S. P. S. Mehta and G. Tewary, 'Kinetics and mechanism of metal ion catalysis: Part II. Oxidation of PhCHO by osmium (VIII) continuously

- regenerated by hexacyanoferrate (III) ion', *Transition Met. Chem.*, **26** (2001) 290 – 294.
- 220.** M. M. Al-Subu, 'Kinetics and mechanism of Osmium (VIII)-catalyzed oxidation of thiomorpholine by alkaline hexacyanoferrate (III)', *Pakistan Journal of applied science*, **2** (2002) 742 – 746.
- 221.** R. Abu-El-Halawa et al., 'Stoichiometry, kinetics and mechanism of oxidation of L-cysteine by hexacyanoferrate (III) in acidic medium', *An-Najah J. Res.*, **4** (1996) 23 – 42.
- 222.** M. E. Reichman et al., 'A further examination of the molecular weight and size of deoxypentose nucleic acid', *J. Am. Chem. Soc.*, **76** (1954) 3047 – 3053.
- 223.** C. M. A. Brett, A. M. Oliviera-Brett, and S. H. P. Serrano, 'An EIS study of DNA-modified electrodes', *Elec. Chim. Acta*, **44** (1999) 4233 – 4239.
- 224.** R. Fukuda, S. Takenaka, and M. Takag, 'Metal ion assisted DNA-interaction of crown ether-linked acididine derivatives', *J. Chem. Soc. Chem. Commun.* (1990) 1028 – 1030.
- 225.** C. Cantor and P. R. Schimmel, *Biophysical Chemistry*, W. H. Freeman, San Francisco, 1980.
- 226.** S. Takenaka, T. Ihara, and M. Takag, 'Bis-9-acridinyl derivatives containing a viologen linker chain: electrochemically active intercalator for reversible labeling of DNA', *J. Chem. Soc. Chem. Commun.* (1990) 1485 – 1487.
- 227.** X. J. Dang et al., 'Inclusion of the parent molecules of some drugs with beta-cyclodextrin studied by electrochemical and spectrometric method', *J. Electroanal. Chem.*, **448** (1998) 61 – 67.

- 228.** M. S. Ibrahim, 'Voltammetric studies of the interaction of nogalamycin antitumor drug with DNA', *Anal. Chim. Acta*, **443** (2001) 63 – 72.
- 229.** H. Berg, G. Horn, and U. Luthardt, 'Interaction of anthracycline antibiotics with biopolymers: polarographic behavior and complexes with DNA', *Bioelectrochem. Bioenergy*, **8** (1981) 537 – 553.
- 230.** J. M. Kauffmann et al., 'Voltammetric oxidation of trazodone', *Electrochem. Acta*, **32** (1987) 1159- - 1162.
- 231.** A. J. Bard, M. T. Carter, and M. Rodriguez, 'Voltammetric studies of the interaction of metal chelates with DNA. 2. Tris-chelated complexes of cobalt(III) and iron(II) with 1,10-phenanthroline and 2,2'-bipyridine', *J. Am. Chem. Soc.* **111** (1989) 8901 – 8911.
- 232.** A. J. Bard and L. R. Faulkner, *Electrochemical Methods Fundamentals and Applications*, Chemical Industry Press, Beijing, (1986) p256.
- 233.** S. Wang, T. Peng, and F. C. Yang, 'Electrochemical determination of interaction parameters for DNA and mitoxantrone in an irreversible redox process', *Biophysical. Chemistry*, **104** (2003) 239 – 248.
- 234.** P. Delahay (Ed.). *New Instrumental Methods in Electrochemistry*, Interscience Publishers Inc., New York, (1954), p125 – 129.
- 235.** I. D. Vilfan et al., 'Characterization of ciprofloxacin binding to the linear single- and double-stranded DNA', *Biochimica et Biophysica Acta*, **1628** (2003) 111 – 122.
- 236.** F. Wang and L. M. Sayre, 'Kinetics and mechanism of aliphatic amine oxidation by aqueous (batho)₂Cu(II)', *J. Am. Chem. Soc.*, **114** (1992) 248 – 255.

237. K. J. Laidler, *Chemical Kinetics*, 2nd edit., McGraw-Hill, New York, (1965) p230.

List of Abbreviations

| | |
|----------|---|
| A | Absorbance (Equation 1) or Frequency factor (Equation 12) |
| A | Surface area |
| ASV | Anodic stripping voltammetry |
| α | Electron transfer coefficient |
| CIP | Ciprofloxacin |
| CE | Capillary electrophoresis |
| C_b | Equilibrium concentration of electro active molecule-binding site complex |
| C_f | Equilibrium concentration of free electro-active molecule |
| CFCE | Carbon fiber column electrode |
| CFDE | Carbon fiber disk electrode |
| C_{NP} | Concentration of nucleotide phosphate |
| CPE | Carbon paste electrode |
| C_s | Concentration of free binding site |
| C_t | Total concentration of electroactive molecule |
| CV | Cyclic voltammetry |
| D | Diffusion coefficient |
| D_f | Diffusion coefficient of free ligand |
| D_b | Diffusion coefficient of ligand-DNA complex |
| DNA | Deoxyribonucleic acid |
| dsDNA | Double-stranded DNA |

| | |
|------------------|--|
| DPP | Differential-pulse polarography |
| E_a | Activation energy |
| E° | Formal electrode potential |
| E_p | Electrode potential |
| EM | Electroactive molecule |
| ENR | Enrofloxacin |
| ϵ | Extinction coefficient |
| ϵ_G | Absorption coefficient of the drug |
| ϵ_{H-G} | Absorption coefficient of the drug-DNA complex |
| F | Farady |
| FT-IR | Fortier-transform infra red |
| FQ | Fluoroquinolone |
| GC | Gas chromatography |
| GCE | Glassy carbon electrode |
| h | Plank's constant |
| HMDE | Hanging mercury drop electrode |
| HPLC | High performance liquid chromatography |
| I_p | Peak current |
| k | Rate constant |
| k° | Standard homogeneous rate constant |
| K | Binding constant |
| K_B | Boltzman constant |
| M | Molar concentration |

| | |
|------------------|---|
| MICs | Minimum inhibitory concentrations |
| MS | Mass spectroscopy |
| <i>n</i> | Number of electrons |
| NAL | Nalidixic acid |
| NMR | Nuclear magnetic resonance |
| NOR | Norfloxacin |
| <i>v</i> | Scan rate |
| PGE | Pencil graphite electrode |
| PPy | Polypyrrole |
| [Pt(terpy)(HET)] | Terpyridine(hydroxyl ethanthiolate) complex |
| Q | Quinolone |
| R | Universal gas constant |
| <i>R</i> | Ratio of nucleotide phosphate concentration and the concentration of electroactive molecule |
| S | Binding site size (base pairs, bp) |
| <i>s</i> | Number of base pairs |
| SPE | Screen printed electrode |
| ssDNA | Single-stranded DNA |
| TLC | Thin layer chromatography |

()

(III)

.

.

J.

()

(III)

.
.

(DNA)

.()

DNA

UV-visible)

.DNA

(spectroscopy

(binding constnt, K)

.DNA

glassy carbon)

(cyclic voltammetry)

(electrode

(D_b) DNA

(D_f)

FQ-DNA) DNA

(binding sites size, s)

(K)

(complex

.Origin

(lectrostatic binding with partial intercalation)

DNA.

ت

(Biosensor)

(DNA)

(DP-ASV)

()

(OsO₄)

(III)